PB-249 062

EVALUATION OF THE MULTIPLE SOURCE GAUSSIAN PLUME DIFFUSION MODEL - PHASE 1

Robert C. Koch, et al

Geomet, Incorporated

Prepared for:

Environmental Protection Agency

April 1973

DISTRIBUTED BY:

NTIS
National Technical Information Service
U. S. DEPARTMENT OF COMMERCE

040038

PB 249 062

EPA-650/4-75-018-a

April 1975

Environmental Monitoring Series

Reproduced by
NATIONAL TECHNICAL
INFORMATION SERVICE
U S Department of Commerce
Springfield VA 22151

TECHNICAL REPORT DATA

(Please read Instructions on the reverse before completing)

1. REPORT NO.

2.

3. RECIPIENT'S ACCESSION NO.

4. TITLE AND SUBTITLE

Evaluation of the Multiple-Source Gaussian Plume
Dispersion Model - Phase I

5. REPORT DATE

April 1973 (issue date)

6. PERFORMING ORGANIZATION CODE

7. AUTHOR(S)

Robert C. Koch
George E. Fisher

8. PERFORMING ORGANIZATION REPORT NO.

GEOMET Report Number EF-186

9. PERFORMING ORGANIZATION NAME AND ADDRESS

GEOMET, Incorporated
15 Firstfield Road
Gaithersburg, Maryland 20760

10. PROGRAM ELEMENT NO.

11. CONTRACT/GRANT NO.

68-02-0281

12. SPONSORING AGENCY NAME AND ADDRESS

Environmental Protection Agency
Research Triangle Park, North Carolina 27711

13. TYPE OF REPORT AND PERIOD COVERED

Final

14. SPONSORING AGENCY CODE

15. SUPPLEMENTARY NOTES

Phase II Report published July 1975 as EPA Report No. EPA-650/4-75-018-b

16. ABSTRACT

Ten different ways of applying the Gaussian plume diffusion model to represent air quality in an urban area are compared. The different techniques include different degrees of detail in representing spatial and temporal variations in emissions and in meteorological conditions. The methods used to represent spatial and temporal variations are described. It is shown that some improvement results from the use of more detailed spatial and temporal variations. It is suggested that greater improvements would result if more detailed measurements of emissions and meteorological conditions were available.

The report places primary emphasis on the use of the Sampled Chronological Input Model (SCIM) as a computer program for the multiple-source Gaussian plume diffusion model; the characteristics of this program are described.

17. KEY WORDS AND DOCUMENT ANALYSIS

a. DESCRIPTORS		b. IDENTIFIERS/OPEN ENDED TERMS	c. COSATI Field/Group
Air Pollution Urban Areas Atmospheric Diffusion Proving Mathematical Models Emission Sequential Sampling	Diurnal Variation	Air Quality Model	1302 0401

PRICES SUBJECT TO CHANGE

18. DISTRIBUTION STATEMENT Release Unlimited	19. SECURITY CLASS *(This Report)* UNCLASSIFIED	21. NO. OF PAGES 180
	20. SECURITY CLASS *(This page)* UNCLASSIFIED	22. PRICE $7.50

EPA Form 2220-1 (9-73)

EPA-650/4-75-018-a

EVALUATION OF THE MULTIPLE SOURCE GAUSSIAN PLUME DIFFUSION MODEL - PHASE I

by

Robert C. Koch and George E. Fisher

Geomet, Inc.
15 Firstfield Road
Gaithersburg, Maryland 20760

Contract No. 68-02-0281
ROAP No. 21ADO
Program Element No. 1AA009

EPA Project Officer: D. Bruce Turner

Meteorology Laboratory
National Environmental Research Center
Research Triangle Park, North Carolina 27711

Prepared for

U. S. ENVIRONMENTAL PROTECTION AGENCY
OFFICE OF RESEARCH AND DEVELOPMENT
WASHINGTON, D. C. 20460

April 1973

ib

EPA REVIEW NOTICE

This report has been reviewed by the National Environmental Research Center - Research Triangle Park, Office of Research and Development, EPA, and approved for publication. Approval does not signify that the contents necessarily reflect the views and policies of the Environmental Protection Agency, nor does mention of trade names or commercial products constitute endorsement or recommendation for use.

RESEARCH REPORTING SERIES

Research reports of the Office of Research and Development, U.S. Environmental Protection Agency, have been grouped into series. These broad categories were established to facilitate further development and application of environmental technology. Elimination of traditional grouping was consciously planned to foster technology transfer and maximum interface in related fields. These series are:

1. ENVIRONMENTAL HEALTH EFFECTS RESEARCH
2. ENVIRONMENTAL PROTECTION TECHNOLOGY
3. ECOLOGICAL RESEARCH
4. ENVIRONMENTAL MONITORING
5. SOCIOECONOMIC ENVIRONMENTAL STUDIES
6. SCIENTIFIC AND TECHNICAL ASSESSMENT REPORTS
9. MISCELLANEOUS

This report has been assigned to the ENVIRONMENTAL MONITORING series. This series describes research conducted to develop new or improved methods and instrumentation for the identification and quantification of environmental pollutants at the lowest conceivably significant concentrations. It also includes studies to determine the ambient concentrations of pollutants in the environment and/or the variance of pollutants as a function of time or meteorological factors.

This document is available to the public for sale through the National Technical Information Service, Springfield, Virginia 22161.

Publication No. EPA-650/4-75-018-a

GEOMET Report Number EF-186

April 1973

EVALUATION OF THE MULTIPLE-SOURCE GAUSSIAN PLUME DIFFUSION MODEL

PHASE I Report

for

Environmental Protection Agency
Research Triangle Park
North Carolina 27711

under

Contract Number 68-02-0281

by

Robert C. Koch
George E. Fisher

TABLE OF CONTENTS

Page

1.0 INTRODUCTION 1

2.0 MODELS 2

2.1 Features of the Multiple-Source Gaussian Plume Diffusion Model 2
2.2 The Simplified Gifford-Hanna Model 18

3.0 MODEL COMPARISONS 21

3.1 Comparisons Between Calculations Using Mean and Variable Emission Rates for SCIM 21
3.2 Comparisons Among Ten Model Variations Using New York City Data 42

4.0 CONCLUSIONS 91

5.0 REFERENCES 94

APPENDIX A - An Algorithm for Estimating Area Source SO_2 Emission Rates

APPENDIX B - Method of Estimating the Height of the Mixing Layer

APPENDIX C - Development of a Method of Estimating Emission Rates for Use in the Simplified Gifford-Hanna Model

APPENDIX D - Frequency Distributions for SCIM Calculations Using 3 to 96 Hour Sampling Intervals

INDEX OF FIGURES

Figure		Page
1	Location of St. Louis Observing Stations Used in Validation Analysis	23
2	Frequency Distribution of Calculated and Measured Two-Hour Concentrations for St. Louis Station #13	25
3	Frequency Distribution of Calculated and Measured Two-Hour Concentrations for St. Louis Station #15	25
4	Frequency Distribution of Calculated and Measured Two-Hour Concentrations for St. Louis Station #17	26
5	Frequency Distribution of Calculated and Measured Two-Hour Concentrations for St. Louis Station #23	26
6	Frequency Distribution of Calculated and Measured Two-Hour Concentrations for St. Louis Station #33	27
7	Frequency Distribution of Calculated and Measured Two-Hour Concentrations for St. Louis Station #4	27
8	Frequency Distribution of Calculated and Measured Two-Hour Concentrations for St. Louis Station #10	28
9	Frequency Distribution of Calculated and Measured Two-Hour Concentrations for St. Louis Station #12	28
10	Frequency Distribution of Calculated and Measured Two-Hour Concentrations for St. Louis Station #28	29
11	Frequency Distribution of Calculated and Measured Two-Hour Concentrations for St. Louis Station #36	29
12	Location of Chicago TAM Stations Used in Validation Analysis	30
13	Frequency Distribution of Calculated and Measured One-Hour Concentrations for Chicago TAM #1	31
14	Frequency Distribution of Calculated and Measured One-Hour Concentrations for Chicago TAM #2	31
15	Frequency Distribution of Calculated and Measured One-Hour Concentrations for Chicago TAM #3	32

(Continued)

INDEX OF FIGURES (Continued)

Figure		Page
16	Frequency Distribution of Calculated and Measured One-Hour Concentrations for Chicago TAM #4	32
17	Frequency Distribution of Calculated and Measured One-Hour Concentrations for Chicago TAM #5	33
18	Frequency Distribution of Calculated and Measured One-Hour Concentrations for Chicago TAM #6	33
19	Frequency Distribution of Calculated and Measured One-Hour Concentrations for Chicago TAM #7	34
20	Frequency Distribution of Calculated and Measured One-Hour Concentrations for Chicago TAM #8	34
21	Locations of Air Quality Measurements in the Immediate Vicinity of New York City	45
22	Frequency Distribution of SCIM Calculated and Measured One-Hour Concentrations for New York City Station #0	51
23	Frequency Distribution of SCIM Calculated and Measured One-Hour Concentrations for New York City Station #1	51
24	Frequency Distribution of SCIM Calculated and Measured One-Hour Concentrations for New York City Station #3	52
25	Frequency Distribution of SCIM Calculated and Measured One-Hour Concentrations for New York City Station #10	52
26	Frequency Distribution of SCIM Calculated and Measured One-Hour Concentrations for New York City Station #14	53
27	Frequency Distribution of SCIM Calculated and Measured One-Hour Concentrations for New York City Station #17	53
28	Frequency Distribution of SCIM Calculated and Measured One-Hour Concentrations for New York City Station #27	54
29	Frequency Distribution of SCIM Calculated and Measured One-Hour Concentrations for New York City Station #28	54

(Continued)

INDEX OF FIGURES (Continued)

Figure | Page

30 Frequency Distribution of SCIM Calculated and Measured One-Hour Concentrations for New York City Station #31 55

31 Frequency Distribution of SCIM Calculated and Measured One-Hour Concentrations for New York City Station #36 55

32 Frequency Distribution of GHM Calculated and Measured One-Hour Concentrations for New York City Station #0 56

33 Frequency Distribution of GHM Calculated and Measured One-Hour Concentrations for New York City Station #1 56

34 Frequency Distribution of GHM Calculated and Measured One-Hour Concentrations for New York City Station #3 57

35 Frequency Distribution of GHM Calculated and Measured One-Hour Concentrations for New York City Station #10 57

36 Frequency Distribution of GHM Calculated and Measured One-Hour Concentrations for New York City Station #14 58

37 Frequency Distribution of GHM Calculated and Measured One-Hour Concentrations for New York City Station #17 58

38 Frequency Distribution of GHM Calculated and Measured One-Hour Concentrations for New York City Station #27 59

39 Frequency Distribution of GHM Calculated and Measured One-Hour Concentrations for New York City Station #28 59

40 Frequency Distribution of GHM Calculated and Measured One-Hour Concentrations for New York City Station #31 60

41 Frequency Distribution of GHM Calculated and Measured One-Hour Concentrations for New York City Station #36 60

42 Variations in Measured and Calculated Mean One-Hour SO_2 Concentration by Hour of the Day 67

43 Variations in Measured and Calculated Mean One-Hour SO_2 Concentrations by Temperature 69

(Continued)

I N D E X O F F I G U R E S (Continued)

Figure		Page
44	Frequency Distribution of SCIM Calculated and Measured 24-Hour Concentrations for New York City Station #0	72
45	Frequency Distribution of SCIM Calculated and Measured 24-Hour Concentrations for New York City Station #1	72
46	Frequency Distribution of SCIM Calculated and Measured 24-Hour Concentrations for New York City Station #3	73
47	Frequency Distribution of SCIM Calculated and Measured 24-Hour Concentrations for New York City Station #10	73
48	Frequency Distribution of SCIM Calculated and Measured 24-Hour Concentrations for New York City Station #14	74
49	Frequency Distribution of SCIM Calculated and Measured 24-Hour Concentrations for New York City Station #17	74
50	Frequency Distribution of SCIM Calculated and Measured 24-Hour Concentrations for New York City Station #27	75
51	Frequency Distribution of SCIM Calculated and Measured 24-Hour Concentrations for New York City Station #28	75
52	Frequency Distribution of SCIM Calculated and Measured 24-Hour Concentrations for New York City Station #31	76
53	Frequency Distribution of SCIM Calculated and Measured 24-Hour Concentrations for New York City Station #36	76
54	Frequency Distribution of GHM Calculated and Measured 24-Hour SO_2 Concentrations for New York City Station #0	77
55	Frequency Distribution of GHM Calculated and Measured 24-Hour SO_2 Concentrations for New York City Station #1	77
56	The Frequency Distribution of 24-Hour SO_2 Concentrations for the Two Sets of GHM Calculations and Measured Values for New York City Station #3	78
57	The Frequency Distribution of 24-Hour SO_2 Concentrations for the Two Sets of GHM Calculations and Measured Values for New York City Station #10	78

(Continued)

INDEX OF FIGURES (Concluded)

Figure		Page
58	The Frequency Distribution of 24-Hour SO_2 Concentrations for the Two Sets of GHM Calculations and Measured Values for New York City Station #14	79
59	The Frequency Distribution of 24-Hour SO_2 Concentrations for the Two Sets of GHM Calculations and Measured Values for New York City Station #17	79
60	The Frequency Distribution of 24-Hour SO_2 Concentrations for the Two Sets of GHM Calculations and Measured Values for New York City Station #27	80
61	The Frequency Distribution of 24-Hour SO_2 Concentrations for the Two Sets of GHM Calculations and Measured Values for New York City Station #28	80
62	The Frequency Distribution of 24-Hour SO_2 Concentrations for the Two Sets of GHM Calculations and Measured Values for New York City Station #31	81
63	The Frequency Distribution of 24-Hour SO_2 Concentrations for the Two Sets of GHM Calculations and Measured Values for New York City Station #36	81

INDEX OF TABLES

Table		Page
1	Comparisons of Calculated Mean SO_2 Concentrations Using SCIM with St. Louis and Chicago Data Sets	35
2	Comparison Statistics for the Distribution of Calculated Hourly SO_2 Concentrations Using SCIM with St. Louis and Chicago Data Sets	37
3	Comparisons Between Calculated and Measured SO_2 Concentrations Using Mean and Variable Emission Rates in the CIGP Model	39
4	Variations in Mean Concentrations for Selected Classifications	41
5	Model-to-Measurement Comparisons of 1-Hour NYC SO_2 Concentrations by Mean, Standard Deviation, RMSE, MAE and Error at Maximum Measurement	61
6	Model-to-Measurement Comparisons of 1-Hour NYC SO_2 Concentrations by Correlation Coefficient, Variance and Regression Coefficients	62
7	Comparisons of 1-Hour SO_2 Concentrations by Hour of the Day and Day of the Week	65
8	Comparisons of 1-Hour SO_2 Concentrations by Temperature, Wind Speed and Stability Classes	66
9	Model-to-Measurement Comparisons of 24-Hour NYC SO_2 Concentrations by Mean, Standard Deviation, RMSE, MAE and Error at Maximum Measurement	82
10	Model-to-Measurement Comparisons of 24-Hour NYC SO_2 Concentrations by Correlation Coefficients, Variance and Regression Coefficients	83
11	Summary of Mean Error and RMSE Associated with Various Sampling Intervals for Proportionate Stratified Sampling in SCIM	86
12	Model Comparisons for Annual Mean SO_2 Concentrations Using New York City Data	88

(Continued)

INDEX OF TABLES (Concluded)

Table		Page
13	Model Comparisons for Annual Mean Particulate Concentrations Using New York City Data	90

Section 1.0

INTRODUCTION

This report describes the work accomplished during Phase I of a research program undertaken by GEOMET, Incorporated for the Environmental Protection Agency to further evaluate and document a Gaussian Plume Urban Diffusion Model. The analysis has concentrated on validation of a steady-state model which uses sampled chronological input data. The model was developed for EPA by GEOMET in previous work (Contract Number CPA 70-94).

The model has been compared with three other models (using the same data base). In future work it will be modified to improve its computational efficiency and to make it compatible with the Implementation Planning Program (IPP). Procedures for preparing emission and meteorological data for use in the model will also be enumerated and evaluated. The use of the statistical portion (Larsen transform) of the Air Quality Display Model (AQDM) and alternative procedures to estimate short-term maximum concentrations will be examined. EPA personnel will be trained to use the model, and a user's manual will be provided.

Section 2.0

MODELS

The models studied in this report include three variations of the multiple-source, Gaussian plume, meteorological diffusion model. Two of the models, the Air Quality Display Model (AQDM) and the Climatological Dispersion Model (CDM), are primarily designed to calculate long-term mean concentrations. The third model, developed by GEOMET under previous EPA sponsorship, is designed to calculate both the long-term mean concentration and the frequency distribution of short-term concentrations using selected chronological data. The frequency distribution is determined by concentrations calculated for a statistically selected set of short-term periods. Representative meteorological characteristics and simulated time-dependent emission characteristics are determined for each selected period. The other two models use mean emission characteristics and a specified set of combinations of meteorological characteristics (wind direction, wind speed and stability). To determine the long-term mean, the calculations for each combination of meteorological conditions are weighted by the relative frequency of occurrence of the combination.

In addition to the three Gaussian plume models, a simple model based on the work of Gifford and Hanna is included.

2.1 FEATURES OF THE MULTIPLE-SOURCE GAUSSIAN PLUME DIFFUSION MODEL

The details and assumptions involved in the development and use of the Gaussian plume model as applied to multiple point sources has been described by many authors (e.g., Calder 1970). They are briefly outlined here for convenient reference.

It is assumed that any long-term period may be represented by a series of quasi-steady-state periods during each of which the following "Gaussian plume" equation describes the concentration at a ground level receptor from an elevated point source.

$$\chi_p = \frac{Q}{\pi u \sigma_y(x)\sigma_z(x)} \exp\left\{- 1/2 \left[\left(\frac{h}{\sigma_z(x)}\right)^2 + \left(\frac{y}{\sigma_y(x)}\right)^2\right]\right\} \qquad (1)$$

where

χ_p = concentration at the receptor ($\mu g/m^3$)
Q = pollutant emission rate at the source ($\mu g/sec$)
u = wind speed (m/sec)
$\sigma_y(x)$ = horizontal diffusion parameter (m)
$\sigma_z(x)$ = vertical diffusion parameter (m)
h = effective height of the source (m)
y = crosswind distance between source and receptor (m)
x = downwind distance from source to receptor (m).

The above equation requires that the value of seven variables be known for each possible pair of source and receptor coordinates. The information requirements are greatly simplified by smoothing the point sources into an area source, since the variables of nearby sources are closely related. The concentration at a single receptor from all sources is

$$\chi_A = \frac{1}{\pi}\int_{0}^{x_d}\int_{y_1}^{y_2} \frac{q(x,y)}{u\sigma_y(x)\;\sigma_z(x)} \exp\left\{-\,1/2\left[\left(\frac{h}{\sigma_z(x)}\right)^2 + \left(\frac{y}{\sigma_y(x)}\right)^2\right]\right\} dy\,dx \quad (2$$

where

$q(x,y)$ = pollutant emission rate per unit area ($\mu g/sec/m^2$)

x_d = distance from receptor to upwind edge of the source area (m)

y_1, y_2 = crosswind distances from receptor to edges of the source area (m).

The largest point sources are judged to be sufficiently different from neighboring sources that they are generally treated independent of the integration procedure indicated above. The summation equation which is applicable to the three model variations treated in this report is

$$\chi = \sum_{i=1}^{N} (\chi_p)_i + \chi_A . \qquad (3)$$

If a long-term period is represented by M discrete quasi-steady-state conditions, the mean concentration over this period is simply the sum of M concentrations each weighted by the relative frequency of occurrence (f_j) of its corresponding steady-state conditions.

$$\overline{\chi} = \sum_{J=1}^{M} f_j\,\chi_j \qquad \text{where } \sum f_j = 1 \qquad (4)$$

It is also of interest to determine the maximum concentration which will occur during a single 3-hour or 24-hour period of a year. This problem is not directly approached in this report but will be a subject to be studied in the second phase of this program.

The six features of the multiple-source Gaussian plume diffusion model which vary in the model's variations studied in this report are:

- Method of defining quasi-steady-state conditions and their frequency of occurrence over a long-term period
- Method of performing the integration operation in Equation (2)
- Method of defining emission rates applicable to a quasi-steady-state period
- Method of estimating the effective source height
- Method of estimating σ_y and σ_z values
- Method of estimating wind speed for use in Equations (1) and (2).

2.1.1 The Sampled Chronological Input Model (SCIM)

The SCI Model is the more detailed of the three variations. The long-term period of interest is defined to be composed of a sequence of equal increment, quasi-steady-state periods of one hour duration. A sampling procedure is used which selects one hour from a specified sampling interval and guarantees that all hours of the day are equally represented in the selected sample. Calculations are made for the selected quasi-steady-state periods, each of which is characterized by a specific wind speed, wind direction, atmospheric stability class, and whatever parameters are required to characterize the time dependence of source emission rates (e.g., temperature, month of the year, hour of the day). The objective of this procedure is to minimize bias due to diurnal and seasonal variations in the model inputs, and to allow the long-term characteristics to be estimated by a reduced number of calculations. All selected quasi-steady-state concentrations are weighted equally in determining the long-term mean concentration.

The integration operation required to calculate concentrations from area sources is performed by using the "narrow plume" assumption. Mathematically, it requires that $\bar{q}(x)$ be defined such that

$$\frac{1}{\sigma_y(x)} \int_{y_1}^{y_2} q(x,y) \exp\left\{-\left[1/2 \frac{y}{\sigma_y(x)}\right]^2\right\} dy = \sqrt{2\pi}\,\bar{q}(x). \qquad (5)$$

This will be generally true as long as the spatial distances between variations in area-source emission rates $q(x,y)$ are large compared to the horizontal diffusion parameters $\sigma_y(x)$. It is assumed that

$$\bar{q}(x) \approx q(x,o). \qquad (6)$$

As a result, Equation (2) becomes

$$\chi_A = \sqrt{\frac{2}{\pi}} \int_0^{x_d} \frac{\bar{q}(x)}{u\sigma_z(x)} \exp\left\{-\,1/2\left[\frac{h}{\sigma_z(x)}\right]^2\right\} dx\,. \qquad (7)$$

This equation may be evaluated by use of the trapezoid rule.*

---

* A slight variation of the trapezoid rule is being used in which small increments in x are gradually increased with increasing x to a uniform increment. This allows the larger variations in the integrand which tend to occur with small, rather than large x, to be more accurately evaluated.

The following equations are used to estimate emission rates for New York City area sources as a function of temperature and hour of the day.

$$\left.\begin{array}{ll} q = q_A \left[A_i + B_i \left(T_i - T\right)\right] & T < T_i \\ q = q_A A_i & T \geq T_i \end{array}\right\} \qquad (8)$$

where

q = area source emission rate for ith hour of the day with temperature T (μg/sec/m^2)

q_A = annual mean area source emission rate (μg/sec/m^2)

A_i, B_i, T_i = empirical parameters for ith hour of the day

T = temperature (°F).

If sufficient data are available, point source emissions may be generated for each hour using a special algorithm. Otherwise, they are treated as constant. For New York City, all point sources were treated as having a constant emission rate. A description of algorithms used for estimating emissions for St. Louis and Chicago was previously reported by Koch and Thayer (1971).

Plume rise for point sources is estimated using the following equations adapted from Briggs (1969). For stable conditions (Turner-Pasquill stability class 5),

$$\Delta H = 2.9 \left(\frac{F\, T_a}{0.03034\, u} \right)^{0.33} \qquad (9)$$

where

ΔH = plume rise (m)

T_a = ambient air temperature (°K)

u = wind speed at stack height (m/sec)

$$F = 2.45 \left(1 - \frac{T_a}{T_s}\right) V_s D_s^2 \qquad (10)$$

where

T_s = stack gas temperature (°K)

V_s = stack gas exit speed (m/sec)

D_s = stack diameter (m) .

For neutral and unstable conditions (Turner-Pasquill stability classes 1 through 4),

$$\Delta H = \frac{3.75\ F^{0.33}\ X^{0.67}}{u} \qquad (11)$$

where

$$X = \begin{Bmatrix} 2.16F^{0.4}\ H^{0.6}, & H \leq 305 \\ 67.3F^{0.4} & , H > 305 \end{Bmatrix} \qquad (12)$$

H = stack height (m) .

The effective source height is

$$h = H + \Delta H. \qquad (13)$$

The integration in Equation (7) is repeated over three effective area source heights. For New York City, the area source emission rates are assigned a height as follows:

Assigned Height (m)	IPP Emission Inventory Reported Height (m)
15	10.0 to 20.1
30	25.0 to 39.9
70	50.0 to 100.0

Estimates of σ_y and σ_z are based on curves published by McElroy (1969) for the Turner-Pasquill stability classes. The curves were extrapolated to distances less than 100 m using the Pasquill-Gifford curves as a guide as previously described by Koch and Thayer (1971). The σ_z values are also modified to accommodate the influence of the mixing layer ceiling as described by Koch and Thayer (1971).

Wind speeds are determined as a function of effective height h as follows:

$$u = u_1 \left(\frac{h}{h_1} \right)^k \qquad (14)$$

where

u_1 = reported wind speed (m/sec)
h_1 = observing height (m)
k = wind profile parameter.

For New York City, k was assigned the following values on the basis of the Turner-Pasquill stability class:

Turner-Pasquill Stability Class	k
1, 2, or 3	0.1
4	0.15
5	0.2

The selection of these values was governed by the results of a previous analysis over New York City (Singer et al. 1970).

2.1.2 The Climatological Dispersion Model

The Climatological Dispersion Model (CDM) was developed as a revised form of a model first proposed by Martin and Tikvart (1968). The model, described in detail by Calder (1971), is similar to the Air Quality Display Model (Section 2.1.3) in the way quasi-steady-states are defined to estimate a long-term mean. There are 576 quasi-steady-state conditions defined by six stability classes, six wind speed classes, and 16 wind direction classes. Each combination is weighted by its relative frequency of occurrence in calculating the long-term mean.

Calder (1971) has shown that the evaluation of Equations (1) through (4) can be greatly simplified by applying the narrow plume assumption to both point and area sources in a slightly different form than presented above for the SCIM. For point sources, the assumption implies that the computations for the contributions of a point source to a receptor location need only consider wind direction class inputs which include the direction from the source to the receptor.

$$(\bar{x}_p)_i = \frac{1}{\theta_k}\left(\frac{Q_i}{X_i}\right)\sum_{j=1}^{N_i} f_j \, S(X_i, h_i ;\, u_j, P_j) \qquad (15)$$

where

$(\bar{x}_p)_i$ = mean concentration at a receptor due to the ith point source ($\mu g/m^3$)

Q_i = source emission rate (μg/sec)

$\theta_k = \frac{2\pi}{N_k}$ = angular width of wind direction class for which the N_i input combinations are defined (radians)

N_k = number of equal wind direction classes

X_i = distance from source to receptor (m)

N_i = number of input combinations defined for direction θ_i (direction from source to receptor)

f_j = relative frequency of occurrence of jth combination of wind speed and stability classes

$$\left.\begin{aligned} S(X_i, h_i; u_j, P_j) &= \sqrt{\frac{2}{\pi}}\left[\frac{1}{u_j \sigma_z(X_i, P_j)}\right] \exp\left\{-1/2\left[\frac{h_i^2}{\sigma_z(X_i, P_j)}\right]^2\right\} \quad (X_i \le X_L) \\ &= \frac{1}{u_j L_j}, \qquad (X_i \ge 2X_L) \end{aligned}\right\} \qquad (16)$$

where

X_L = distance such that $\sigma_z(X_L, P_j) = 0.47L_j$

L_j = mixing ceiling attributed to jth input combination (m)

P_j = stability class for jth input combination

u_j = wind speed for jth input combination.

Linear interpolation is used between X_L and $2X_L$. Equation (16) permits the effect of the mixing layer depth to be treated in a form recommended by Pasquill. This effect is treated in the SCIM by modifying σ_z.

For area sources, the computation for each set of inputs is equivalent to the SCIM except that $\overline{q}(x)$ is defined:

$$\overline{q}(x) = \frac{1}{22.5} \int_{\theta_i - \theta_k/2}^{\theta_i + \theta_k/2} q(x,\theta)\, d\theta \qquad (17)$$

where

$q(x,\theta)$ = area source emission rate

θ_i = median wind direction of class containing direction from source to receptor.

The integral is evaluated by the trapezoid rule using an increment of 22.5° for θ. The integrals indicated by Equation (2) are then evaluated using Equation (7) and the trapezoid rule using an increment of 100 m for X. The model was applied with θ_k equal to 22.5° corresponding to 16 equal wind direction classes.

A uniform effective area source height is assumed. Plume rise for point sources is estimated by the Briggs equations as follows:

- For stable conditions (Turner-Pasquill stability class 5),

$$x_f = 1.00323\, u \left(\frac{T_a}{\partial\theta/\partial z} \right)^{0.5}$$

where

x_f = distance to final rise, m

u = wind speed at stack level, m/sec

T_a = ambient air temperature, °K

$\frac{\partial\theta}{\partial z}$ = vertical potential temperature gradient, °K/m

$$= \begin{cases} 0.02, \text{ Pasquill Category E} \\ 0.035, \text{ Pasquill Category F} \end{cases}$$

(1) Distance from source to receptor < x_f,

$$\Delta H = \frac{1.6\, F^{1/3}\, x^{2/3}}{u}$$

where F is given by Equation (10)

x = distance from source to receptor

(2) Distance from source to receptor $\geq x_f$, use minimum of ΔH_1 and ΔH_2,

$$\Delta H_1 = 2.4 \left[\frac{T_a F}{9.80616\, \mu \left(\frac{\partial\theta}{\partial z} \right)} \right]^{1/3}$$

$$\Delta H_2 = 5F^{1/4} \left[\frac{9.80616}{T_a} \left(\frac{\partial\theta}{\partial z} \right) \right]^{-3/8}$$

- For neutral and stable conditions (Turner-Pasquill stability classes 1, 2, 3, and 4),

$$\Delta H = \begin{cases} \dfrac{1.6\ F^{1/3}\ x^{2/3}}{\mu}, & x < 3.5\ X^* \\ \dfrac{1.6\ F^{1/3}\ (3.5\ X^*)^{2/3}}{\mu}, & x \geq 3.5\ X^* \end{cases}$$

$$\text{where } X^* = \begin{cases} 14\ F^{5/8}, & F < 55 \\ 34\ F^{2/5}, & F \geq 55. \end{cases}$$

The diffusion parameter σ_z is calculated as power functions of distance using stability dependent parameters a, b, and c. The functions are based on the Pasquill-Gifford values, but the stability classes are modified to characterize an urban atmosphere. The stability classes are defined using the Turner-Pasquill rules as in the SCIM. During daytime hours, the assigned stability class is made one class more unstable (except the most unstable class); during nighttime hours, when the most stable class occurs, one class less stable is assigned. As a result, only four stability classes are used. The σ_z values are further modified using the virtual source concept with an assumed initial value of 30 m for sources with an effective height of 20 m or less. The initial value is decreased linearly with increasing source height to zero for effective heights which exceed 50 m.

The mixing layer depth is treated as a function of stability. The neutral stability class is subdivided into day and night subclasses. The height is determined as follows:

Stability Class*	Mixing Layer Depth (L)
Very unstable (1)	1.5 Times Mean Afternoon Maximum
Unstable (2)	Mean Afternoon Maximum
Slightly Unstable (3)	Mean Afternoon Maximum
Day, Neutral (4)	Mean Afternoon Maximum
Night, Neutral (4)	0.5 Times (Mean Afternoon Maximum plus 100 m)
Stable (5)	100 m

* Numbers in parenthesis indicate Turner-Pasquill stability class.

The wind speeds are determined for each source as a function of the effective source height using a wind profile power law as in the SCIM.

2.1.3 The Air Quality Display Model

The Air Quality Display Model (AQDM) is based more directly on the ideas of Martin and Tikvart than the preceding CDM. It was implemented for EPA as a component of an air quality planning tool known as the Implementation Planning Program (IPP) by the TRW Systems Group (1969). In this model, the quasi-steady-states used to determine a long-term mean are defined by 480 combinations of 16 wind direction classes, six wind speed classes, and five stability classes for which the joint frequency distribution is known. A mean value is assigned for each class and the calculations for each combination are averaged by weighting them by their relative frequency of occurrence.

The concentrations from area sources, Equation (2), are evaluated by subdividing the area into grid squares (not necessarily of equal size) and replacing each grid square by a virtual point source. The virtual point source definition which is employed is:

$$X_o = \frac{\sqrt{A'}}{2 \tan (11.25°)} \tag{18}$$

where

X_o = virtual distance (m)

A' = area of an area source grid square lying within a 22.5° sector upwind of the receptor (m^2).

The distance from the source to the receptor is assumed to be $X_o + X_i$ which replaces X_i in Equation (15). However, the σ_z values in Equation (16) are evaluated using X_i. Equation (15) is used to evaluate the contributions from point and area sources. An additional modification of Equation (15) is used to associate each source with the two neighboring wind direction classes whose medians (θ_k and θ_{k+1}) define an interval which includes the direction (θ) from the source to the receptor. The emission rate Q_i in Equation (15) is multiplied by

$$\frac{\theta_{k+1} - \theta}{\theta_{k+1} - \theta_k} \text{ and } \frac{\theta - \theta_k}{\theta_{k+1} - \theta_k}$$

for use with wind classes k and k+1, respectively. For area source grid squares, Q_i is reduced by multiplying by A'/A where A is the area of the grid square and A' is defined above.

Emission rates are treated as constant. For point sources, the plume rise is estimated by a stability dependent modification of Holland's equation.

$$\Delta h = \frac{VD}{u}\left[1.5 + 0.00268\ PD\left(\frac{T_s - T_a}{T_s}\right)\right](1.4 - 0.1\ S) \qquad (19)$$

where

Δh = plume rise (m)
V = stack gas exit speed (m/sec)
D = stack exit diameter (m)
u = wind speed (m/sec)
P = atmospheric pressure (mb)
T_s = stack gas exit temperature (°K)
T_a = atmospheric temperature (°K)
S = Turner-Pasquill stability class (1 to 5).

Since the area source is represented by a set of points, one for each grid square, an area source height may be defined for each area grid square.

The σ_z values are determined by functions which were fitted to the Pasquill-Gifford curves as for CDM. The Turner (1964) definitions of the stability classes are used except that class 4 values are used for class 5 occurrences. Mixing layer depths are defined by stability class as in CDM, except that class 4 is not subdivided. Instead, three-fifths of the class 4 stability occurrences are treated as having the daytime class 4 depth and two-fifths as having the nighttime class 4 depth.

No vertical variation in wind speed is computed as with SCIM and CDM.

2.2 THE SIMPLIFIED GIFFORD-HANNA MODEL

A simple model was selected to compare with the three variations of the Gaussian plume model. The simplified version of the Gifford-Hanna model recently described by Hanna (1971) was used for this purpose. The model is

$$\chi = C \frac{Q}{u} \tag{20}$$

where

χ = concentration at a receptor location ($\mu g/m^3$)
Q = area source strength surrounding the receptor ($\mu g/m^2/sec$)
u = wind speed (m/sec)
C = dimensionless constant.

Recently, Gifford (1972) recommended the following values for C:

Atmospheric Stability	C
Stable	600
Neutral	200
Unstable	50

For a long period, a value of 225 was recommended. The constant C is related to other parameters in the original Gifford-Hanna model as follows

$$C = \sqrt{\frac{2}{\pi}} \left(\frac{2N+1}{2} \Delta X\right)^{1-b} \frac{1}{a(1-b)} \tag{21}$$

where

N = number of grid squares (ΔX on a side) from receptor to edge of area source

a,b = parameters of the vertical diffusion function (σ_z) of the Gaussian plume equation

$\sigma_z = aX^b$.

Empirical estimates of C were reported by Gifford and Hanna (1973) based on particulate and SO_2 data for 44 U.S. cities. The estimates were based on long-term mean concentrations. For particulates, the empirical constant ranged from a low of 57 to a high of 634. The mean value was 219. The estimates of C reported for SO_2 data varied from 7 to 218 with a mean of 50. Gifford and Hanna suggested that the lower values for SO_2 result from the large fraction of SO_2 emitted by tall stacks. The validation analysis in this study used C = 50 for SO_2 emissions and C = 225 for particular emissions, for both long- and short-term concentrations. No attempt was made to further relate C to stability conditions.

Methods of estimating Q from emission inventory data are discussed and compared in Appendix C. The method used in comparisons with other models was the following:

1. Determine annual emissions applicable to 1 km squares.
2. For each receptor location, get the average emission rate for s^2 1 km squares centered on each receptor location, as required by the criteria below.

Pollutant	Criteria (ton/km^2/day)(1)	Use $Q = Q_s^*$ where s is
SO_2	(a) $Q_9^* > 0.701$ and $Q_{37}^* > 0.512$	9 km
	(b) $Q_9^* < 0.701$ and $Q_{37}^* < 0.512$	37 km
	(c) Neither (a) nor (b)	31 km
Particulates	(a) $Q_3^* > 0.128$ and $Q_{28}^* > 0.082$	3 km
	(b) $Q_3^* < 0.128$ and $Q_{28}^* < 0.082$	39 km
	(c) Neither (a) nor (b)	19 km

(1) Q_s^* is the average emission rate from the s^2 grid squares whose center grid square contains the receptor (s must be an odd integer).

It should be noted that the grid size criteria were developed by correlating the effective emission rate for different grid sizes with SO_2 measurements which were later used in the validation study. This results in an advantage to the Gifford-Hanna model over other model results used in this study.

The wind speed used in this model is based on the same input as that used in the other models, the three-hourly airport observation measured at LaGuardia Airport. However, the wind speed was assumed constant with height.

Section 3.0

MODEL COMPARISONS

Calculations using the four models described in Section 2.0 have been compared against each other and against measured values. Each model was run in its normal mode. In addition, certain simplifications were made by averaging the inputs used for the model. The model comparisons which follow include consideration of 10 different variations of models and inputs.

Two model comparison tasks were carried out. The first task was to compare calculations for SCIM which were obtained in a preceding program (Contract No. CPA 70-94, "Validity and Sensitivity of the Gaussian Plume Urban Diffusion Model") with calculations made using the same model and data set, except that mean rather than time-dependent emission rates were used for all sources. These calculations involved a 3-month data period for St. Louis and a 1-month data period for Chicago, for sulfur dioxide emissions.

The second task was to compare 10 different combinations of variations in input and model with each other and with measured values using a 1-year data set for New York City. The comparisons include 3-hourly, 24-hourly, and annual concentrations of sulfur dioxide emissions, and annual concentrations of particulate matter emissions.

3.1 COMPARISONS BETWEEN CALCULATIONS USING MEAN AND VARIABLE EMISSION RATES FOR SCIM

Calculations of SO_2 concentrations made with the SCIM were previously compared with measurements obtained for a 1-month period in

Chicago and a 3-month period in St. Louis. In these calculations emission rates were varied from hour to hour as a function of production and other activity factors and temperature-dependent space heating requirements. A new corresponding set of calculations has been made using the same model inputs for each hour except for the emission rates. At each location (St. Louis and Chicago) a new emission rate was computed for each source by taking the mean of the values attributed to each hour of the data period. The previously obtained calculations are referred to as variable Q calculations; the new calculations, mean Q calculations.

The St. Louis data set consists of hourly estimates of source strengths, source height, and meteorological conditions for an 89-day period (December 1, 1964 to February 28, 1965). The data includes SO_2 emission rates for 1200 squares (5000 ft on a side) and 51 stacks. Hourly estimates of wind speed and direction are the vector average of measurements from the three wind measuring stations and the TV tower shown in Figure 1. The Pasquill-Turner stability classification is based on hourly airport observations reported by Lambert Field (Figure 1). A wind profile power law is included based on measurements from three heights on the TV tower. The mixing layer depth for each hour is based on hourly interpolation of the mean layer depth estimated from 00Z and 12Z radiosonde soundings for Columbia, Missouri and Peoria, Illinois. More details concerning the data set are given in a previous report (Koch and Thayer 1971). Measured 2-hour SO_2 concentrations are included for 10 locations (Figure 1). As a result, two corresponding hourly calculations for each location must be averaged to compare with the measured concentrations. The cumulative

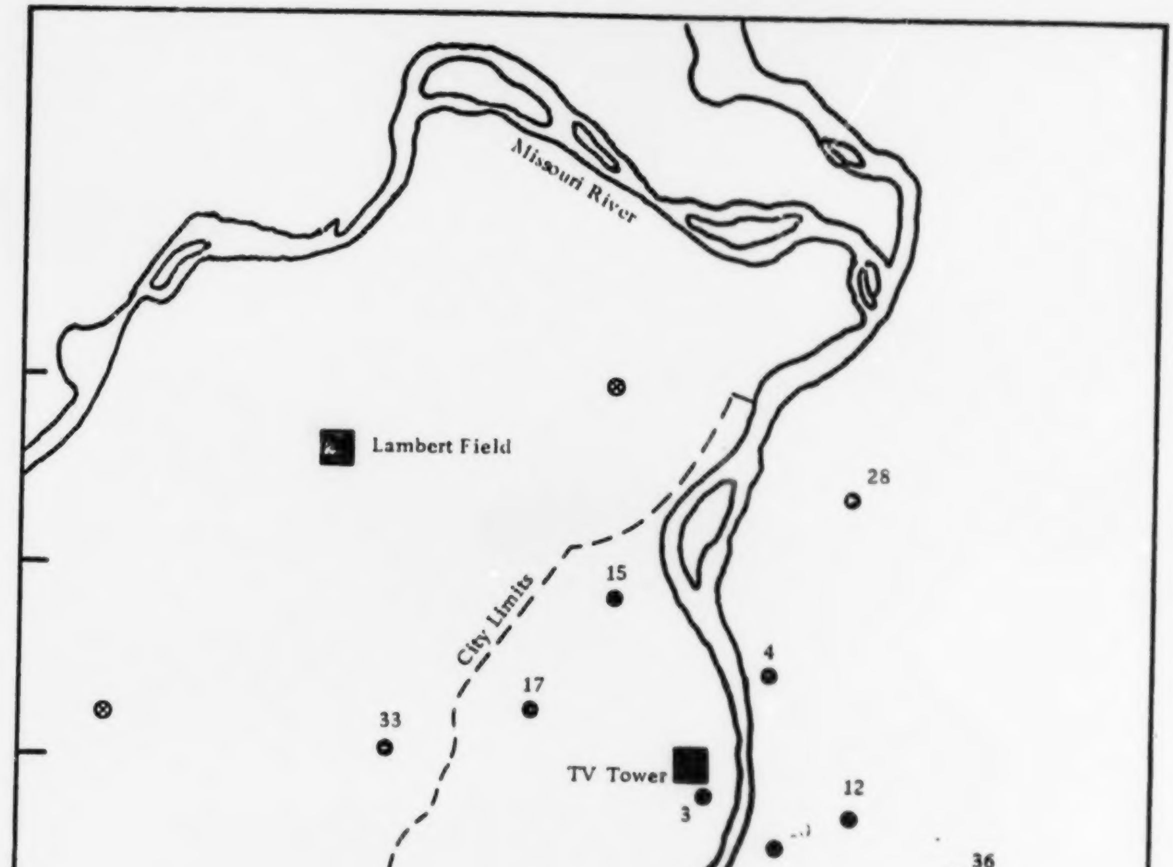

Figure 1. Location of St. Louis Observing Stations Used in Validation Analysis

frequency distribution of calculated (mean Q and variable Q) and measured 2-hour concentrations of SO_2 for each receptor location are shown in Figures 2 through 11.

The Chicago data sets consists of hourly estimates of inputs similar to the St. Louis data set for the period January 1 to 31, 1967. However, the SO_2 emission rates include three estimates for each of 600 squares (1 mile on a side) and one estimate for each of 85 stacks. The wind speed and direction are the vector average of eight measurements (one at each TAM location in Figure 12). The Pasquill-Turner stability classification is based on hourly airport observations at Midway Airport (Figure 12). The wind profile power law is determined as a function of the stability classification. The mixing layer depth is derived from radiosonde soundings for Green Bay, Wisconsin and Peoria, Illinois. Measured 1-hour SO_2 concentrations are included for eight locations shown in Figure 12. The cumulative frequency distribution of calculated (mean Q and variable Q) and measured 1-hour concentrations of SO_2 for each receptor location are shown in Figures 13 through 20.

3.1.1 Model-To-Model Comparisons

Tests were made to determine if the mean and frequency distribution of SO_2 concentrations calculated for a receptor location are significantly different between using mean Q and variable Q inputs. Comparison results for calculated mean values are shown in Table 1. The principal result to be noted in Table 1 is that at all of the eight Chicago stations and 8 of the 10 St. Louis stations, the difference in the two means

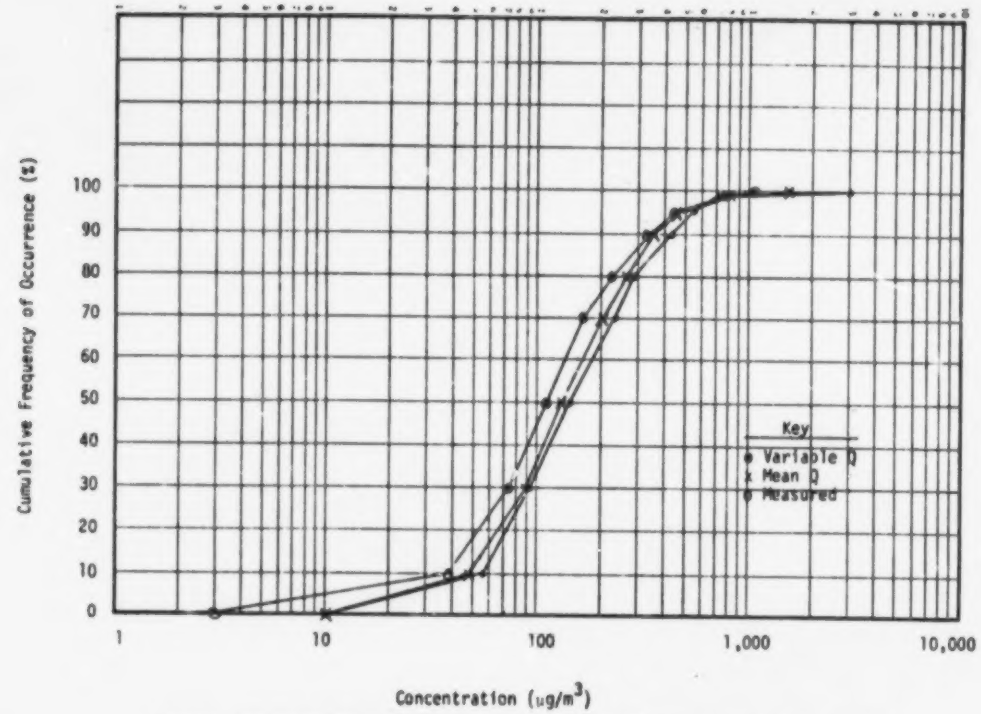

Figure 2. Frequency Distribution of Calculated and Measured Two-Hour Concentrations for St. Louis Station #13

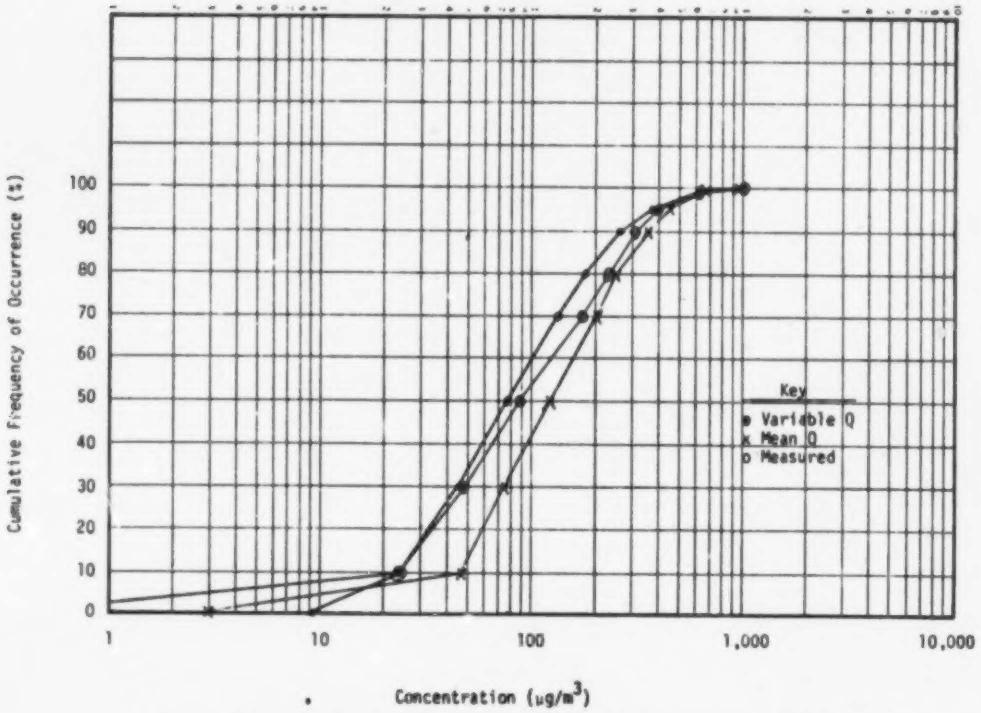

Figure 3. Frequency Distribution of Calculated and Measured Two-Hour Concentrations for St. Louis Station #15

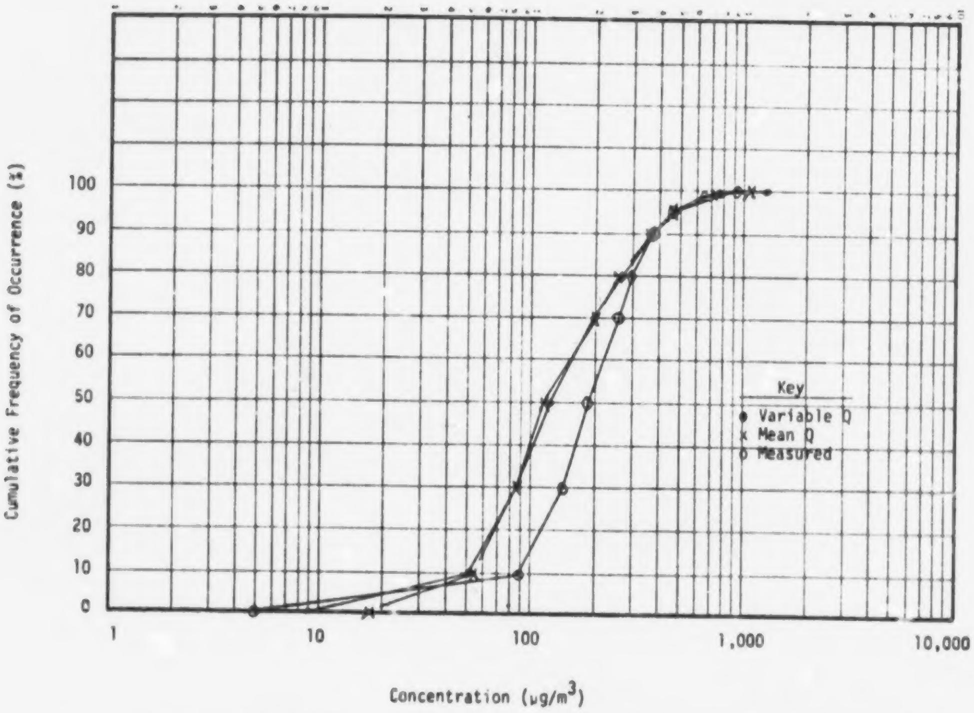

Figure 4. Frequency Distribution of Calculated and Measured Two-Hour Concentrations for St. Louis Station #17

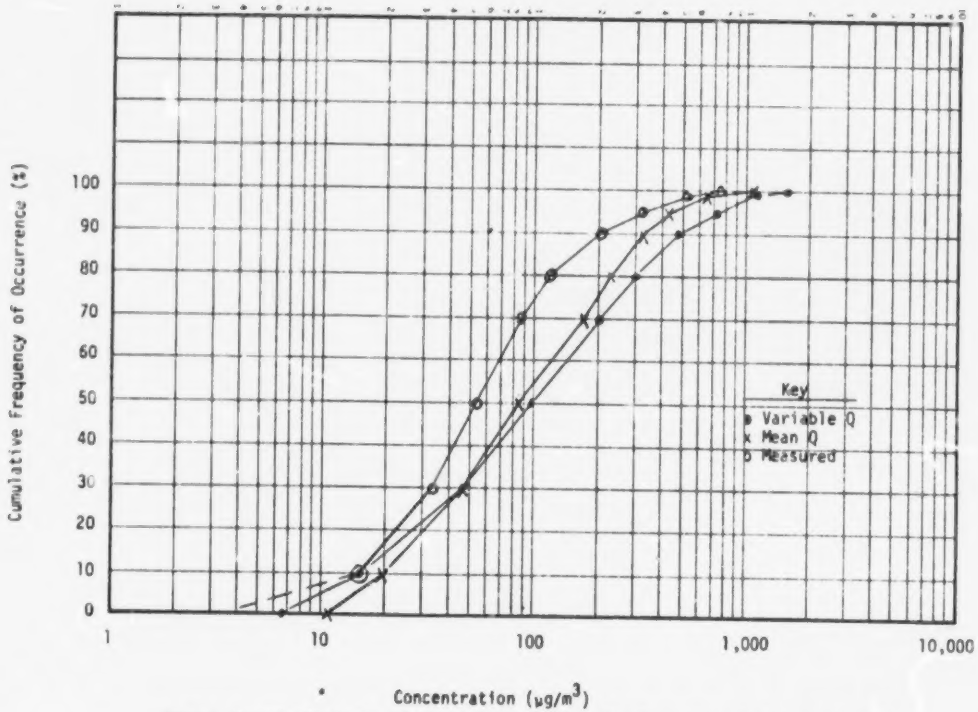

Figure 5. Frequency Distribution of Calculated and Measured Two-Hour Concentrations for St. Louis Station #23

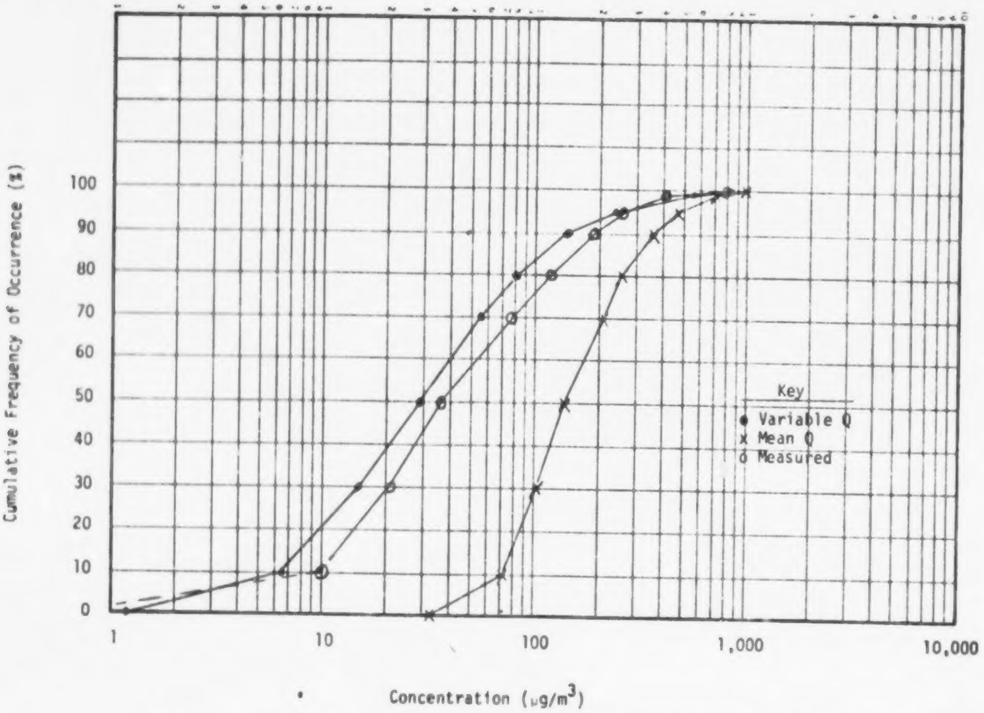

Figure 6. Frequency Distribution of Calculated and Measured Two-Hour Concentrations for St. Louis Station #33

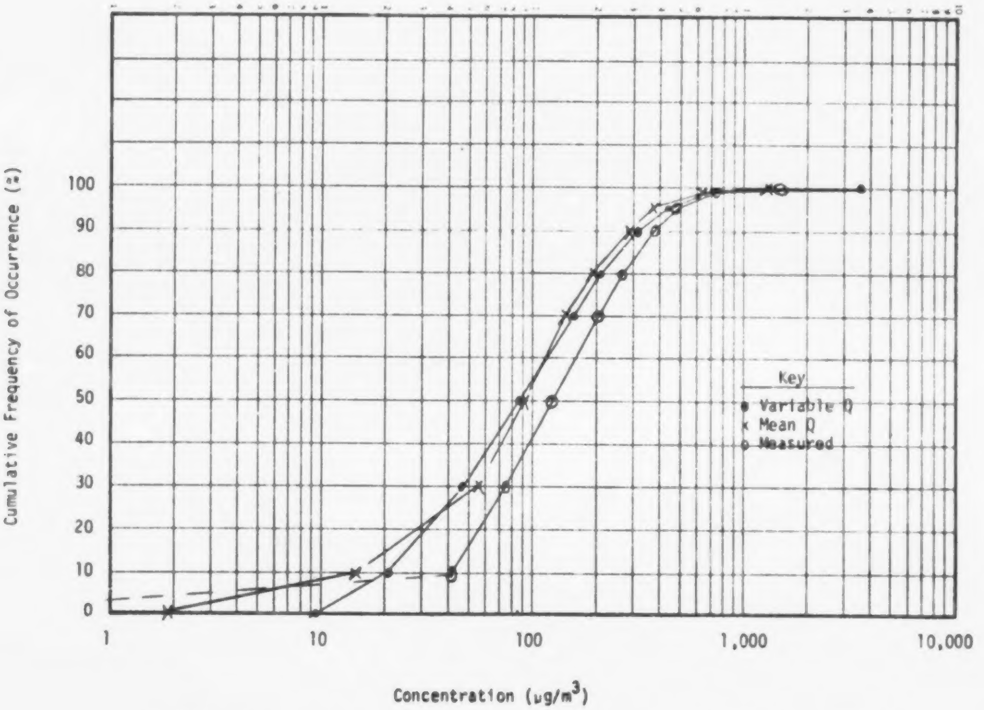

Figure 7. Frequency Distribution of Calculated and Measured Two-Hour Concentrations for St. Louis Station #4

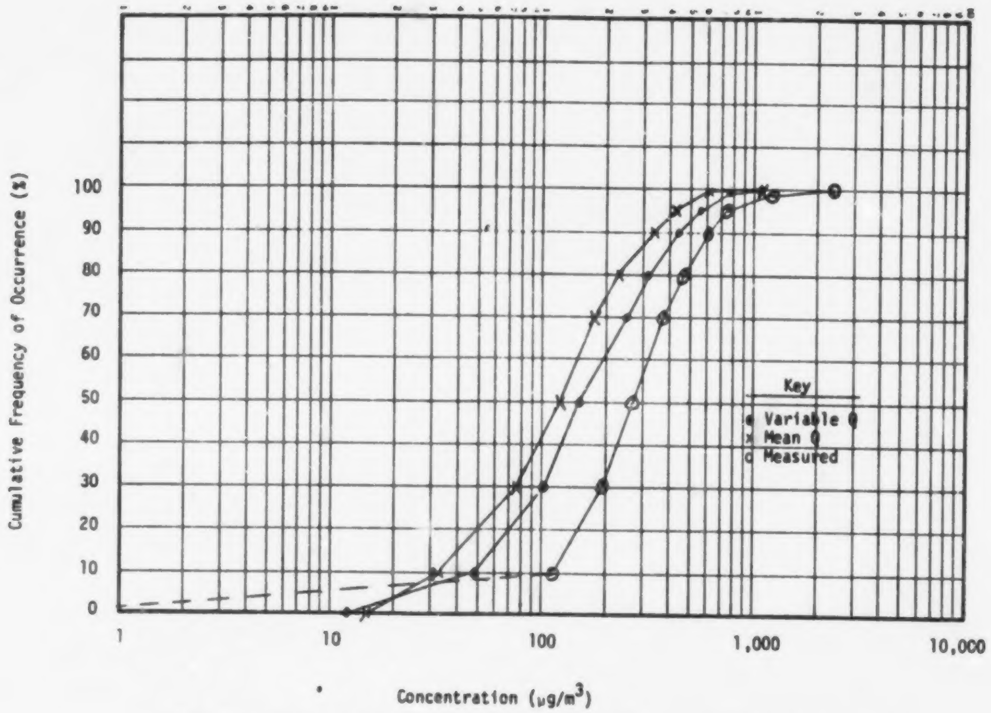

Figure 8. Frequency Distribution of Calculated and Measured Two-Hour Concentrations for St. Louis Station #10

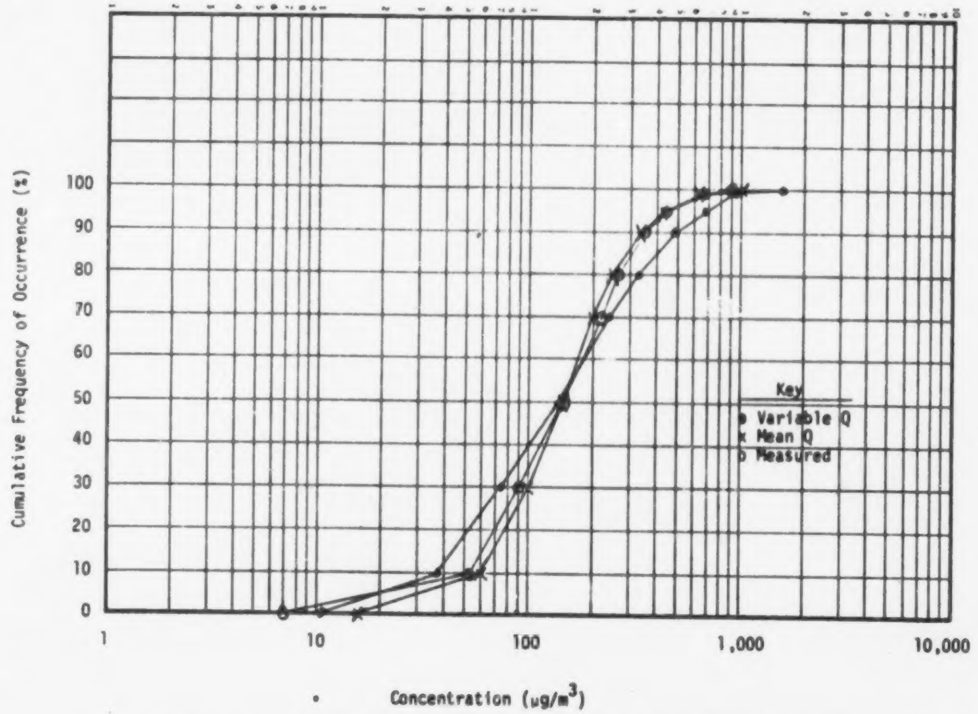

Figure 9. Frequency Distribution of Calculated and Measured Two-Hour Concentrations for St. Louis Station #12

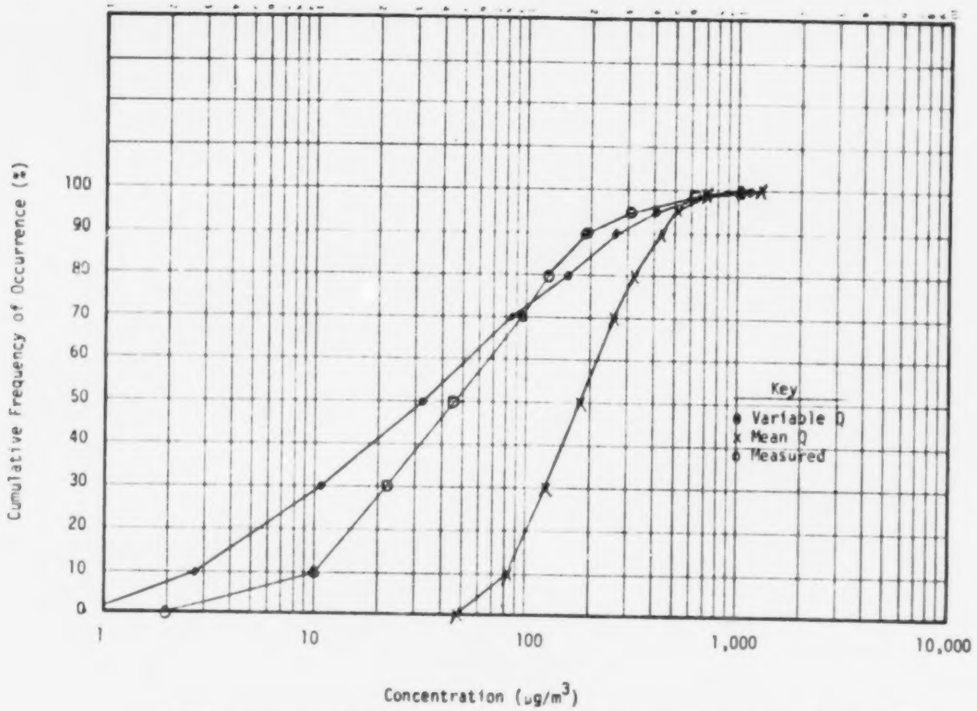

Figure 10. Frequency Distribution of Calculated and Measured Two-Hour Concentrations for St. Louis Station #28

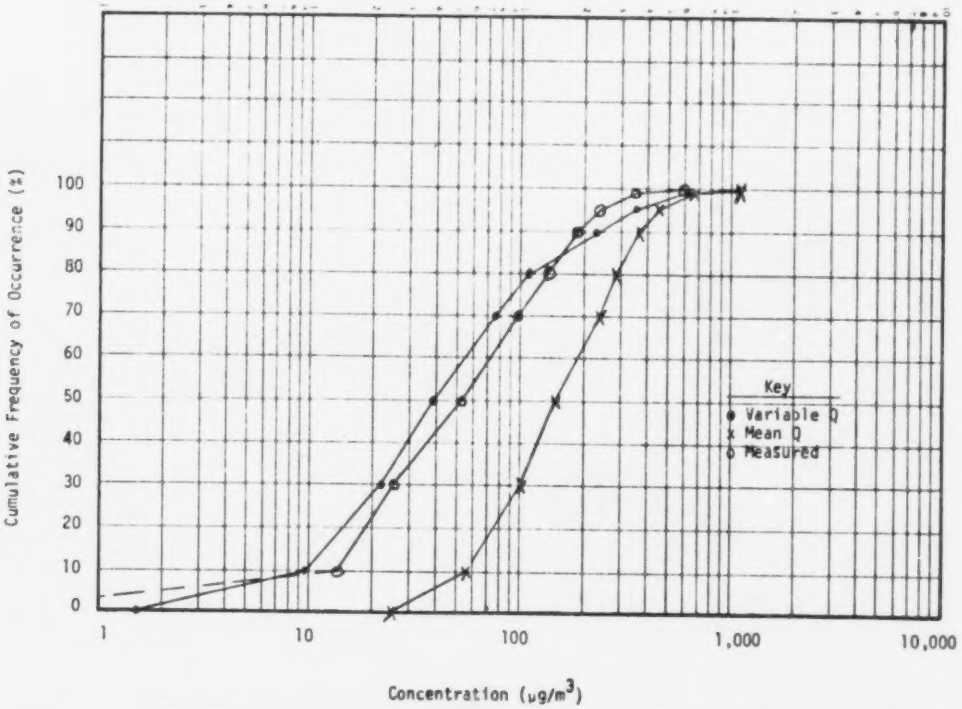

Figure 11. Frequency Distribution of Calculated and Measured Two-Hour Concentrations for St. Louis Station #36

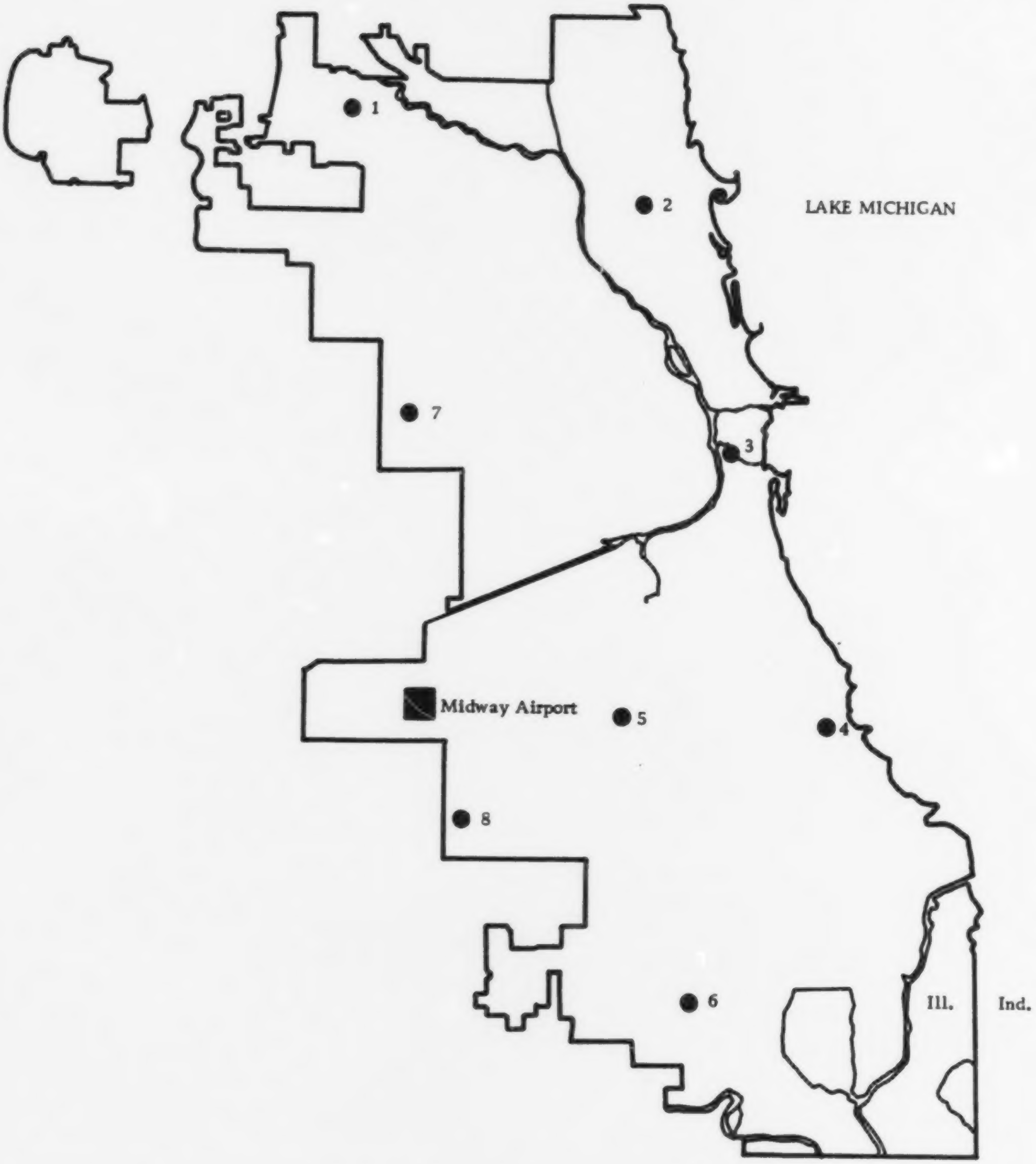

Figure 12. Location of Chicago TAM Stations Used in Validation Analysis

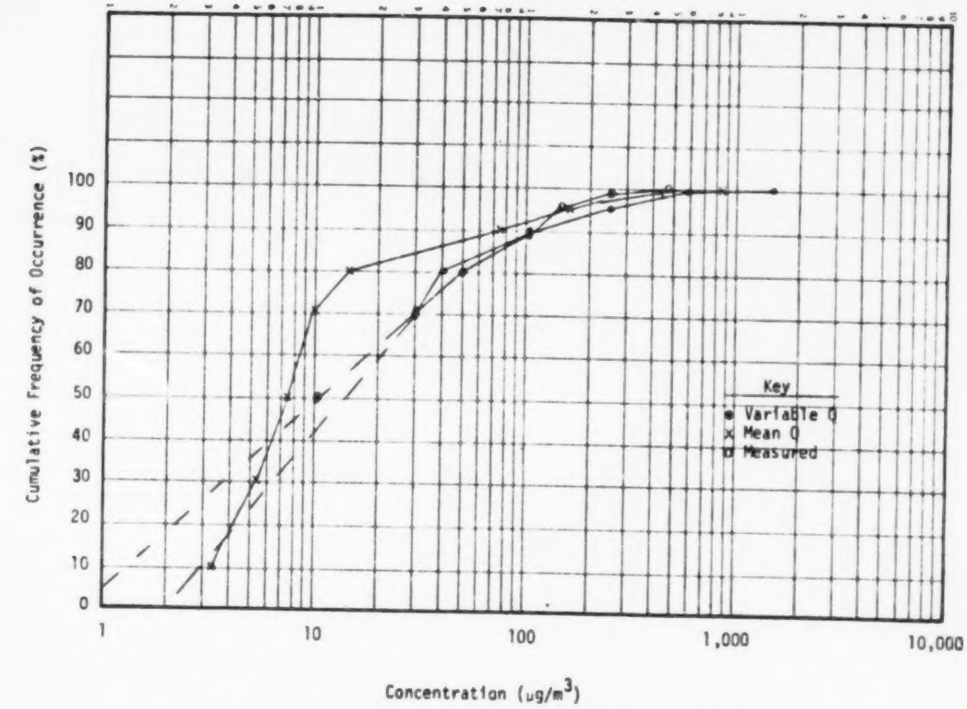

Figure 13. Frequency Distribution of Calculated and Measured One-Hour Concentrations for Chicago TAM #1

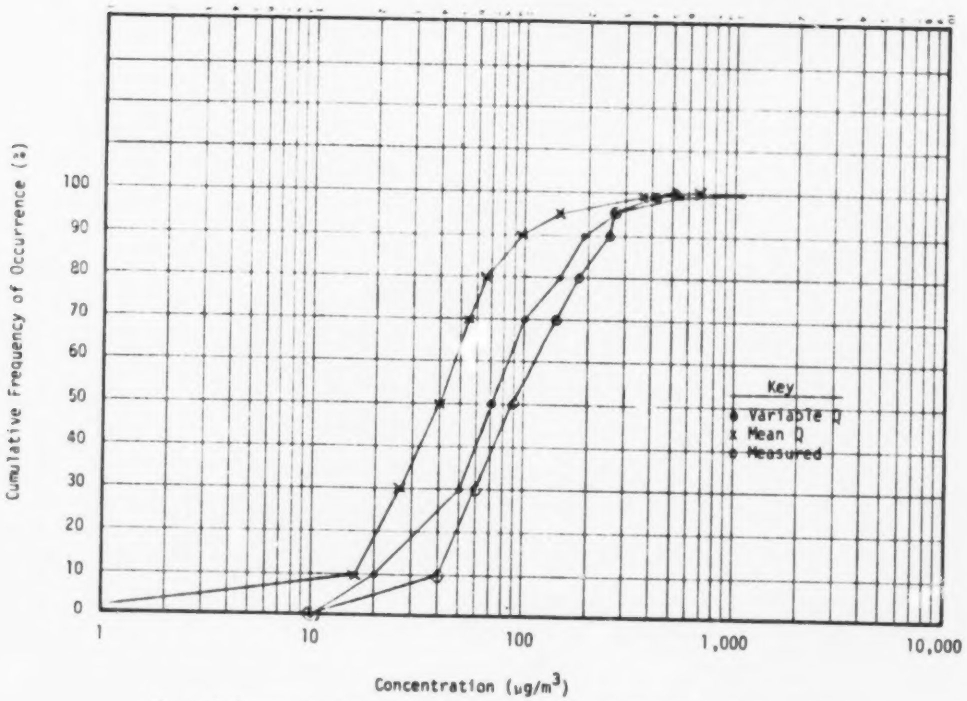

Figure 14. Frequency Distribution of Calculated and Measured One-Hour Concentrations for Chicago TAM #2

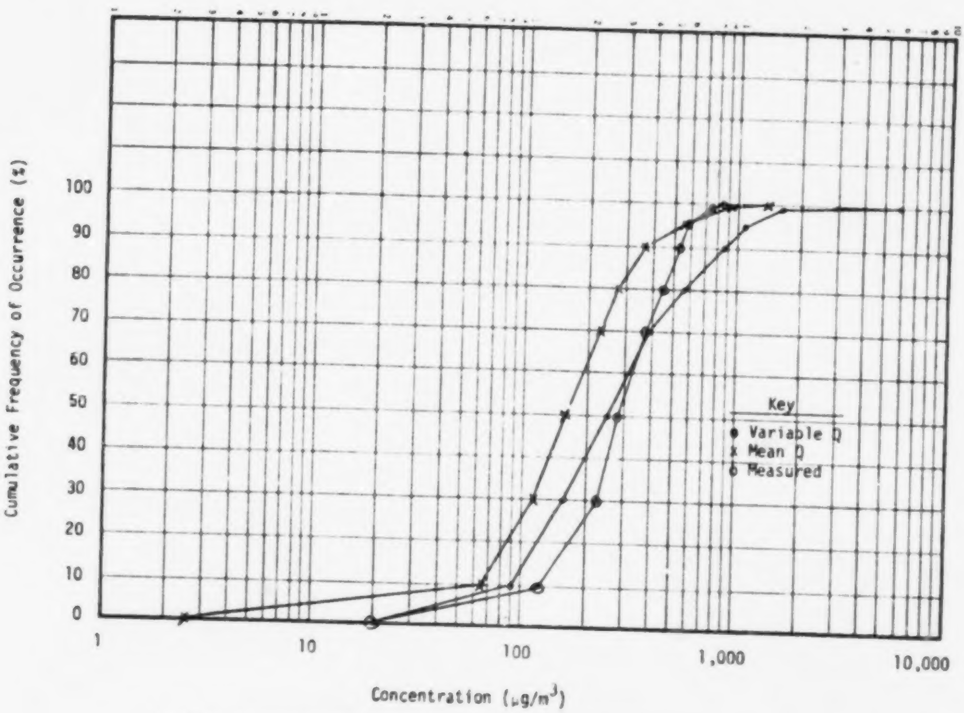

Figure 15. Frequency Distribution of Calculated and Measured One-Hour Concentrations for Chicago TAM #3

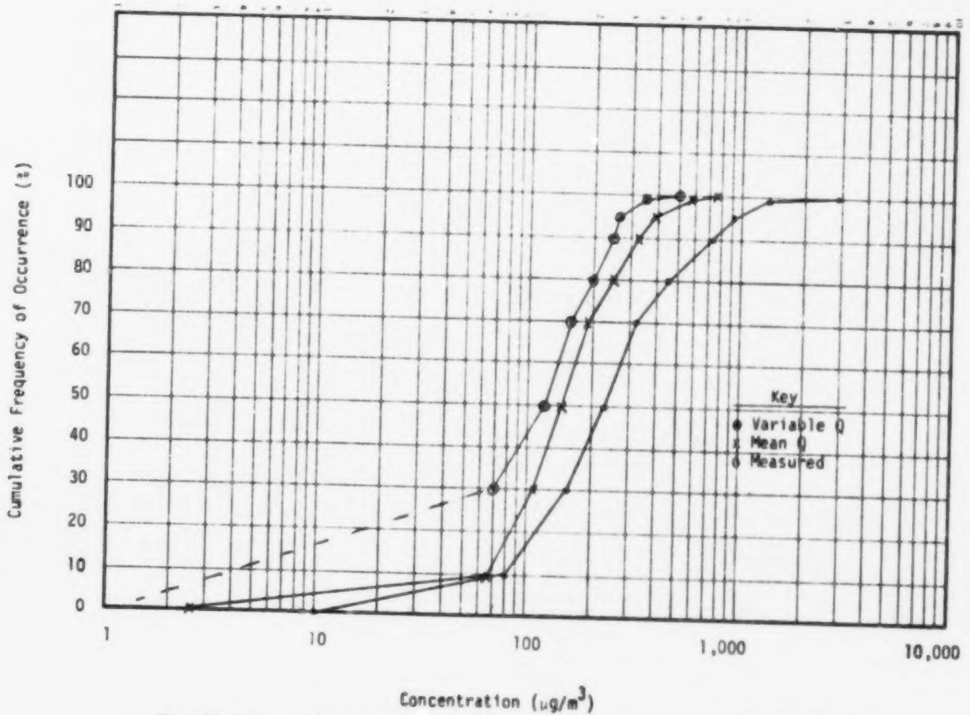

Figure 16. Frequency Distribution of Calculated and Measured One-Hour Concentrations for Chicago TAM #4

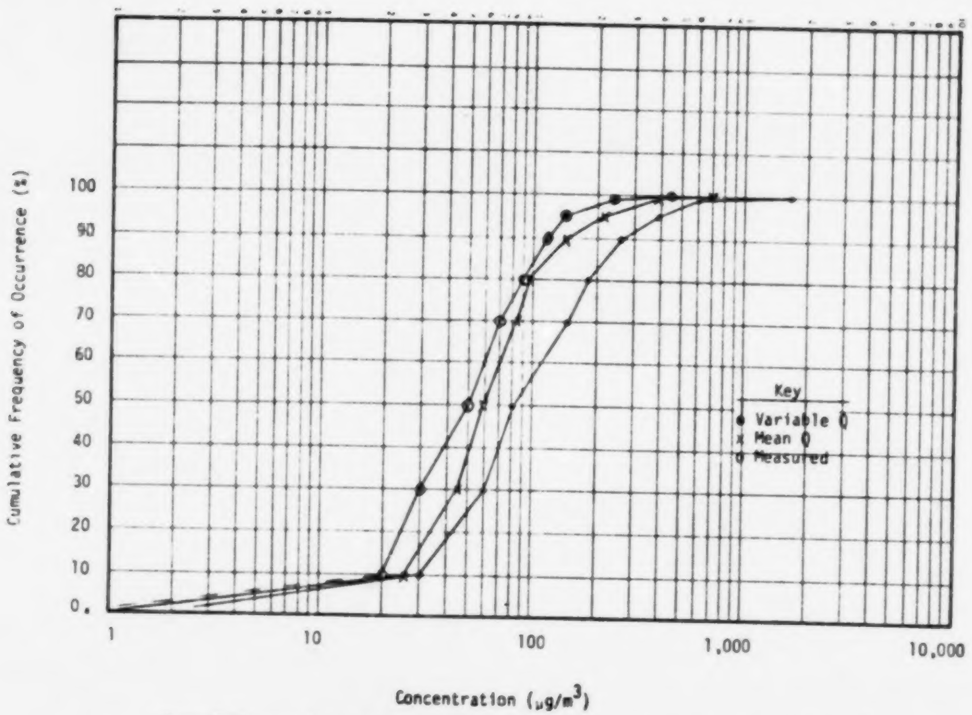

Figure 17. Frequency Distribution of Calculated and Measured One-Hour Concentrations for Chicago TAM #5

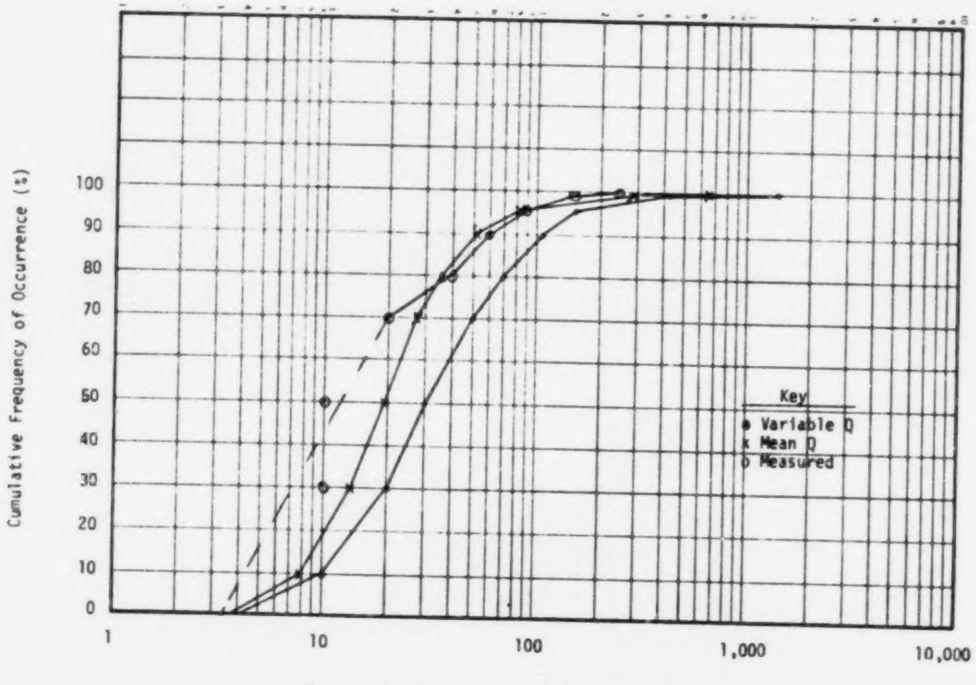

Figure 18. Frequency Distribution of Calculated and Measured One-Hour Concentrations for Chicago TAM #6

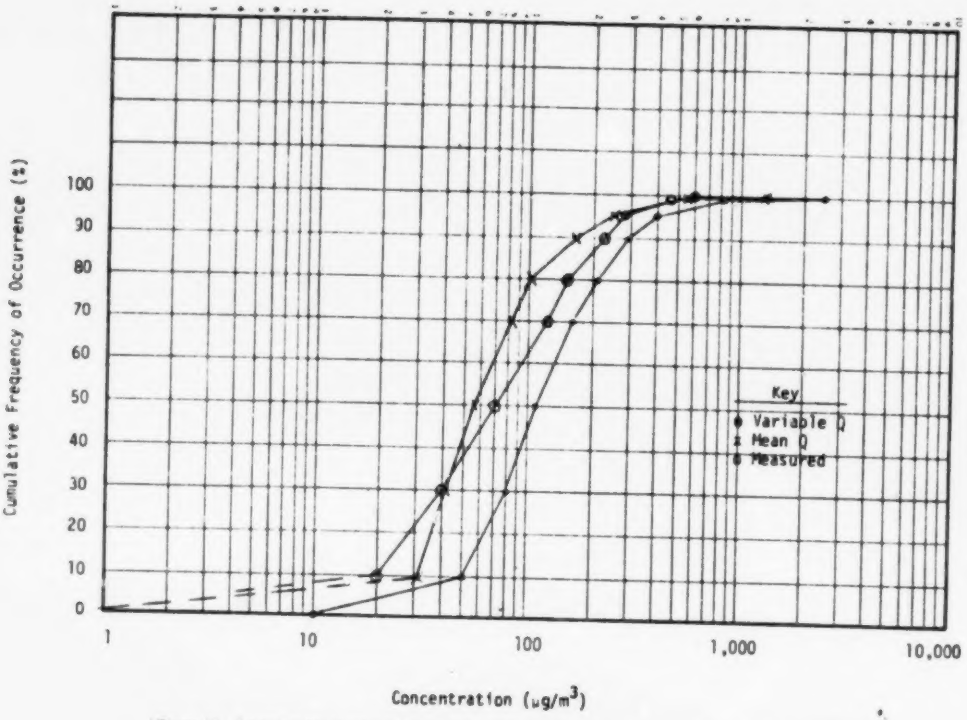

Figure 19. Frequency Distribution of Calculated and Measured One-Hour Concentrations for Chicago TAM #7

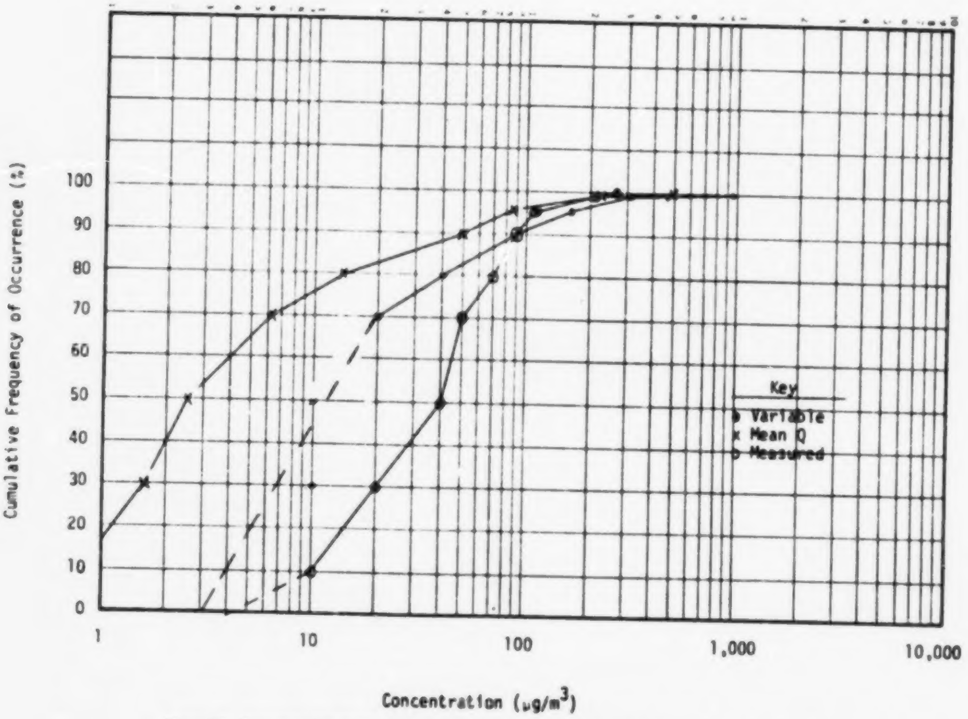

Figure 20. Frequency Distribution of Calculated and Measured One-Hour Concentrations for Chicago TAM #8

Table 1. Comparisons of Calculated Mean SO_2 Concentrations Using SCIM with St. Louis and Chicago Data Sets

Location	Station	Model Means ($\mu g/m^3$)			Paired Comparison Statistics		
		Mean Q	Variable Q	(Mean Q-Variable Q) Difference	Number of Comparisons	t-statistic	Significance Level
St. Louis	3	177	195	-17	2118	-4.12	<0.005
St. Louis	15	167	123	43	2118	10.45	<0.005
St. Louis	17	175	181	-6	2118	-1.61	>0.10
St. Louis	23	145	185	-40	2121	-6.05	<0.005
St. Louis	33	186	60	126	2121	36.09	<0.005
St. Louis	4	135	143	-8	2121	-1.60	>0.10
St. Louis	10	154	208	-53	2121	-11.36	<0.005
St. Louis	12	175	221	-45	2121	-9.82	<0.005
St. Louis	28	214	94	119	2121	24.23	<0.005
St. Louis	36	197	93	104	2121	29.62	<0.005
Chicago	1	28	47	-18	727	-8.37	<0.005
Chicago	2	58	105	-47	727	-14.78	<0.005
Chicago	3	207	378	-170	727	-14.61	<0.005
Chicago	4	180	327	-147	727	-17.81	<0.005
Chicago	5	78	128	-50	727	-13.15	<0.005
Chicago	6	30	57	-27	727	-10.12	<0.005
Chicago	7	83	158	-75	727	-19.05	<0.005
Chicago	8	16	36	-20	727	-7.54	<0.005

is highly significant. Clearly, the method by which hourly emissions are estimated has an important impact on the mean estimated for a 1-month or 3-month period. It is interesting that at the eight Chicago stations, the mean Q estimates are all less than the variable Q estimates. At the St. Louis stations, the three largest differences are the result of high mean Q estimates. Since these differences are all attributable to the emission algorithm, it is clear that the algorithm can act either to increase or decrease the mean calculated value over a long-term period. The non-linear correlation between changes in emission rates and changes in the rate of diffusion through the atmosphere is indicated by these results.

Since the means of the two sets of calculations are significantly different, it is not surprising that the distributions about these means are different. The standard deviation of the calculations for each station is shown in Table 2. Except for one St. Louis station, the corresponding standard deviations for calculations using the two types of emission rates are significantly different at the one percent level based on the F-test statistic. The distributions were also compared by means of the nonparametric Kolmogorov-Smirnov statistic. All the distributions are significantly different at the five percent level using this statistic, and all but two are significantly different at the one percent level. The results of the Kolmogorov-Smirnov test are the more conclusive because it is likely that the distributions are not normal as is assumed in the F-test.

Table 2. Comparison Statistics for the Distribution of Calculated Hourly SO_2 Concentrations Using SCIM with St. Louis and Chicago Data Sets [(1)]

Location	Station	Standard Deviation[(2)]		Kolmogorov-Smirnov (K-S) Statistic	Probability of Exceeding (K-S) Statistic
		Mean Q	Variable Q		
St. Louis	3	181	205	1.475	0.026
St. Louis	15	154	139	7.145	0.0
St. Louis	17	168*	172*	1.613	0.011
St. Louis	23	166	261	2.487	0.0
St. Louis	33	152	105	21.894	0.0
St. Louis	4	159	204	3.009	0.0
St. Louis	10	147	182	4.652	0.0
St. Louis	12	144	239	3.746	0.0
St. Louis	28	158	174	21.004	0.0
St. Louis	36	160	151	16.382	0.0
Chicago	1	71	110	6.950	0.0
Chicago	2	64	115	6.242	0.0
Chicago	3	161	403	5.140	0.0
Chicago	4	136	314	6.242	0.0
Chicago	5	72	140	4.616	0.0
Chicago	6	51	96	5.376	0.0
Chicago	7	91	159	8.182	0.0
Chicago	8	41	76	9.048	0.0

(1) Based on a 3-month period for St. Louis and a 1-month period for Chicago.

(2) All standard deviations are significantly different at one percent level using F-test except values marked by an asterisk.

3.1.2 Model-To-Measurement Comparisons

Having determined that there is a significant difference between calculations made using hourly variations in emission rates and calculations made using mean values, it is of interest to determine whether one gives significantly better agreement with corresponding measured values. Table 3 shows some comparison statistics. For the St. Louis data, the use of variable emission rates yields a calculated mean closer to the measured mean at 7 of 10 stations. For the Chicago data, the variable emission rate calculations are closer at only 3 of 8 stations. Three sets of paired comparisons statistics are shown in Table 3, including mean absolute error (MAE), root-mean-square error (RMSE), and correlation coefficient. The variable emission rate calculations show better agreement with measured values based on MAE and RMSE than the mean emission rate calculations for St. Louis stations. For Chicago stations the reverse is true. Using correlation coefficients, the variable emission rate calculations show the better agreement with measured values at both locations. Except for correlation coefficients, the mean emission rate calculations are best for Chicago stations and the variable emission rate calculations are best for St. Louis stations.

The model-to-model comparisons shown in Tables 1 and 2 indicate that the model is sensitive to hourly variations in emission rates such as are represented by the algorithm which has been employed. However, the validation results suggest that the algorithm has some, but limited, skill in representing these hourly variations. Another possibility is that other sources of error are so large that they mask the effects of changes in emission rates. Since the emission algorithm uses only

Table 3. Comparisons Between Calculated and Measured SO_2 Concentrations[1]
Using Mean and Variable Emission Rates in the CIGP Model

Station	Location	Mean[2]			Mean Absolute Error		Root-Mean-Square Error		Correlation Coefficient	
		Observed	Mean Q	Variable Q	Mean Q	Variable Q	Mean Q	Variable Q	Mean Q	Variable Q
St. Louis	3	156	178*[3]	196	132	130*	202*	211	0.118	0.201*
St. Louis	15	137	168	118*	148	87*	202	134*	-0.080	0.448*
St. Louis	17	212	174	181*	128	114*	180	163*	0.170	0.390*
St. Louis	23	89	140*	190	112*	142	171*	259	0.185	0.241*
St. Louis	33	73	184	62*	143	53*	195	104*	0.014	0.393*
St. Louis	4	175	133	141*	137	115*	105*	213	0.073	0.293*
St. Louis	10	335	157	207*	224	202*	312	286*	0.127	0.235*
St. Louis	12	179	176*	210	102*	120	149*	195	0.359	0.460*
St. Louis	28	87	224	95*	178	80*	238	153*	-0.047	0.362*
St. Louis	36	80	194	89*	134	64*	188	122*	0.200	0.440*
Chicago	1	33	29*	47	27*	40	61*	100	0.559*	0.467
Chicago	2	114	55	99*	83*	90	119*	130	0.071	0.148*
Chicago	3	312	209	379*	171*	220	223*	400	0.242	0.303*
Chicago	4	123	172*	315	96*	200	140*	330	0.165	0.372*
Chicago	5	62	80*	128	45*	80	75*	150	0.355*	0.277
Chicago	6	23	31*	58	27*	50	57*	100	0.179	0.180*
Chicago	7	102	85*	158	70*	100	114*	170	0.284	0.320*
Chicago	8	43	17	36*	42*	50	59*	80	0.216*	0.072

---

(1) Three-month period for St. Louis and 1-month period for Chicago.

(2) The means shown here may differ slightly from those shown in Table 1 because hours when no observed value was reported are omitted.

(3) An asterisk indicates the better of the corresponding mean Q and variable Q results.

temperature, time of day and day of the week as variables, it is possible to examine the validity of the model with different combinations of these variables and to determine whether there is any detectable bias. This has been done in Table 4 for classes of hour of the day, day of the week and temperature. With regard to hour of the day, the St. Louis measurements show two peaks, one in late morning and one in late evening. The calculations using variable emission rates also show two peaks, but they precede the measured peaks by one class. The amplitude of the calculated cycles, although small, agrees with the amplitude of the measured cycles. Calculations using a mean emission rate show a single unlikely peak occurring during the early morning hours. In the Chicago data, the measurements also show two peaks, although the second peak in the early evening is very weak. The calculations using variable emission rates are in phase with the Chicago measurements but the amplitude of the cycle is greatly magnified. The single cycle of the calculations using mean emission rates agrees more closely with the Chicago measurements.

There does not appear to be any systematic variation in the measured or calculated class means by day of the week. However, both measured and calculated class means show a trend from high to low values with increasing temperature. The trend is more pronounced in the Chicago measurements than in the St. Louis measurements. The temperature dependence is exaggerated in the calculations based on variable emission rates. It appears that many sources were incorrectly assumed to have a high degree of temperature dependency.

Table 4. Variations in Mean Concentrations for Selected Classifications

		Mean 3-Month Concentration ($\mu g/m^3$) Over 10 St. Louis Stations				Mean 1-Month Concentration ($\mu g/m^3$) Over 8 Chicago Stations		
			Calculated				Calculated	
Classification	No. of Cases	Measured	Variable Q	Mean Q	No. of Cases	Measured	Variable Q	Mean Q
Hours								
00-04	1578	145	148	209	908	79	152	86
04-08	1595	161	167	180	896	113	213	101
08-12	1613	165	140	138	893	106	123	69
12-16	1480	128	123	132	904	92	103	64
16-20	1540	153	175	185	897	98	154	84
20-24	1585	173	154	188	685	95	133	86
Day of the Week								
Monday	1294	154	141	164	836	87	123	72
Tuesday	1330	166	157	171	850	88	140	76
Wednesday	1376	164	159	180	703	124	229	96
Thursday	1367	141	148	153	707	102	140	90
Friday	1338	153	151	176	716	110	121	72
Saturday	1377	148	130	155	742	91	109	66
Sunday	1309	155	173	208	901	82	160	96
Temperature								
<15F	806	161	217	178	738	128	280	93
15F to 24.9F	1795	150	202	191	1000	95	155	81
25F to 34.9F	2748	154	161	181	2365	89	122	82
35F to 44.9F	2099	168	129	163	848	102	125	72
45F to 54.9F	1359	144	95	156	309	85	95	95
55F to 64.9F	495	139	73	138	180	73	46	52
>65F	89	124	84	132	15	44	23	36

In view of the sensitivity shown by the model-to-model comparisons, the variable emission rate is a desirable approach where pollution emissions have significant time-dependent variations. It appears that the emission algorithms used for St. Louis and Chicago are introducing significant errors, and that data must be sought which can be used to make more reasonable estimates of the variations in emission rates.

3.2 COMPARISONS AMONG TEN MODEL VARIATIONS USING NEW YORK CITY DATA

A validation study of the three Gaussian plume models and the simplified Gifford-Hanna model, described in Section 2.0, was carried out using data applicable to the vicinity of New York City for 1969. There are various ways of preparing input for use in these models. In particular, the emission rates, stability conditions or wind speed may be assumed to be constant throughout the data period or varied from hour to hour. Altogether 10 combinations of models and data conditioning were analyzed. The material which follows describes the combinations, describes the New York City data, presents the method of analysis, presents and discusses the results, and summarizes the findings.

3.2.1 Description of the Ten Model and Data Conditioning Combinations

For the SCIM, area source emissions and the meteorological conditions of atmospheric stability and height of the mixing layer (grouped together) are treated either as varying from hour to hour or as being constant throughout the data period. Three combinations of input data conditioning were analyzed, including:

- Area source emission rates, atmospheric stability and height of the mixing layer variable
- Area source emission rates constant, but atmospheric stability and height of the mixing layer variable
- Area source emission rates, atmospheric stability and height of the mixing layer constant.

For the simplified Gifford-Hanna Model (GHM), area source emissions and wind speed are treated as both varying from hour to hour or as both being constant throughout the data period. In addition, the calculated concentration at a receptor due to point sources (as estimated by SCIM with variable atmospheric stability and mixing layer height) are either added or not added to the GHM calculations. This results in four variations of this model, including:

- Constant area source emission rates and wind speed, without point sources
- Variable area source emission rates and wind speed, without point sources
- Constant area source emission rates and wind speed, with point sources
- Variable area source emission rates and wind speed, with point sources.

Calculations for CDM, which treat atmospheric stability and height of the mixing layer as either both variable or both constant, were furnished by Mr. D. B. Turner of the Division of Meteorology, EPA/NERC/RTP. Statistical results of model-to-measurement comparisons for these calculations are included in this report for comparison with the other models. Calculations for AQDM (no variations) also were furnished by Mr. Turner and are included for comparison.

3.2.2 Description of the Data

Three types of data for New York City which were used to test the validity of the models are described here, including air quality measurements, pollutant emission information and meteorological measurements. The air quality and meteorological measurements were made during 1969, and the emission information is applicable to 1969.

3.2.2.1 Air Quality Data

The air quality measurements consist of annual mean concentrations of SO_2 and particulate aerosols and hourly concentrations of SO_2. The annual mean concentrations were measured at 127 locations in the New York - New Jersey - Connecticut Air Quality Control Region. SO_2 was measured at 75 locations and particulate aerosols were measured at 114 locations. Hourly mean concentrations of SO_2 were measured at 39 locations in New York City. The 10 locations shown in Figure 21, representing different geographic characteristics, were selected for use in this analysis. All 127 of the locations measuring annual concentrations were used. The locations in the immediate vicinity of the New York City limits are shown in Figure 21.

3.2.2.2 Emission Data

The emission information consists of: (1) emission inventory data prepared for the Implementation Planning Program (IPP) for the

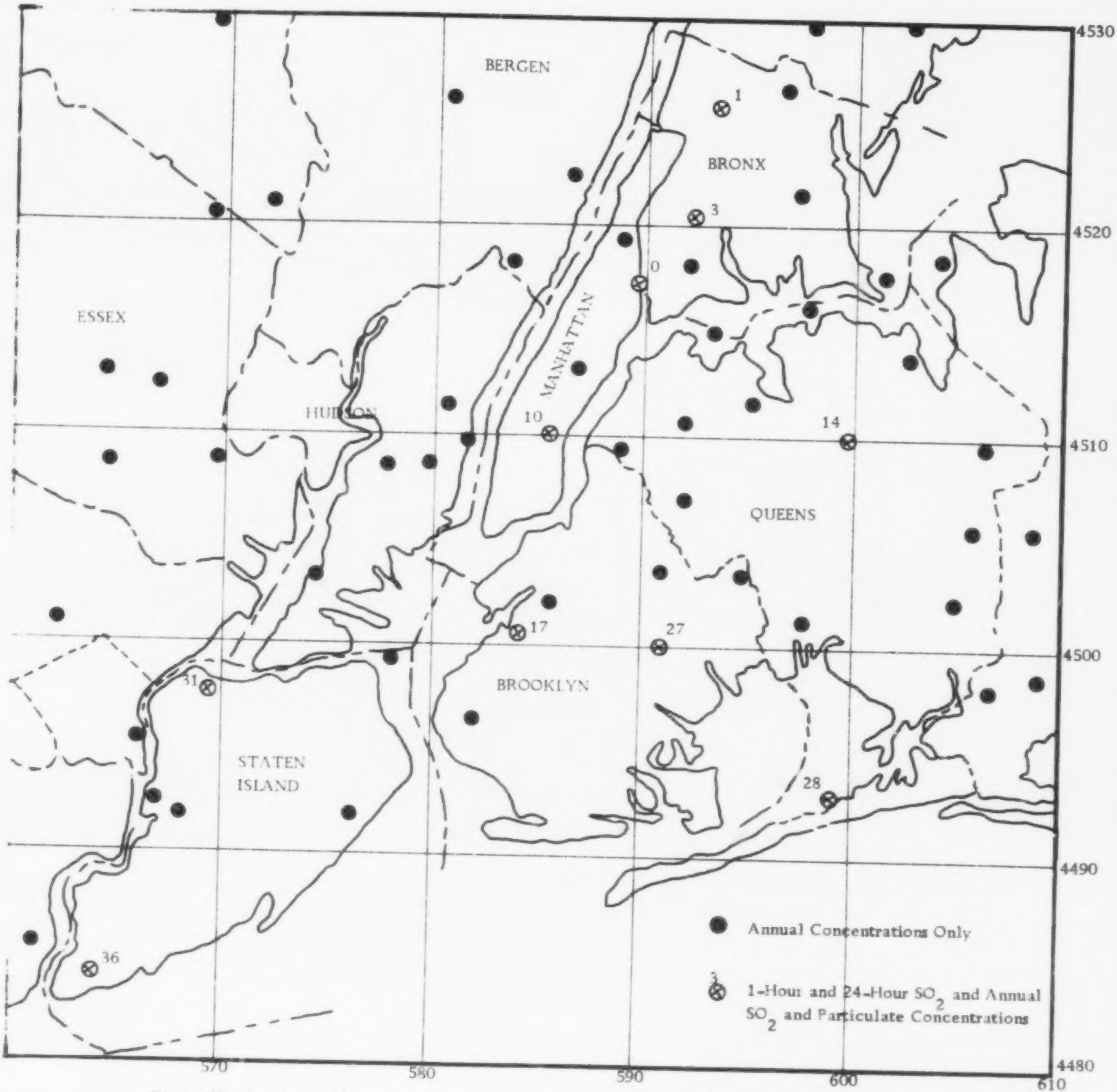

Figure 21. Locations of Air Quality Measurements in the Immediate Vicinity of New York City

New Jersey - New York - Connecticut AQCR, and (2) time and temperature dependent weighting factors which when multiplied by the annual emission rate of area sources provide an estimate applicable to a particular hour.

The IPP data includes 675 point sources and 871 area sources. For each point the available information includes Transverse Mercator Projection Coordinates (TMPC), Standard Industrial Code (SIC), annual SO_2 and particulate emission rates, stack height, stack diameter, stack gas exit velocity and stack gas exit temperature. Each area source is defined for a specified square area varying between 1 and 100 km^2. The available information includes the TMPC of the southwest corner, the size of the area, the annual SO_2 and particulate emission rates, and the effective height of the emissions.

The weighting factor used to determine area source emissions for a particular hour is a function of temperature and time of day; its development is described in Appendix A. The area source emission rate algorithm is

$$Q_i = Q_A K_i$$

where

Q_i = emission rate for the ith hour of the year ($\mu g/m^2/sec$)

$$K_i = [(1-F_h) J_i L_1 + F_h (\bar{T}_i - T_i) I_i K L_2] \text{ for } T_i < \bar{T}_i$$
$$K_i = [(1-F_h) J_i L_i] \text{ for } T_i \geq \bar{T}_i \tag{22}$$

Q_A = mean annual area source emission rate ($\mu g/m^2/sec$)

F_h = 0.29 = fraction of emissions attributed to space heating requirements

J_i = base level emission coefficient for hour i (day/hr)

$\overline{T}_i$ = threshold temperature for hour i (°F)

T_i = observed temperature for hour i (°F)

I_i = temperature sensitivity factor for hour i (Index/°F)

K = constant $\equiv$ 0.0002337 yr/Index hr

L_1 = unit conversion $\equiv$ 24 hr/day

L_2 = unit conversion $\equiv$ 8760 hr/yr.

The numerical values of the terms J_i, $\overline{T}_i$ and I_i are given in Appendix A. A value of K_i was computed for each 3-hour temperature observation obtained for 1969.

3.2.2.3 Meteorological Data

The meteorological measurements consist of 3-hourly synoptic weather observations reported for LaGuardia Airport and twice daily radiosonde observations reported for Kennedy Airport. The observations from the 3-hourly weather report for LaGuardia Airport which were used in this study were:

- Wind direction (nearest 10° azimuth)
- Wind speed (observing height of 6.1 m)
- Temperature
- Cloud cover (tenths)
- Height of cloud ceiling.

The first observation period of each day was 0100 EST. Twelve hours for which the reported wind speed was calm or less than 1 m/sec were excluded from the data set. The validation was limited to the use of 3-hourly observations since this is what is routinely available from NOAA's National Weather Records Center in Ashville. As a result, the validation findings indicate what can be expected from routine as opposed to research use of the models tested.

The radiosonde observations were used to estimate the height of the surface-based mixing layer. The details of the parcel method used to define the height are described in Appendix B. The height derived for the morning sounding was assumed to be applicable to the hours of 0100, 0400 and 0700. The height derived for the afternoon sounding was assumed to be applicable to the hours of 1300, 1600, 1900, and 2200. An average of the morning and afternoon values was used for 1000. If a sounding was missing, the height assigned to the previous 24-hour period was used. An annual mean mixing height was determined by averaging all the 3-hourly values. Heights in excess of 5000 m were treated as being 5000 m. The resulting annual mean was 979 m which is about midway between the annual morning and afternoon mixing layer heights recently reported by Holzworth (1972) for New York City.

Two other annual mean meteorological values which were used in this study were 5.1852 m/sec for wind speed and neutral (Pasquill-Turner class 4) for atmospheric stability.

3.2.3 Comparison Statistics

Model-to-measurement comparison statistics were obtained for each of the 10 model and data conditioning combinations. The statistics are listed and compared in the following sections. All the statistics are standard and require no special explanation. Error as used in these statistics refers to calculated minus measured concentration.

3.2.4 Results of Model-to-Measurement Comparisons

The ability of all four models to estimate long-term concentrations accurately is evaluated. Only the SCIM and GHM are appropriate for testing for short-term concentration estimates. The short-term concentration calculations, which are compared with measured hourly mean concentrations of SO_2, are presented first.

3.2.4.1 One-Hour SO_2 Comparisons for SCIM and GHM

Using SCIM and GHM, the SO_2 concentration was calculated at each of 10 receptor locations for every third hour of the year, for which a measured concentration was available, beginning 0100 on January 1, 1969. For each hour selected, SCIM calculations were made in three ways:

- With variable area source emissions (using Equation (4) for K_i) and variable stability and mixing layer height (variable Q, S, and H)
- With mean area source emissions ($K_i=1$) and variable stability and mixing layer height (mean Q, variable S and H)
- With mean area source emissions, stability (Pasquill-Turner class 4) and mixing layer height (979 m) (mean Q, S, and H).

The GHM calculations were made in two ways:

- With variable area source emissions and wind speed, and without the inclusion of any contributions from point sources
- With variable area source emissions and wind speed, and with point source contributions as calculated by SCIM added to the basic GHM calculations.

The frequency distribution of 1-hour concentrations for each of the three types of SCIM calculations and for the measured values are shown on log-normal graphs for each of the 10 stations in Figures 22 through 31. The corresponding frequency distributions for the two types of GHM calculations and for measured values are similarly plotted in Figures 32-41. The curves are close to straight lines; therefore, it is reasonable to expect that they may be approximated by log-normal distribution functions. This hypothesis will be tested during Phase II. The GHM graphs clearly show that the model calculations with point source concentrations added give better agreement with the frequency distribution of measured concentrations at 8 of the 10 New York City stations. Of the other two (Stations #0 and #1), only Station #0 shows better agreement with calculations without point source concentrations. The SCIM frequency distributions based on variable S and H differ very little and agree best with the measured frequency distributions at Stations #14, 17, 27, 28, and 31. Only at Station #0 does the SCIM frequency distribution based on mean Q, S and H agree best with measured values.

A summary of model-to-measurement comparison statistics is given in Tables 5 and 6. Table 5 includes a comparison of the means and standard deviations of measured and calculated concentrations for each station. The root-mean-square errors (RMSE), the mean absolute errors (MAE), and the error (calculated minus observed) concentration corresponding to the measured maximum concentration are also included for each set of model calculations. Table 6 shows correlation coefficients and linear regression characteristics for model-to-measurement comparisons. The tabulated regression characteristics of measured on calculated concentrations include the variance attributed to the regression relationship and the two slope and intercept regression coefficients.

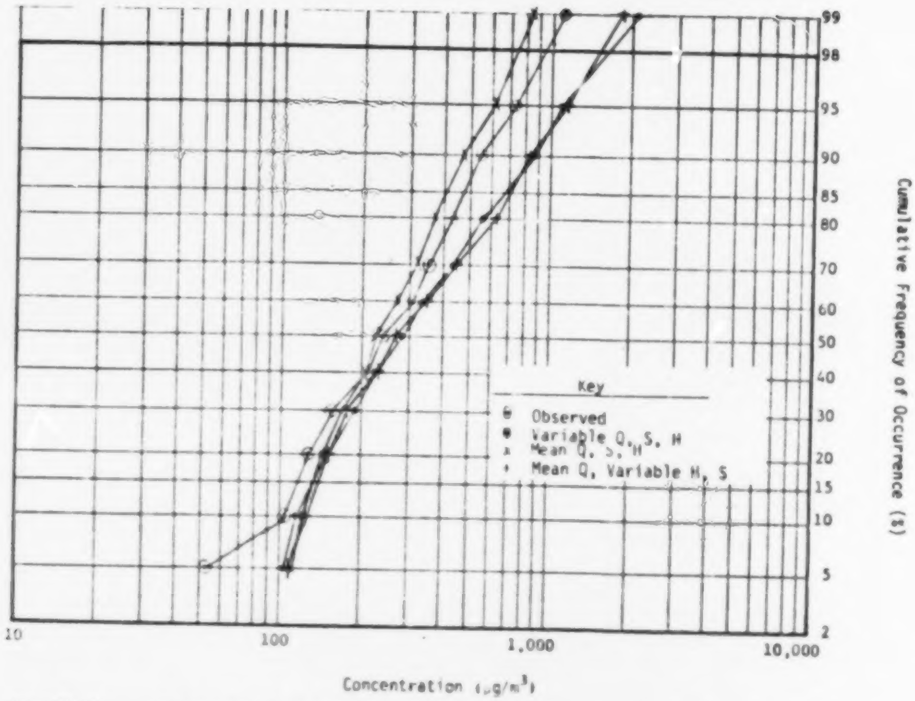

Figure 22. Frequency Distribution of SCIM Calculated and Measured One-Hour Concentrations for New York City Station #0

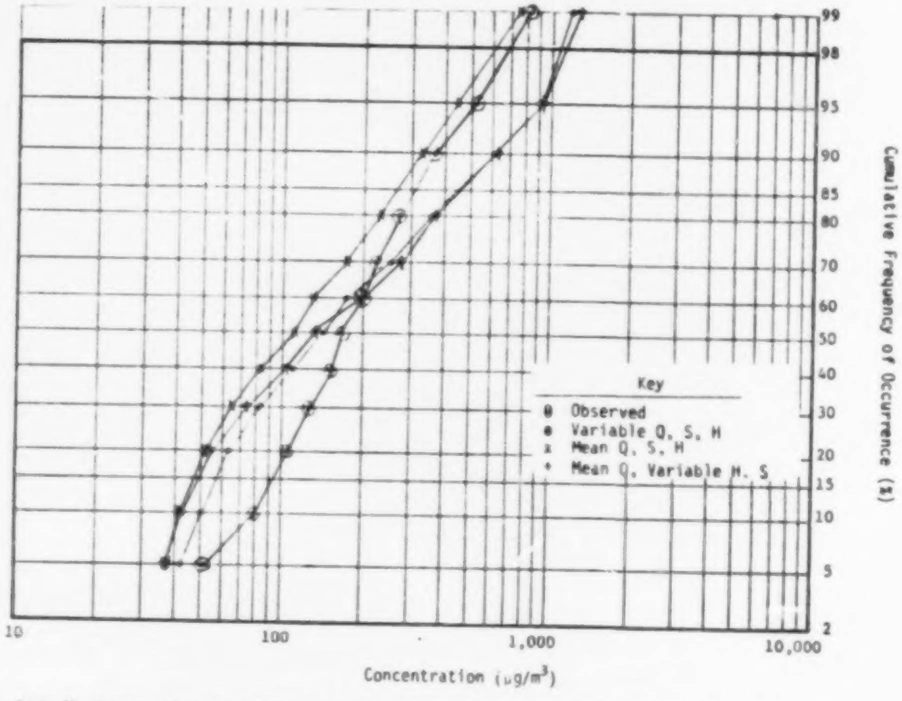

Figure 23. Frequency Distribution of SCIM Calculated and Measured One-Hour Concentrations for New York City Station #1

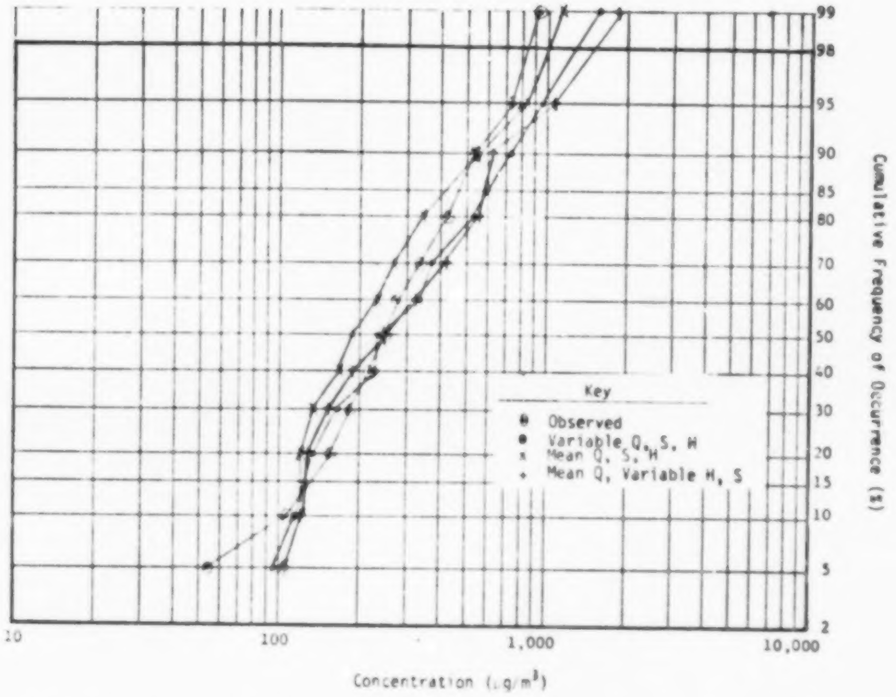

Figure 24. Frequency Distribution of SCIM Calculated and Measured One-Hour Concentrations for New York City Station #3

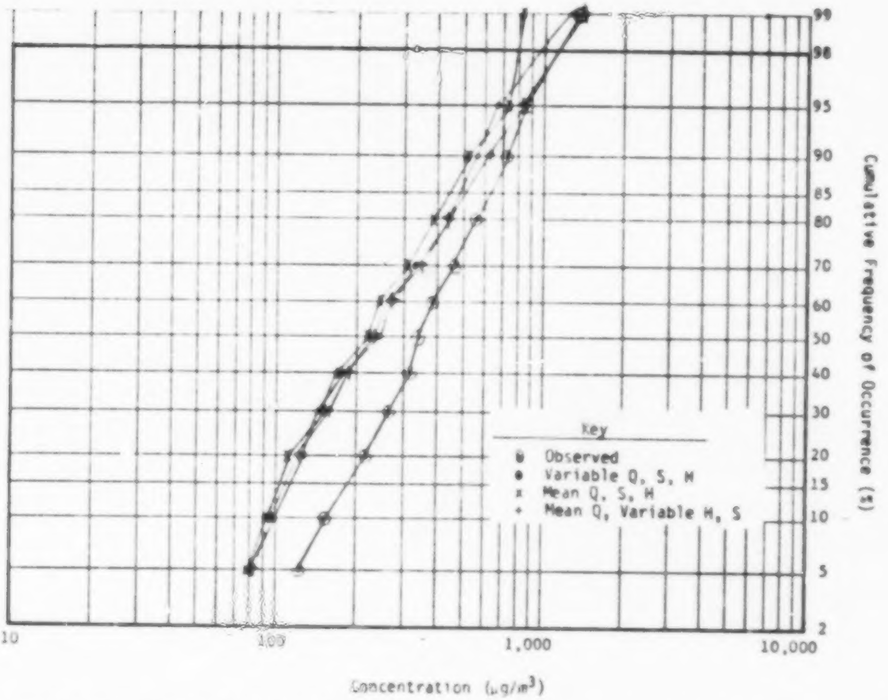

Figure 25. Frequency Distribution of SCIM Calculated and Measured One-Hour Concentrations for New York City Station #10

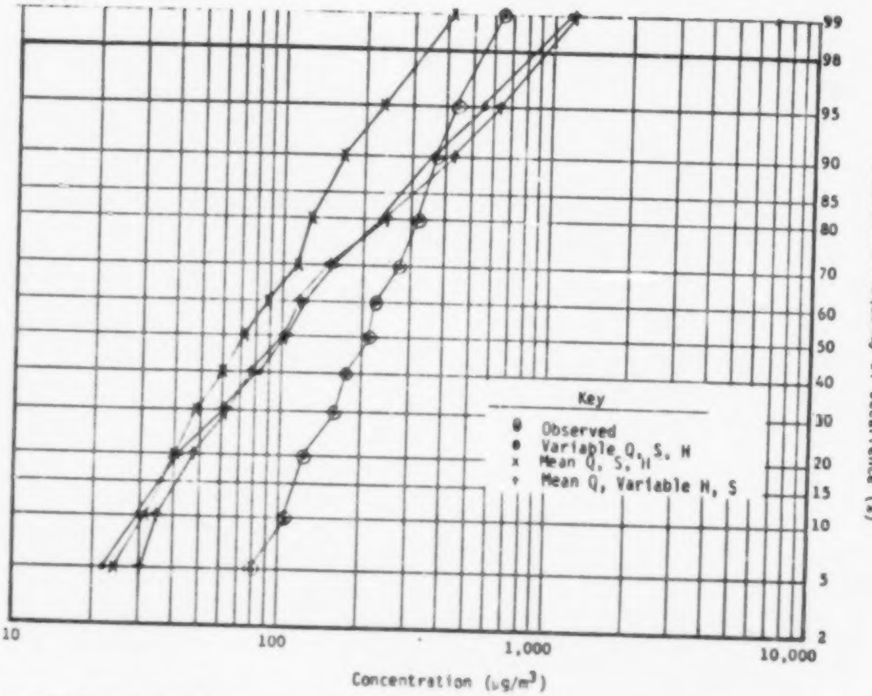

Figure 26. Frequency Distribution of SCIM Calculated and Measured One-Hour Concentrations for New York City Station #14

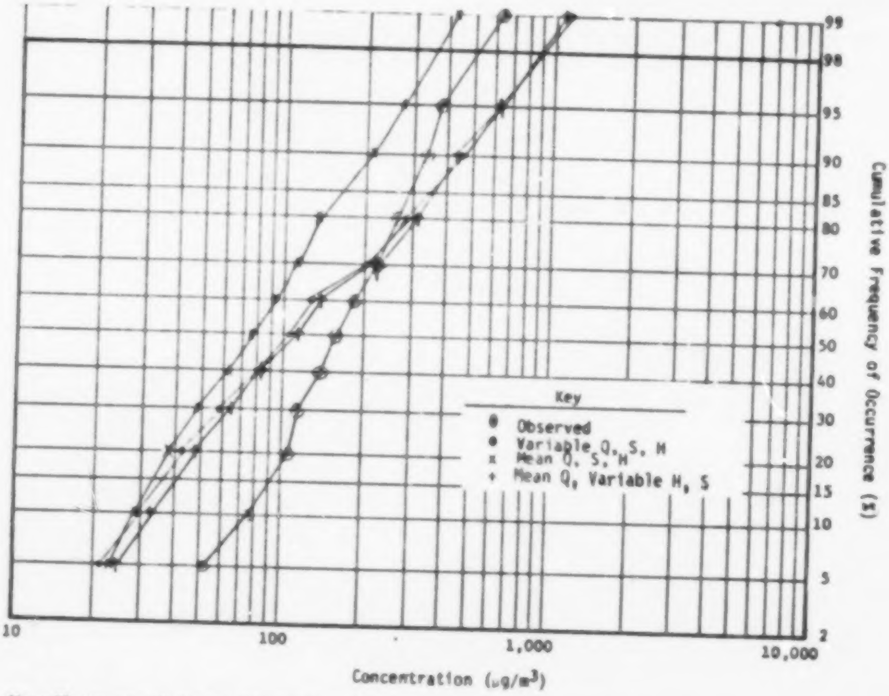

Figure 27. Frequency Distribution of SCIM Calculated and Measured One-Hour Concentrations for New York City Station #17

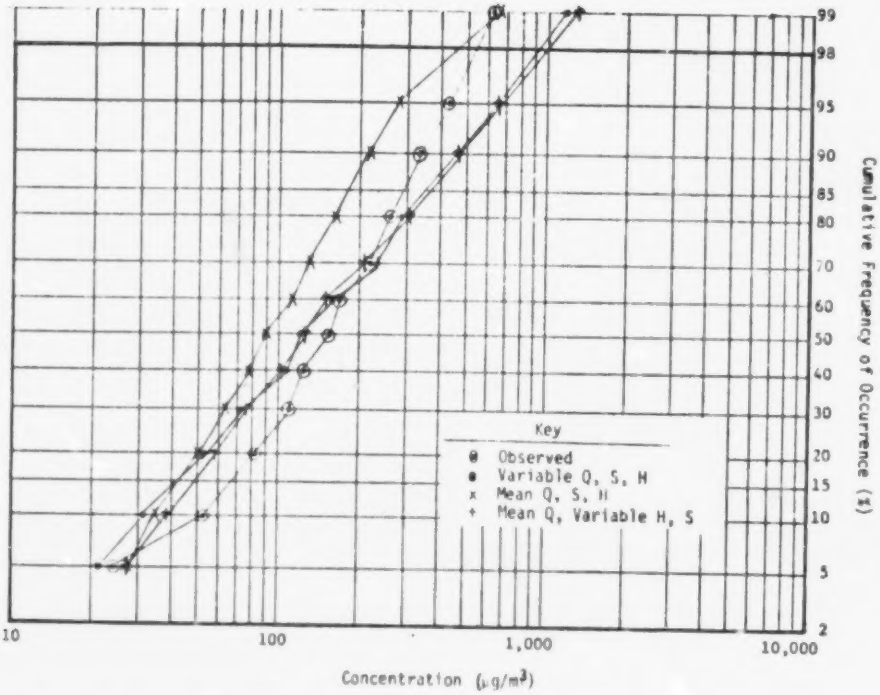

Figure 28. Frequency Distribution of SCIM Calculated and Measured One-Hour Concentrations for New York City Station #27

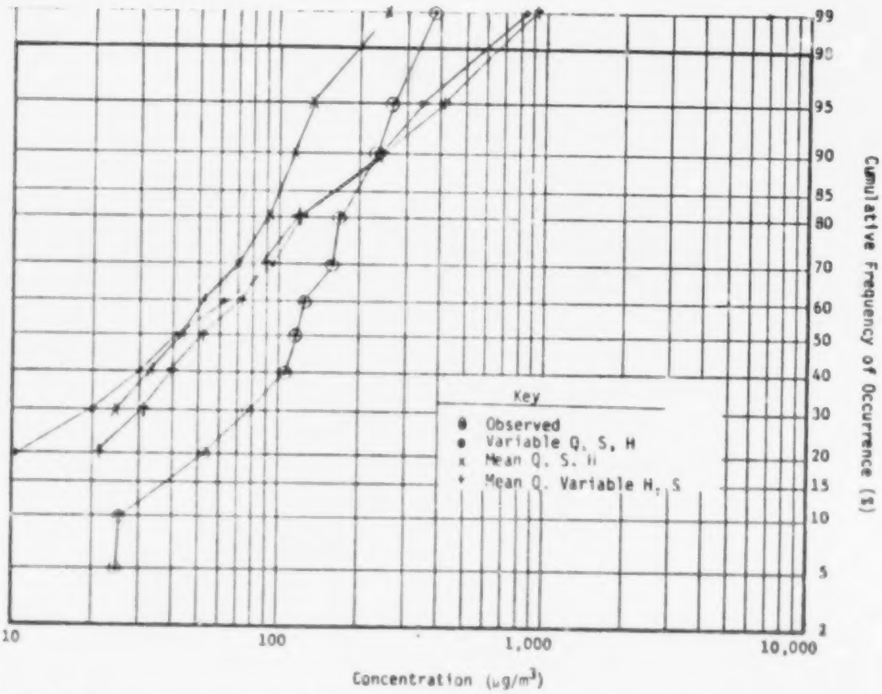

Figure 29. Frequency Distribution of SCIM Calculated and Measured One-Hour Concentrations for New York City Station #28

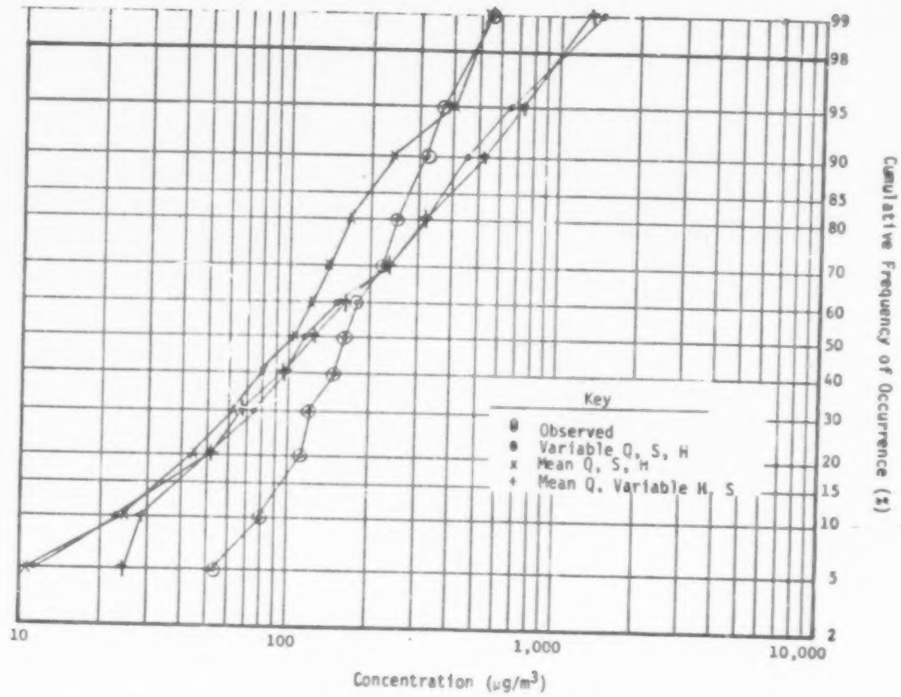

Figure 30. Frequency Distribution of SCIM Calculated and Measured One-Hour Concentrations for New York City Station #31

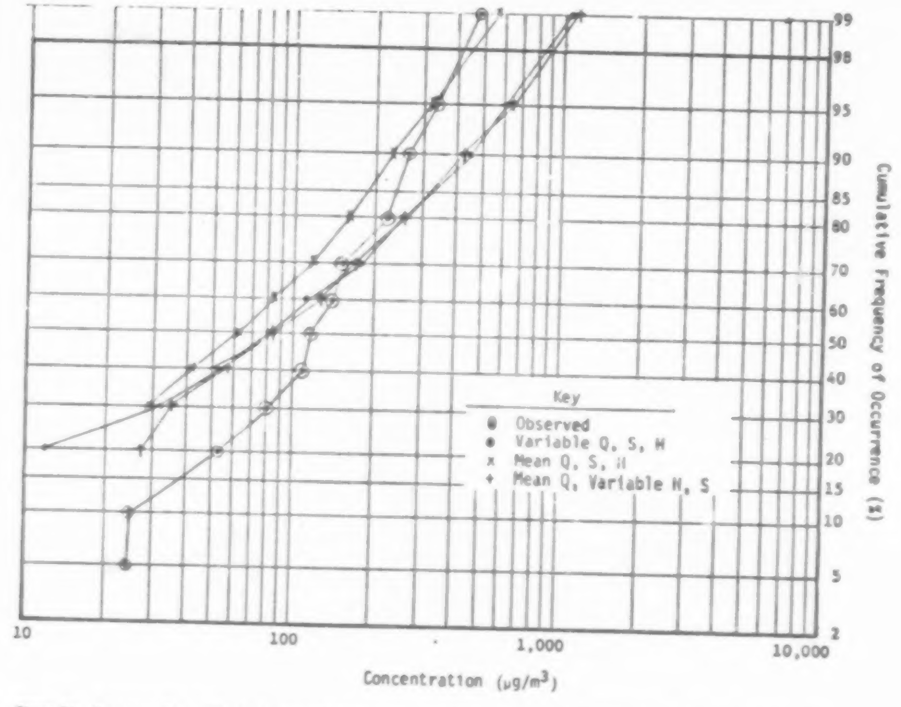

Figure 31. Frequency Distribution of SCIM Calculated and Measured One-Hour Concentrations for New York City Station #36

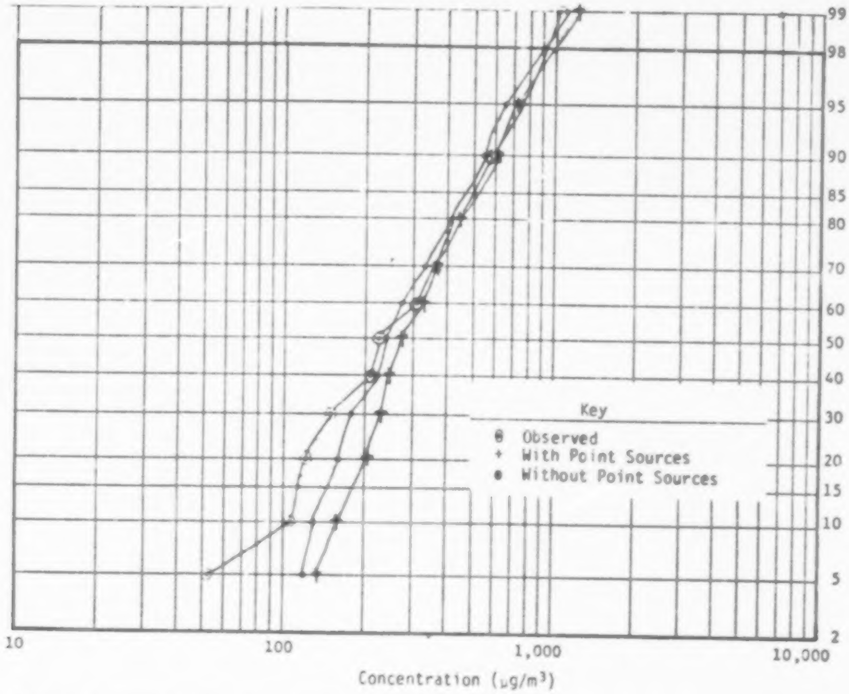

Figure 32. Frequency Distribution of CHM Calculated and Measured One-Hour Concentrations for New York City Station #0

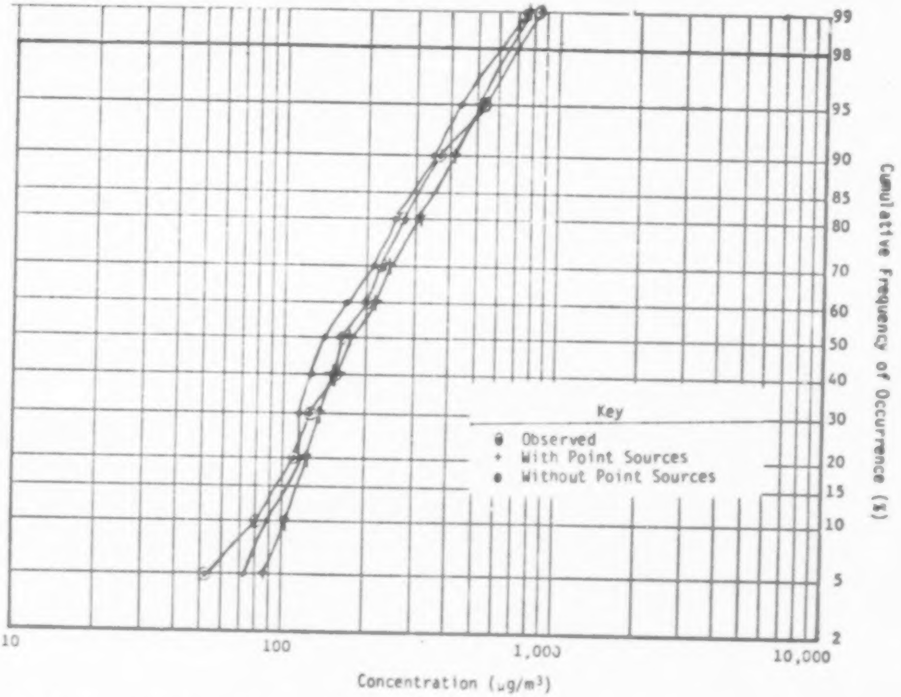

Figure 33. Frequency Distribution of CHM Calculated and Measured One-Hour Concentrations for New York City Station #1

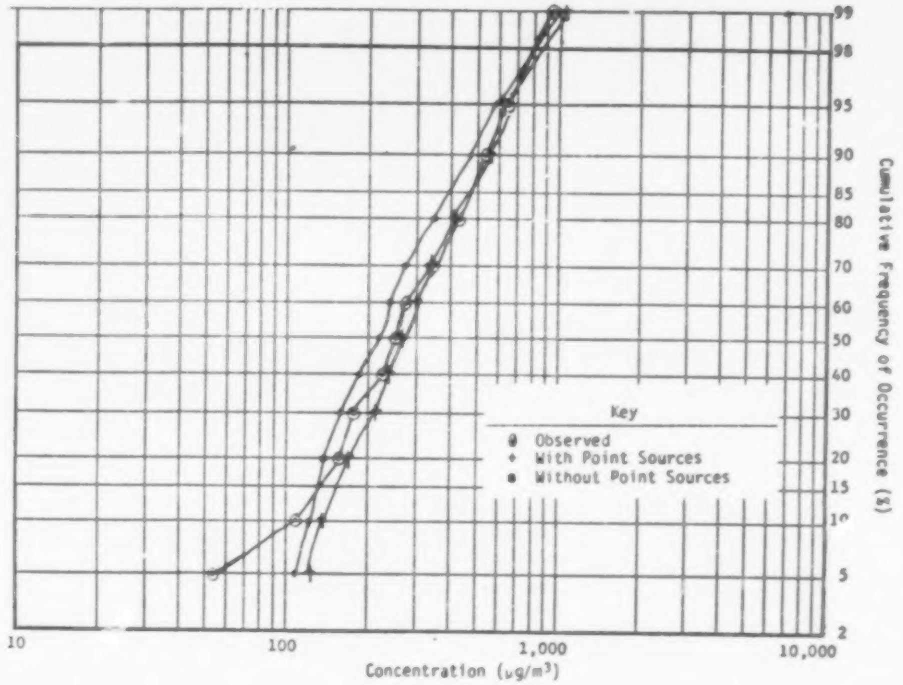

Figure 34. Frequency Distribution of CDM Calculated and Measured One-Hour Concentrations for New York City Station #3

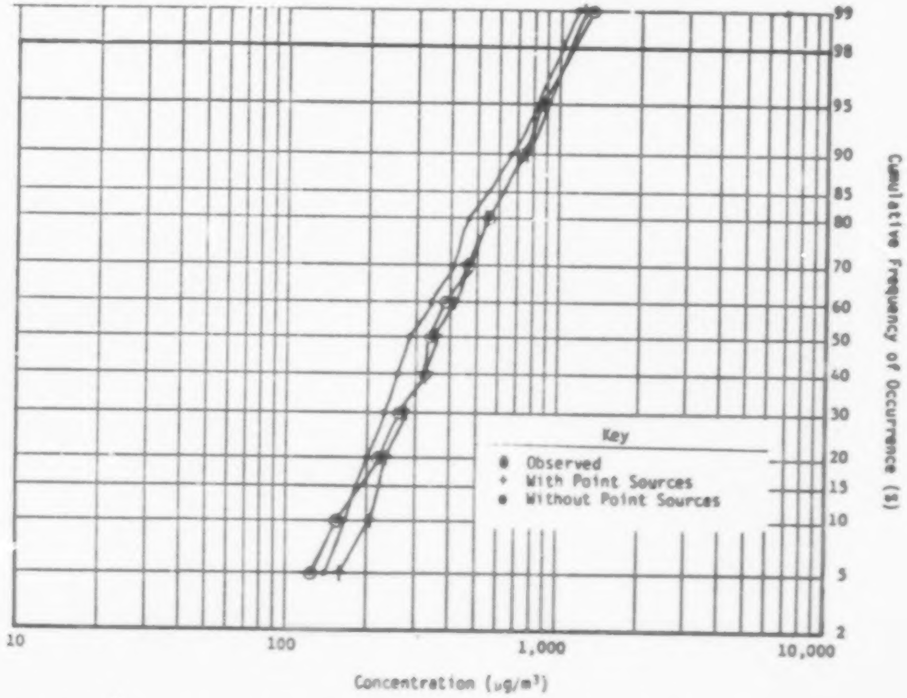

Figure 35. Frequency Distribution of CDM Calculated and Measured One-Hour Concentrations for New York City Station #10

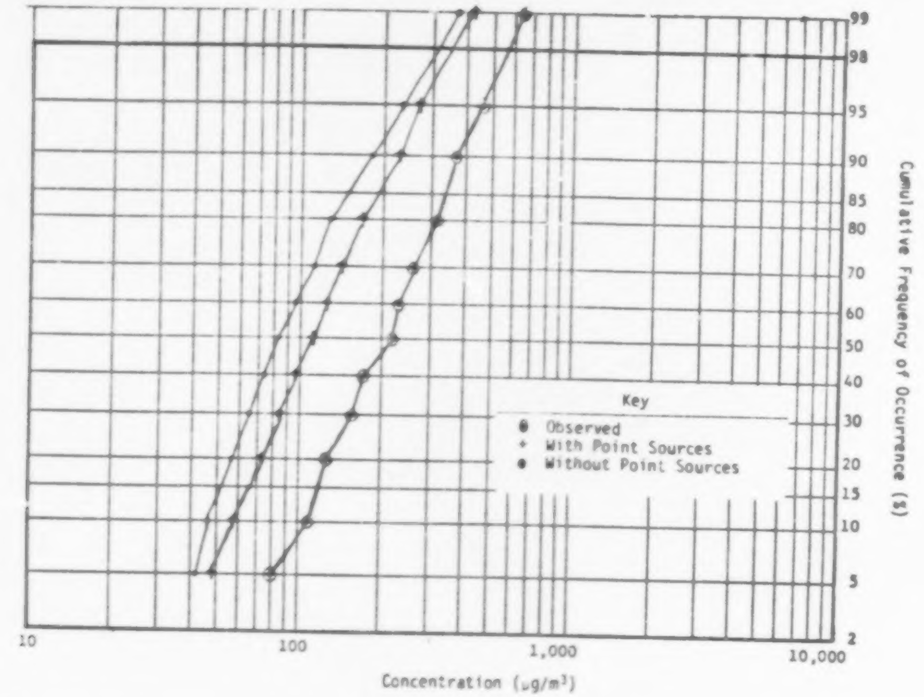

Figure 36. Frequency Distribution of CHM Calculated and Measured One-Hour Concentrations for New York City Station #14

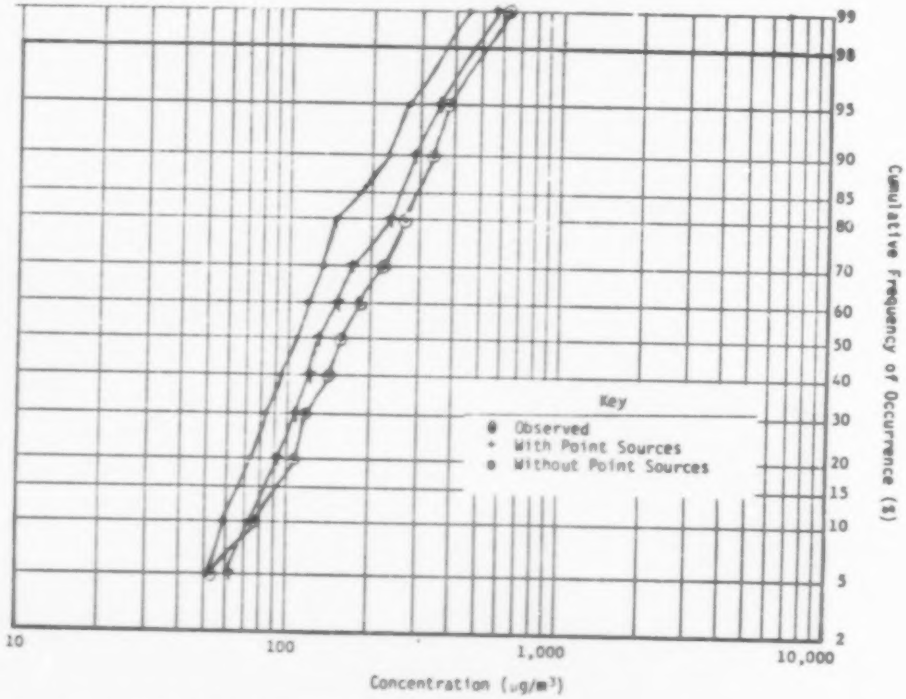

Figure 37. Frequency Distribution of CHM Calculated and Measured One-Hour Concentrations for New York City Station #17

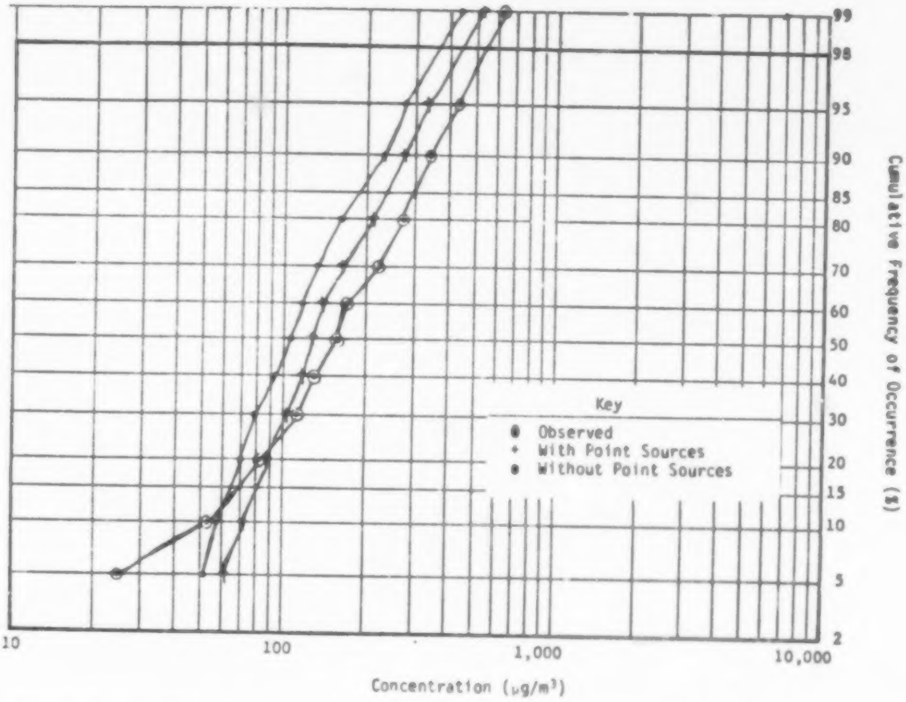

Figure 38. Frequency Distribution of CHM Calculated and Measured One-Hour Concentrations for New York City Station #27

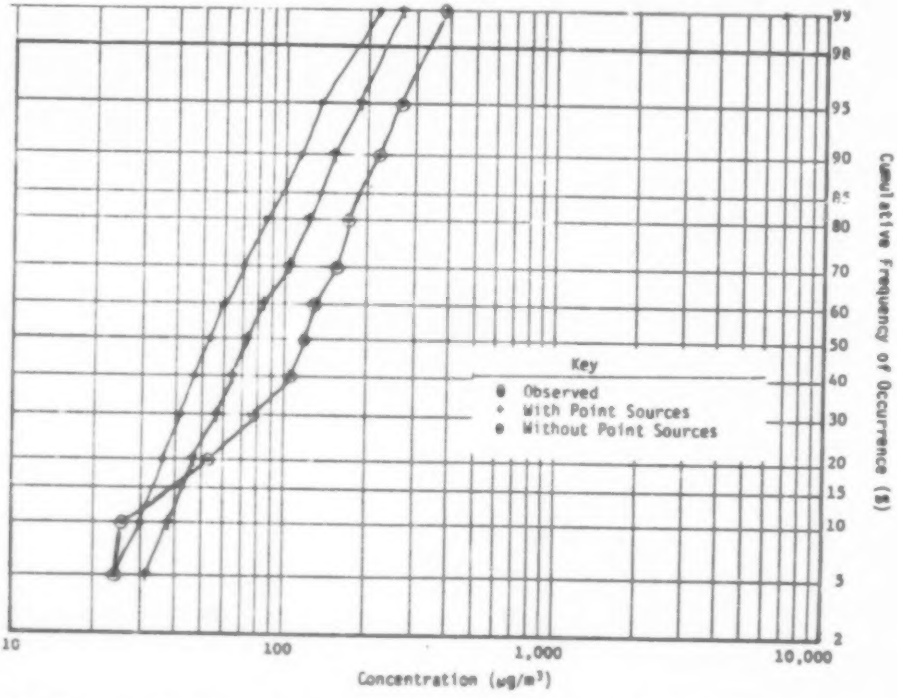

Figure 39. Frequency Distribution of CHM Calculated and Measured One-Hour Concentrations for New York City Station #28

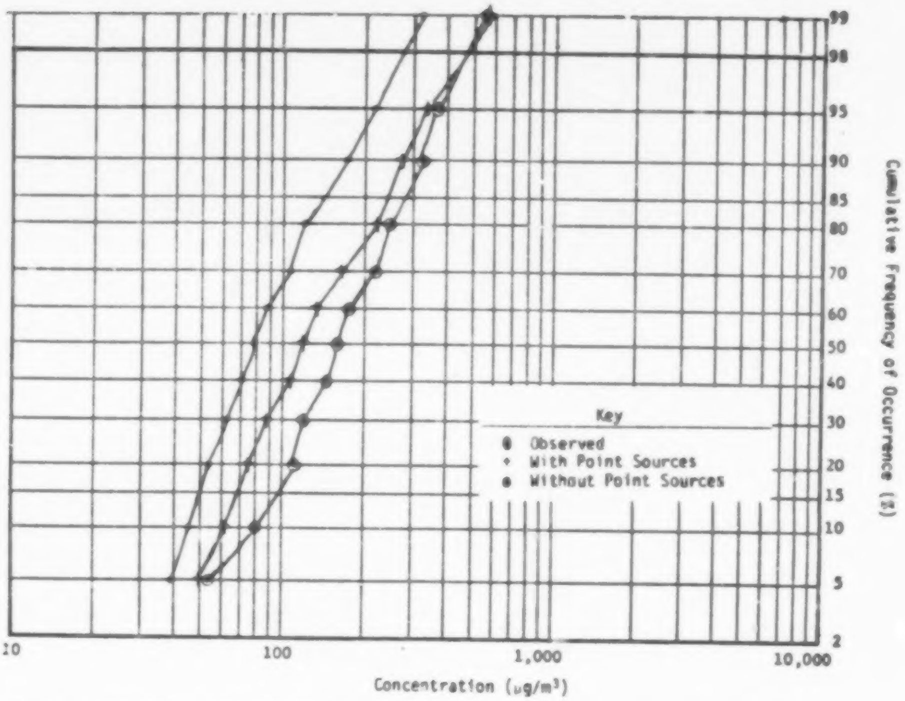

Figure 40. Frequency Distribution of CHM Calculated and Measured One-Hour Concentrations for New York City Station #31

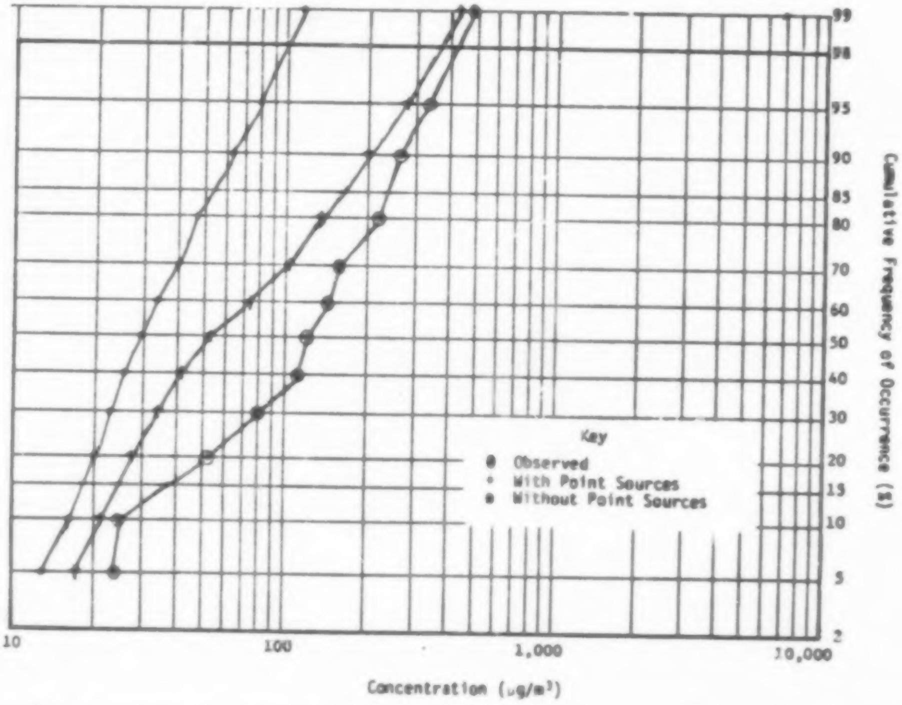

Figure 41. Frequency Distribution of CHM Calculated and Measured One-Hour Concentrations for New York City Station #36

Table 5. Model-to-Measurement Comparisons of 1-Hour NYC SO_2 Concentrations by Mean, Standard Deviation, RMSE, MAE and Error at Maximum Measurement

		NYC Station Number									
		0	1	3	10	14	17	27	28	31	36
	Number of Comparisons	2892	1213	1489	1670	1641	1768	1702	1381	1783	1475
Mean ($\mu g/m^3$)	Measured	304	212	296	420	230	193	188	127	187	145
	SCIM (Variable Q, S, H)	421	271	374	307	172	192	210	98	214	164
	SCIM (Mean Q, Var. S, H)	440	281	390	320	184	196	211	102	221	174
	SCIM (Mean Q, S, H)	282	157	248	224	94	102	118	50	121	100
	GHM (without points)	308	196	270	369	105	130	128	65	97	37
	GHM (with points)	350	226	313	424	131	169	156	90	156	94
Standard Deviation ($\mu g/m^3$)	Measured	220	157	192	327	127	119	129	88	108	105
	SCIM (Variable Q, S, H)	421	405	388	281	223	235	255	180	297	221
	SCIM (Mean Q, Var. S, H)	421	412	408	272	243	229	252	184	281	239
	SCIM (Mean Q, S, H)	170	148	163	137	73	87	97	55	96	119
	GHM (without points)	200	125	173	236	68	84	81	41	60	23
	GHM (with points)	209	140	181	247	76	103	91	54	121	102
Root Mean Square Error ($\mu g/m^3$)	SCIM (Variable Q, S, H)	400	392	400	410	216	237	251	188	295	219
	SCIM (Mean Q, Var. S, H)	455	416	433	430	238	242	268	195	285	244
	SCIM (Mean Q, S, H)	261	201	240	402	185	165	165	128	146	151
	GHM (without points)	219	165	238	350	176	142	144	109	144	147
	GHM (with points)	227	168	236	354	156	137	137	104	145	146
Mean Absolute Error ($\mu g/m^3$)	SCIM (Variable Q, S, H)	233	192	228	256	146	152	146	112	159	137
	SCIM (Mean Q, Var. S, H)	289	219	254	277	160	156	159	118	166	146
	SCIM (Mean Q, S, H)	188	142	168	257	147	125	118	96	110	110
	GHM (without points)	154	111	167	207	137	103	103	79	108	111
	GHM (with points)	160	114	166	213	118	98	97	75	99	104
	Maximum Measured ($\mu g/m^3$)	2242	1350	1723	6711	1345	1009	1178	836	1072	903
Error at Maximum Measured ($\mu g/m^3$)	SCIM (Variable Q, S, H)	934	-351	-1463	-6502	-406	-745	-867	-827	-943	-641
	SCIM (Mean Q, Var. S, H)	-258	-508	-1469	-6512	-778	-852	-934	-827	-942	-696
	SCIM (Mean Q, S, H)	-1546	-940	-1579	-6511	-1218	-953	-1052	-832	-941	-706
	GHM (without points)	-1373	-1134	-1490	-6429	-1044	-630	-966	-787	-1009	-850
	GHM (with points)	-1123	-892	-1473	-6358	-1022	-629	-902	-787	-911	-714

Table 6. Model-to-Measurement Comparisons of 1-Hour NYC SO_2 Concentrations by Correlation Coefficient, Variance and Regression Coefficients

		NYC Station Number									
		0	1	3	10	14	17	27	28	31	36
	Number of Comparisons	2892	1213	1489	1670	1614	1768	1702	1381	1783	1475
Correlation Coefficient	SCIM (Variable Q, S, H)	0.43	0.30	0.23	0.17	0.40	0.24	0.29	0.17	0.21	0.26
	SCIM (Mean Q, Var. S, H)	0.20	0.20	0.16	0.03	0.33	0.15	0.14	0.12	0.18	0.19
	SCIM (Mean Q, S, H)	0.13	0.20	0.13	0.02	0.29	0.14	0.15	0.05	0.19	0.18
	GHM (without points)	0.46	0.34	0.16	0.28	0.29	0.24	0.29	0.19	0.21	0.33
	GHM (with points)	0.46	0.36	0.21	0.26	0.36	0.27	0.31	0.14	0.24	0.13
Reduction of Variance by Linear Regression	SCIM (Variable Q, S, H)	0.18	0.09	0.05	0.03	0.16	0.06	0.08	0.03	0.04	0.06
	SCIM (Mean Q, Var. S, H)	0.04	0.04	0.02	0.00	0.11	0.02	0.02	0.02	0.03	0.04
	SCIM (Mean Q, S, H)	0.02	0.04	0.02	0.00	0.08	0.07	0.02	0.00	0.04	0.03
	GHM (without points)	0.21	0.11	0.03	0.08	0.08	0.06	0.09	0.04	0.04	0.11
	GHM (with points)	0.21	0.13	0.04	0.07	0.13	0.07	0.09	0.02	0.06	0.02
Slope of Regression Line	SCIM (Variable Q, S, H)	0.22	0.12	0.11	0.20	0.23	0.12	0.15	0.08	0.08	0.12
	SCIM (Mean Q, Var. S, H)	0.10	0.08	0.08	0.04	0.17	0.08	0.07	0.06	0.07	0.08
	SCIM (Mean Q, S, H)	0.17	0.21	0.15	0.06	0.50	0.18	0.20	0.08	0.22	0.16
	GHM (without points)	0.50	0.42	0.18	0.38	0.53	0.34	0.47	0.41	0.37	1.51
	GHM (with points)	0.49	0.41	0.22	0.35	0.61	0.31	0.44	0.22	0.21	0.13
Intercept of Regression Line	SCIM (Variable Q, S, H)	210	181	254	360	191	170	157	119	171	125
	SCIM (Mean Q, Var. S, H)	258	191	267	407	198	176	172	121	172	131
	SCIM (Mean Q, S, H)	255	179	259	407	182	174	163	123	161	129
	GHM (without points)	148	130	247	279	173	148	128	100	151	89
	GHM (with points)	133	120	227	271	150	141	119	107	154	133

Several general results may be noted by comparing the statistics for the three SCIM calculations. The results obtained using variable Q, S, and H are very similar to the results obtained using mean Q, variable S, and H inputs; however, higher correlations and slightly smaller errors are observed using variable Q. When the variable Q, S, and H results are compared with the mean Q, S, and H results, the differences are more striking. The calculated mean is closer to the measured mean at 7 out of 10 receptors using the variable inputs, while the root-mean-square error is smaller at all receptors using the mean inputs. The correlation coefficients are higher at all receptors using the variable inputs. The frequency distributions of errors for each set of calculations was also examined. It was found that the variable input calculations produce some large overprediction errors not found with mean input calculations. In view of the similar results obtained using mean and variable Q with variable S and H, these large errors must be due to inaccurate estimates of the atmospheric stability or the mixing layer height.

The GHM results are slightly, but consistently, better for the calculations with point source concentrations than for the calculations without point sources. The correlation coefficients with point sources are higher at 7 of the 10 stations; the RMSE is smaller at 6 stations; the error at the minimum measured concentration is smaller at 9 stations.

The results in Tables 5 and 6 suggest that SCIM with Variable Q, S and H and GHM with point sources gave the best overall results. Of these two, SCIM produced better results for estimating the mean and the maximum measured concentration. GHM produced smaller RMSE's and better correlation as indicated by the correlation coefficient and the regression characteristics.

In order to get more insight into the validation results, the results were stratified by classes of five different parameters. For each parameter, the mean of each class was determined for each set of model calculations and for the measured values. The class means for hour of the day and day of the week are shown in Table 7. The class means for temperature, wind speed, and stability are shown in Table 8.

With regard to day of the week, observations for Sunday were available for only 1 station (#0). The means for Sunday were made comparable to other days of the week by multiplying the Sunday mean by the ratio of the annual mean for all stations to the annual mean for Station #0. None of the six columns in Table 7 show any important variation by day of the week.

The results by hour of the day are listed in Table 7 and plotted in Figure 42. With small exceptions all five sets of calculated results follow the general trend of the measured values. Calculations using SCIM with mean Q, S, and H underestimate the magnitude of the cycle of measured values while the other four sets of calculations overestimate the cycle. This result suggests there is a need to include model parameters with diurnal variations, and that the diurnal variation is easily overestimated. Clearly, the diurnal cycle of stability, mixing layer depth and emissions as represented in SCIM exaggerate the diurnal cycle of measured values. The GHM calculations which do not include a stability parameter show a better correspondence to the diurnal cycle of measured values. The addition of point sources in GHM calculations, while not changing the amplitude of the diurnal cycle, brings it into better agreement with measured values.

Table 7. Comparisons of 1-Hour SO_2 Concentrations by Hour of the Day and Day of the Week

			SCIM ($\mu g/m^3$)			GHM ($\mu g/m^3$)	
Classification	Number of Cases	Measured ($\mu g/m^3$)	Variable Q, S, H	Mean Q, Variable S and H	Mean Q, S and H	Without Points	With Points
Hour							
01	2143	209	269	341	169	156	194
04	2116	237	311	372	183	180	221
07	2111	303	444	336	190	302	352
10	2077	258	223	223	168	188	236
13	2134	223	166	191	142	139	180
16	2146	214	163	179	136	139	177
19	2146	231	226	219	137	176	211
22	2141	226	247	268	154	171	209
Day							
Monday	1796	232	239	253	154	171	210
Tuesday	3191	242	245	257	155	175	216
Wednesday	3350	232	229	243	149	165	205
Thursday	3362	233	264	272	158	184	224
Friday	3193	238	241	252	152	176	217
Saturday	1710	240	306	308	182	206	254
Sunday*	412	(215)	(270)	(269)	(152)	(178)	(218)

* Sunday values were observed only for Station #0. The tabulated values were normalized by multiplying the Sunday mean by the ratio of the mean of all station measurements to the mean of all Station #0 measurements.

Table 8. Comparisons of 1-Hour SO_2 Concentrations by Temperature, Wind Speed and Stability Classes

	Number of Cases	Measured ($\mu g/m^3$)	SCIM ($\mu g/m^3$) Variable Q, S, H	SCIM ($\mu g/m^3$) Mean Q, Variable S, H	SCIM ($\mu g/m^3$) Mean Q, S, H	GHM ($\mu g/m^3$) Without Points	GHM ($\mu g/m^3$) With Points
Temperature (°F)							
<15	36	363	248	146	132	288	320
15 to 24.9	511	322	316	180	123	281	306
25 to 34.9	2595	299	268	196	131	230	256
35 to 44.9	2573	306	290	238	147	221	255
45 to 54.9	2401	279	258	258	154	185	223
55 to 64.9	3316	210	261	315	170	162	202
≥ 65	5582	167	225	295	179	141	194
Wind Speed (m/sec)							
≤ 1.5	55	226	937	1054	625	680	763
>1.5 to 2.0	724	258	799	893	402	456	515
>2.0 to 2.5	728	254	506	544	285	342	396
>2.5 to 3.0	989	278	446	467	248	288	335
>3.0 to 4.0	2570	252	325	338	194	221	266
>4.0 to 5.0	2901	228	232	246	159	166	210
>5.0 to 6.0	2952	230	210	211	135	148	190
>6.0 to 8.0	4699	228	146	146	107	123	158
>8.0 to 10.0	1271	231	114	103	82	111	136
>10.0	271	230	106	83	67	114	132
Stability (Turner-Pasquill)							
1	17	143	162	255	332	316	340
2	559	213	374	434	273	239	302
3	1784	235	284	300	201	193	248
4	11667	236	188	185	133	160	198
5	2987	248	482	533	218	247	284

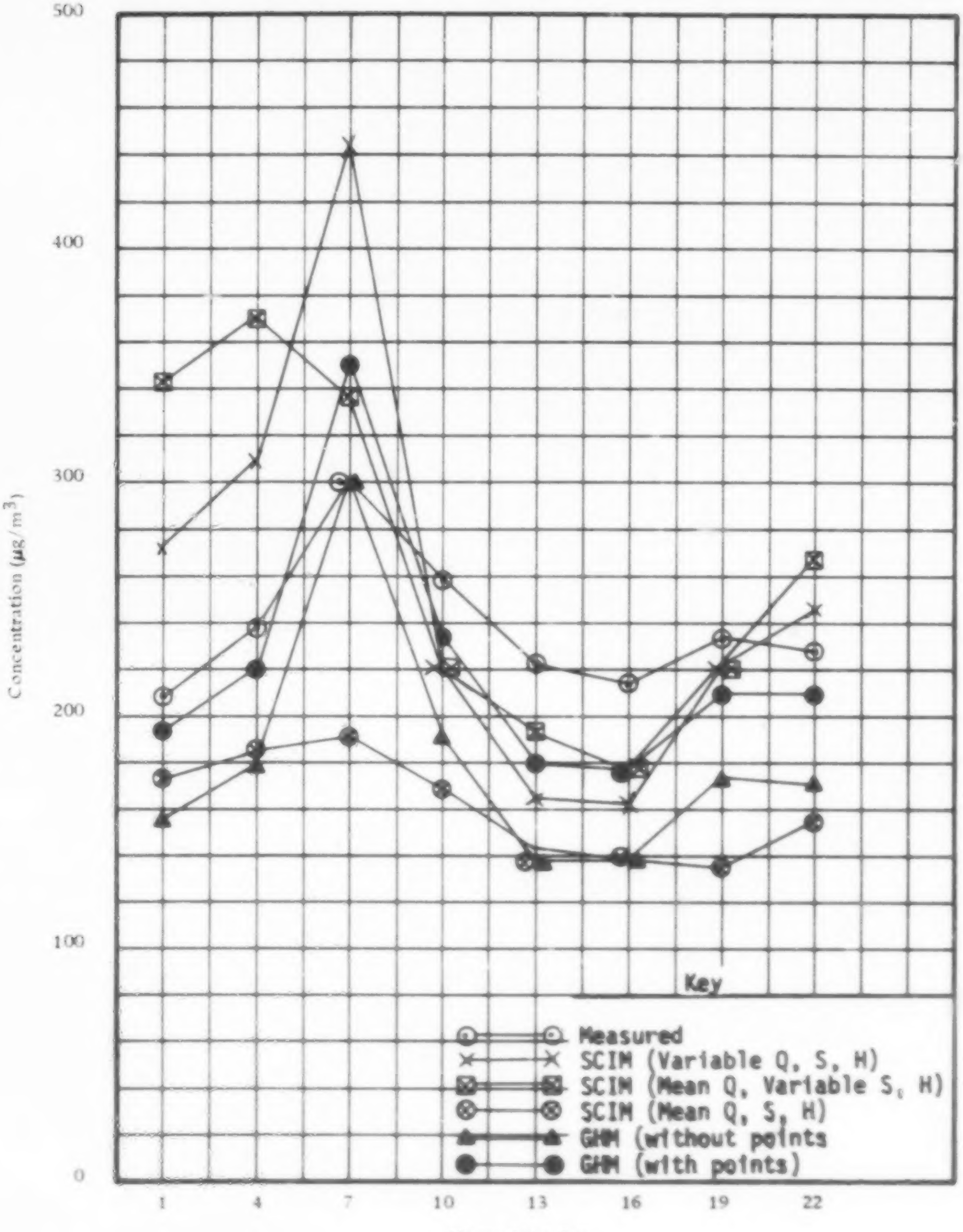

Figure 42. Variations in Measured and Calculated Mean One-Hour SO_2 Concentration by Hour of the Day

Temperature-dependent trends are tabulated in Table 8 and shown graphically in Figure 43. The importance of the temperature-dependent emission algorithm is suggested by the observation that the two sets of calculations based on mean Q run counter to the trend of the three sets of calculations using a variable Q and the measured values.

All five sets of calculated results show an important wind speed dependence in Table 8. This dependence is not evident in the measured concentrations. It is difficult to explain the measured results, since they are contrary to results observed at other locations such as Chicago, and St. Louis (Koch and Thayer 1971). Normally, if the wind speed is increased one would expect the pollutant concentration to decrease because the pollutant is diluted by a larger volume of air. However, for this particular data some compensating effect occurred, such as a decrease in diffusion or an increase in emissions. Clearly, the compensating effect is not accounted for in the models.

Stratifying the calculated and measured concentrations by stability class (Table 8) also shows some systematic errors in the models. The results for class 1 are inconclusive due to the small number of cases, less than two per station. For the remaining four stability classes, all five model results show the same pattern in varying magnitudes. The means decrease from class 2 to class 4 and then increase for class 5. The magnitude of the variations are especially large for the two SCIM results with variable stability inputs. The pattern contradicts the pattern of measured concentrations which show a small consistent increase from class 2 to class 5. Since wind speed tends to be light with very stable and unstable conditions, it is likely that the difference between

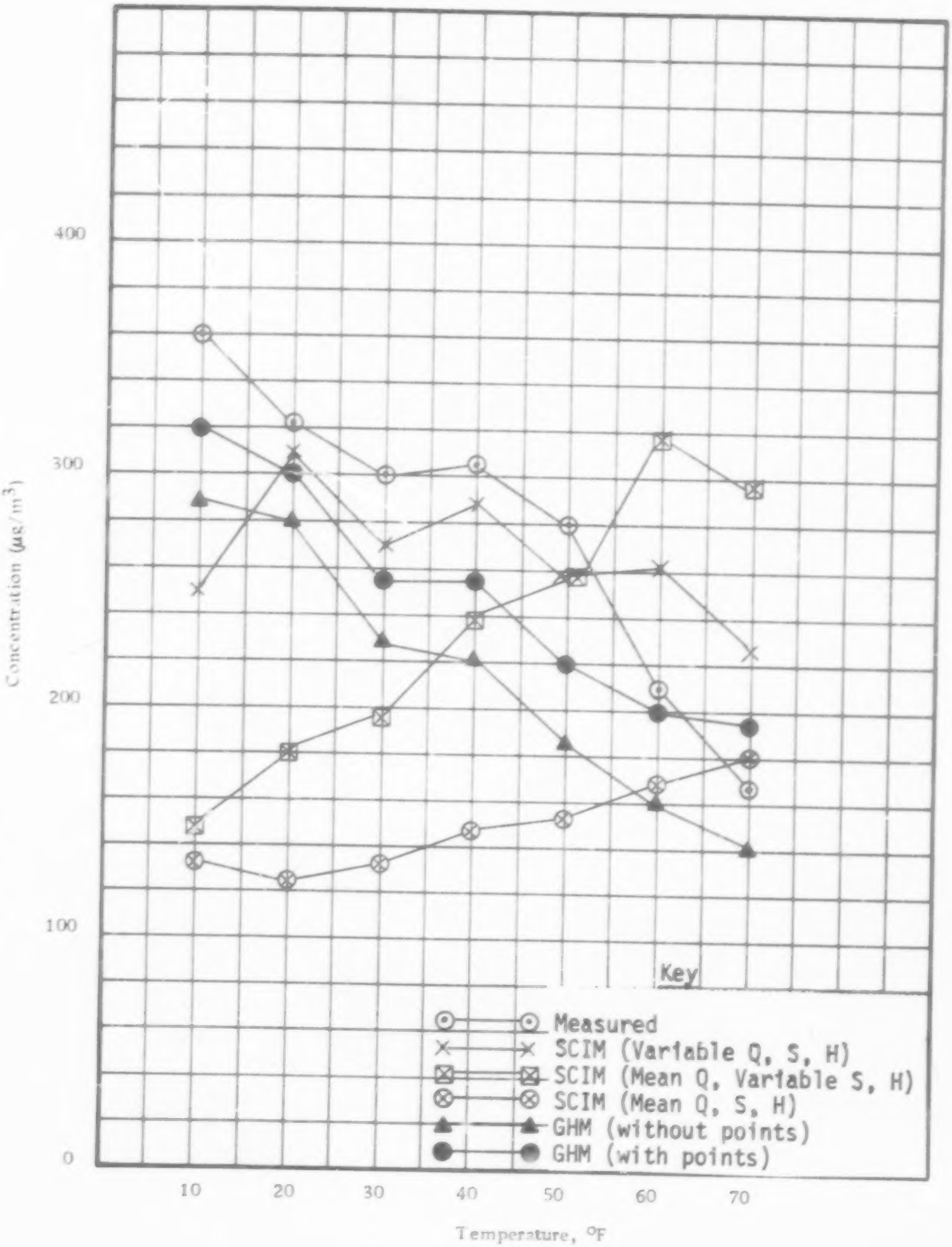

Figure 43. Variations in Measures and Calculated Mean One-Hour SO_2 Concentrations by Temperature

measured values and the three sets of calculated means without a stability dependent parameter (SCIM with mean Q, S and H, and the two GHM's) are due to the effects of wind speed on the model calculations. Although the use of a mean wind speed is shown in Section 3.2.4.4 to improve annual mean concentrations calculated using the GHM with point sources added, this seems undesirable because it amounts to suppressing a measured variation in atmospheric conditions. It is more desirable to find modifications to the models or to other model inputs which represent the compensating effects and leave the model compatible with results for other locations.

In view of the interrelationships between the parameters considered above, it is not possible to isolate the sources of error. However, it appears that some hypotheses can be drawn which are worthy of future study. The rate of change of mean calculated concentration with temperatures for the two best performing models (SCIM with variable Q, S and H, and GHM with points) is less than the rate of change of mean measured concentration with temperature. These models also show a larger mean diurnal variation than the measured values. These results suggest that the emission algorithm overestimates the diurnal factor and underestimates the fraction of emissions which are temperature-dependent. Another hypothesis is that SCIM overestimates diffusion effects associated with changes in atmospheric stability. This might be due to the inadequacy of the meteorological measurements based on the Turner-Pasquill index to represent stability variations. Of course, there are other possible sources of error which have not been investigated. These include the effective height of the area source emissions, the allocation of emissions to geographical areas in the emission inventory, and the diurnal variations in the mixing layer height, to mention a few.

3.2.4.2 Twenty-four Hour SO_2 Comparisons for SCIM and GHM

The calculated and measured concentrations were averaged for each 24-hour period and compared. The frequency distributions for each of the three sets of SCIM calculations and the set of measured values are shown in Figures 44 through 53 by receptor location. These figures agree with the results of the preceding figures for hour concentrations. They suggest that both sets of calculations based on variable S and H inputs more closely approximate the distribution of measured concentrations than the calculations based on mean S and H inputs. The frequency distribution of 24-hour SO_2 concentrations for the two sets of GHM calculations and the measured values at each of 10 New York City sampling stations are shown in Figures 54 through 63. Of the two model calculations the frequency distribution of calculations using point sources more closely coincides with the frequency distribution of measured values at 7 of 10 stations. For two stations (#0 and #1), the calculations without points show better agreement with measured values. The measurements at the other station (#3) are about equally matched by both sets of calculations.

Statistical comparisons of the five sets of model calculations with measured values are given in Tables 9 and 10. As with the hourly concentrations, the 24 hourly concentrations show that, of the three sets

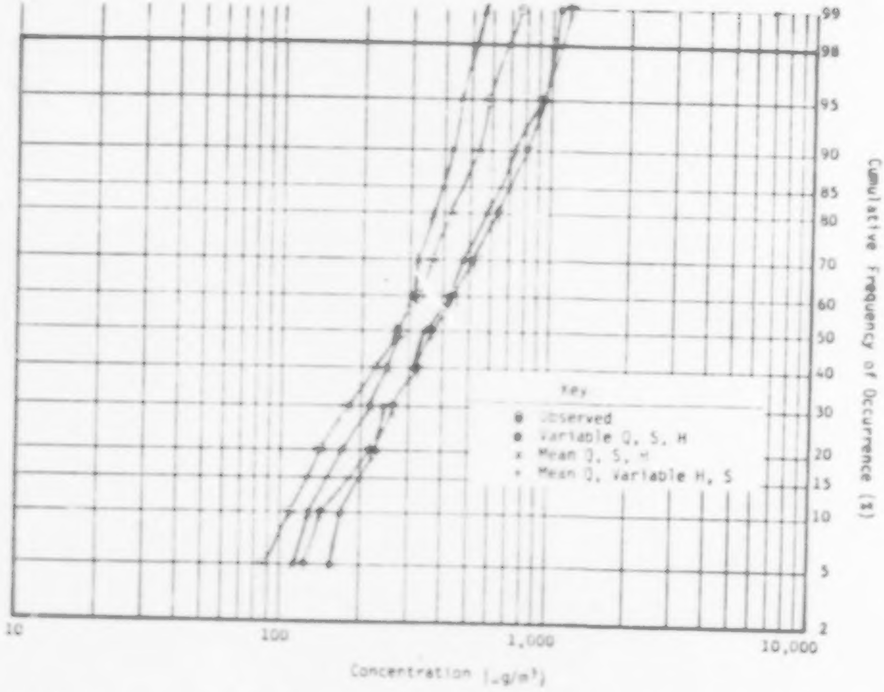

Figure 44. Frequency Distribution of SCIM Calculated and Measured 24-Hour Concentrations for New York City Station #0

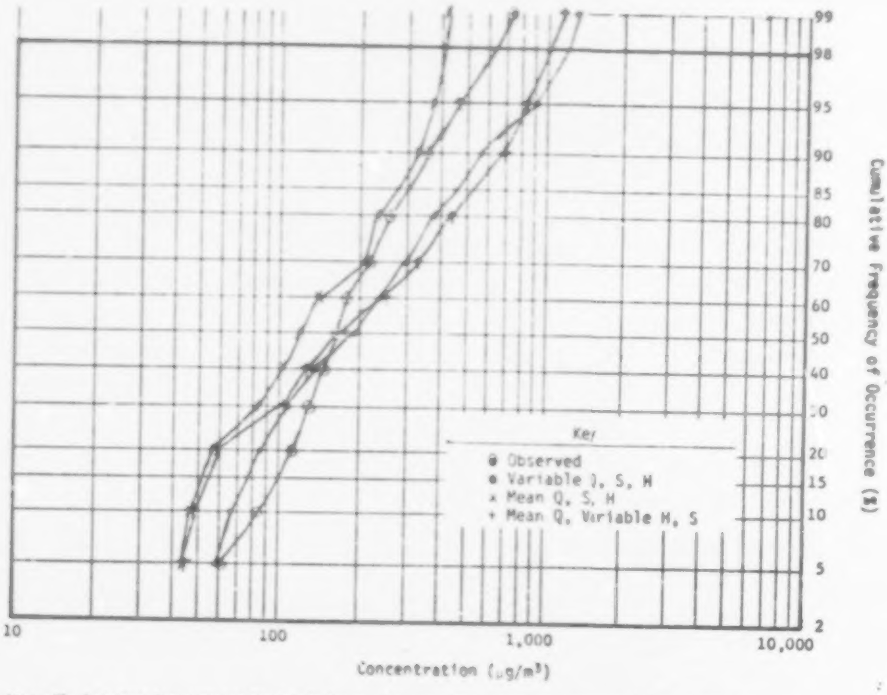

Figure 45. Frequency Distribution of SCIM Calculated and Measured 24-Hour Concentrations for New York City Station #1

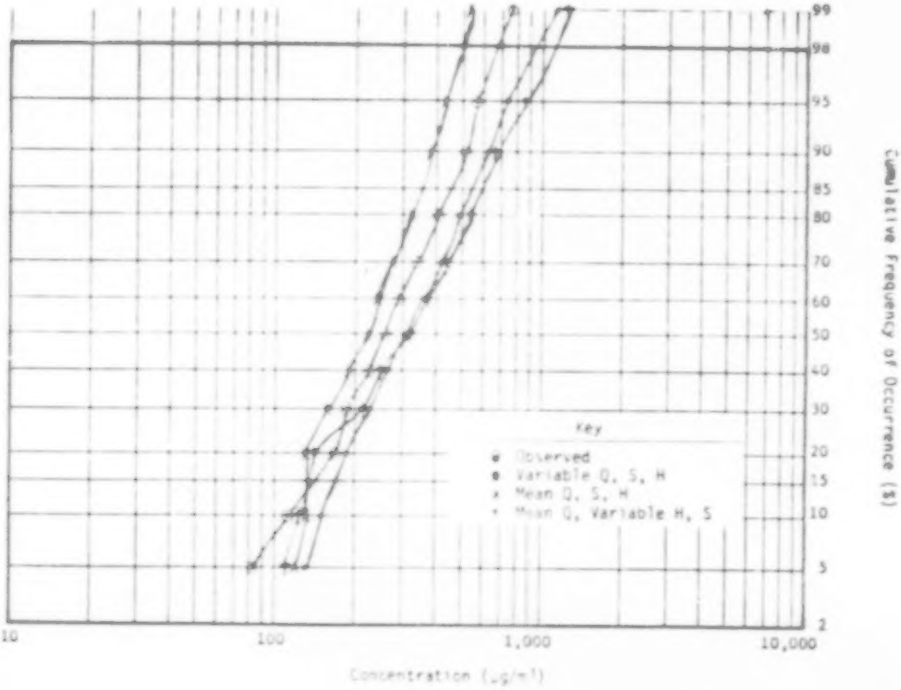

Figure 46. Frequency Distribution of SCIM Calculated and Measured 24-Hour Concentrations for New York City Station #1

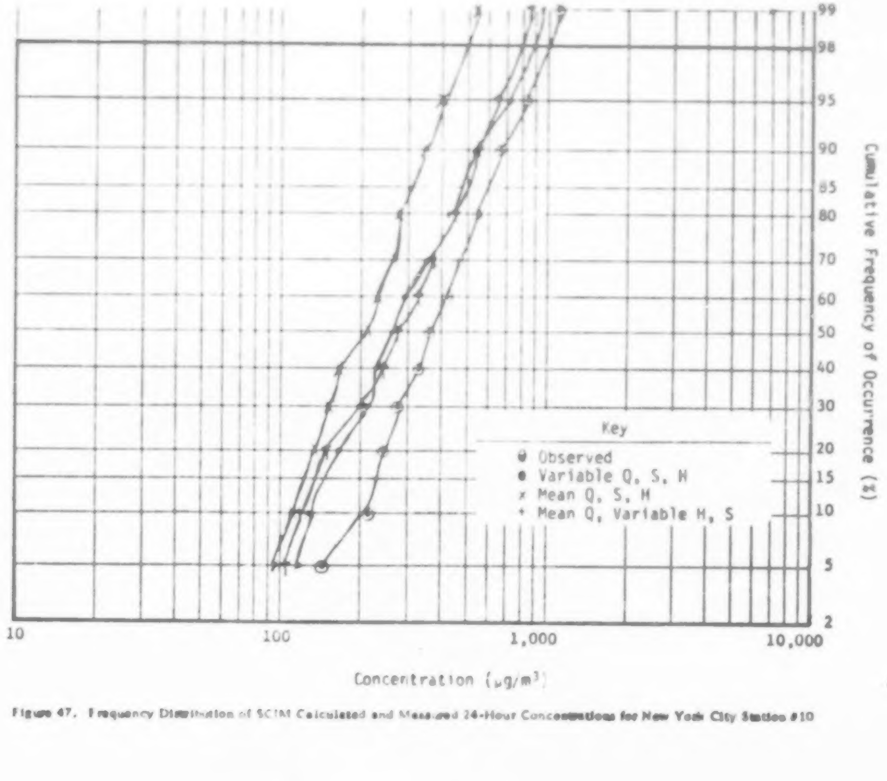

Figure 47. Frequency Distribution of SCIM Calculated and Measured 24-Hour Concentrations for New York City Station #10

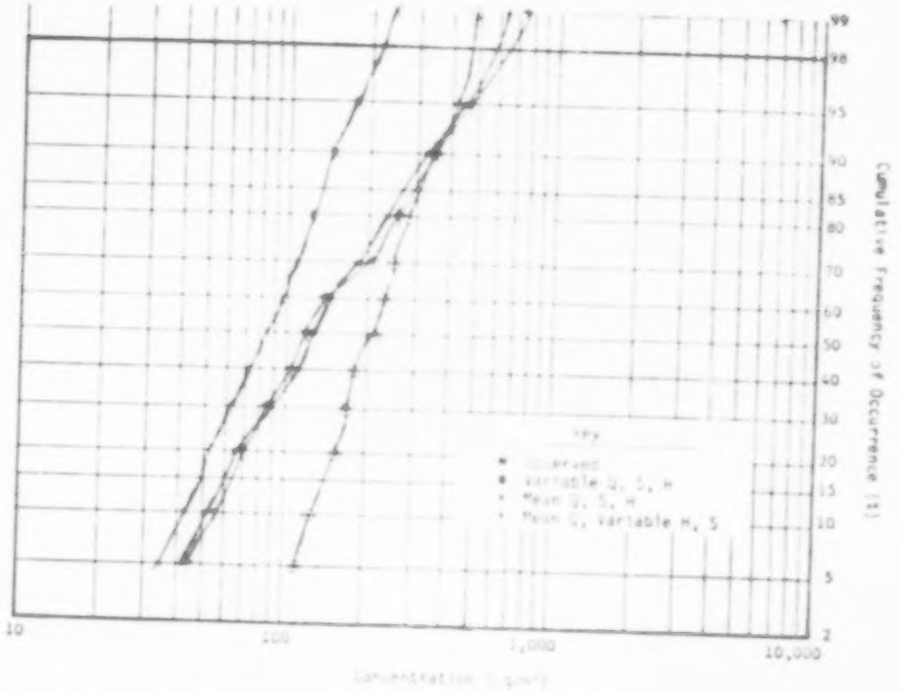

Figure 48. Frequency Distribution of SCIM Calculated and Measured 24-Hour Concentrations for New York City Station #14

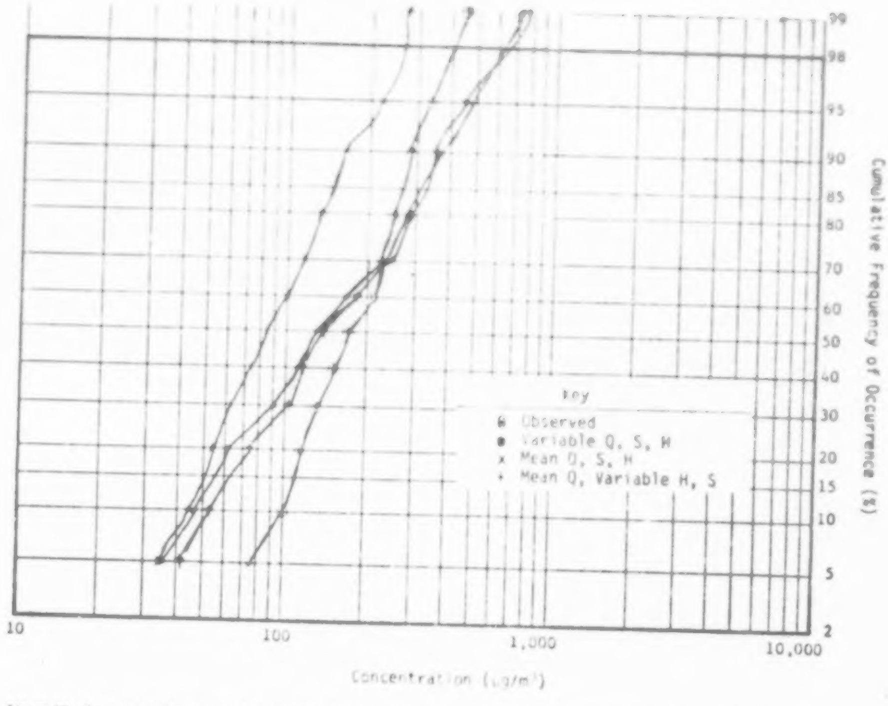

Figure 49. Frequency Distribution of SCIM Calculated and Measured 24-Hour Concentrations for New York City Station #17

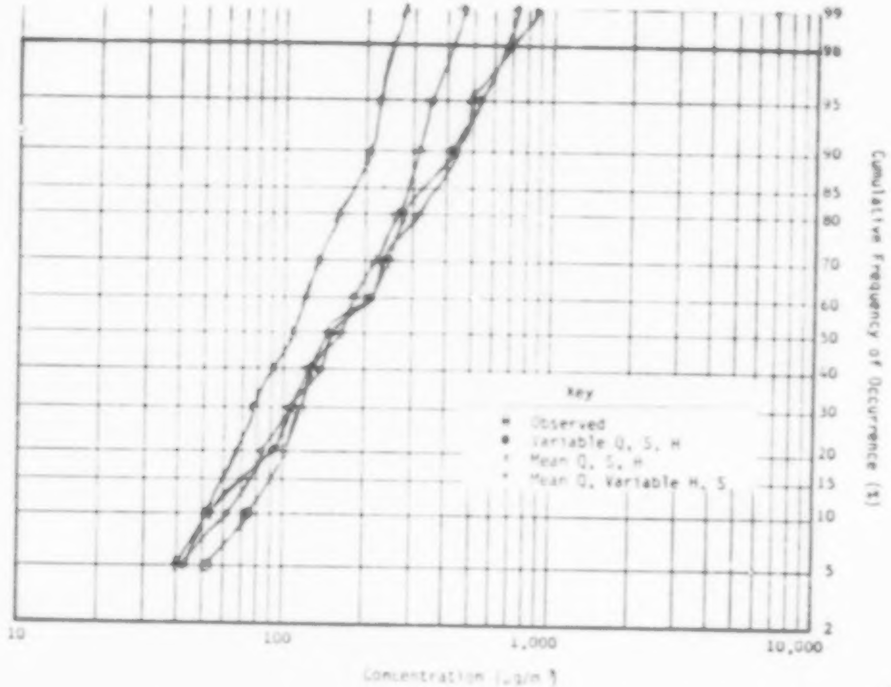

Figure 50. Frequency Distribution of SCIM Calculated and Measured 24-Hour Concentrations for New York City Station #27

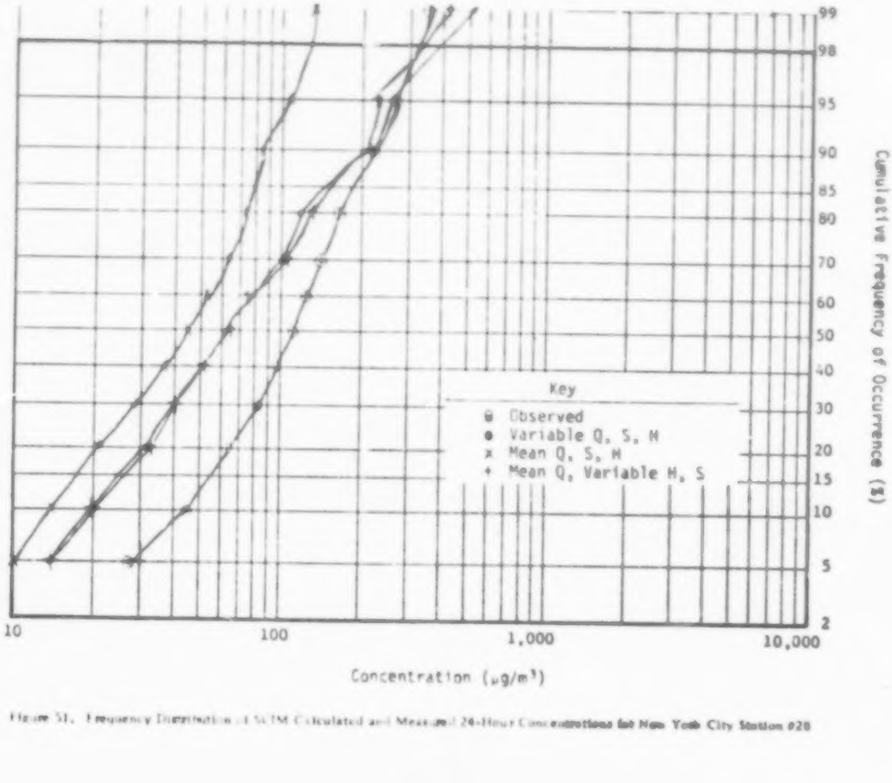

Figure 51. Frequency Distribution of SCIM Calculated and Measured 24-Hour Concentrations for New York City Station #28

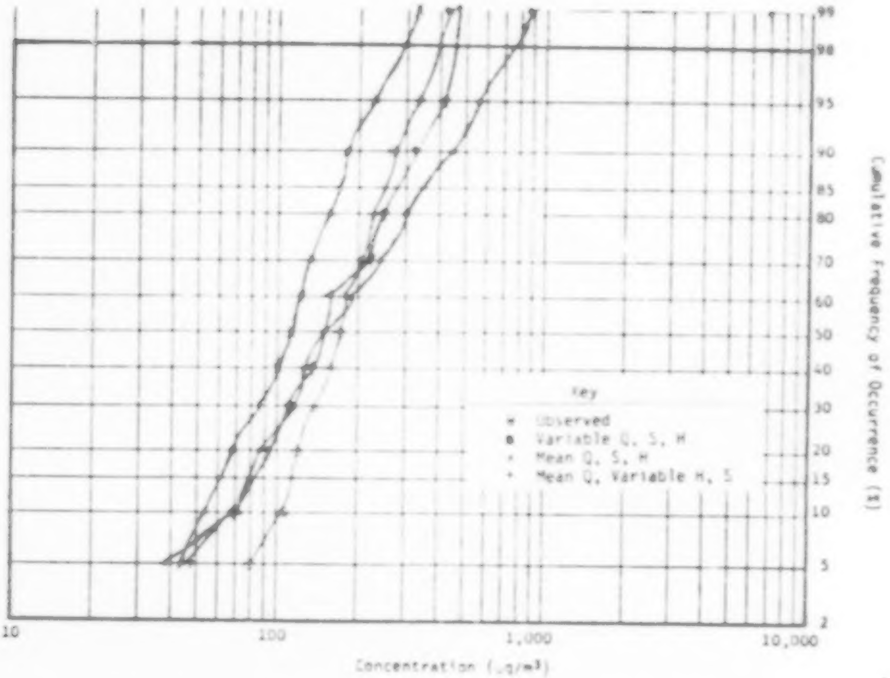

Figure 52. Frequency Distribution of SCIM Calculated and Measured 24-Hour Concentrations for New York City Station #31

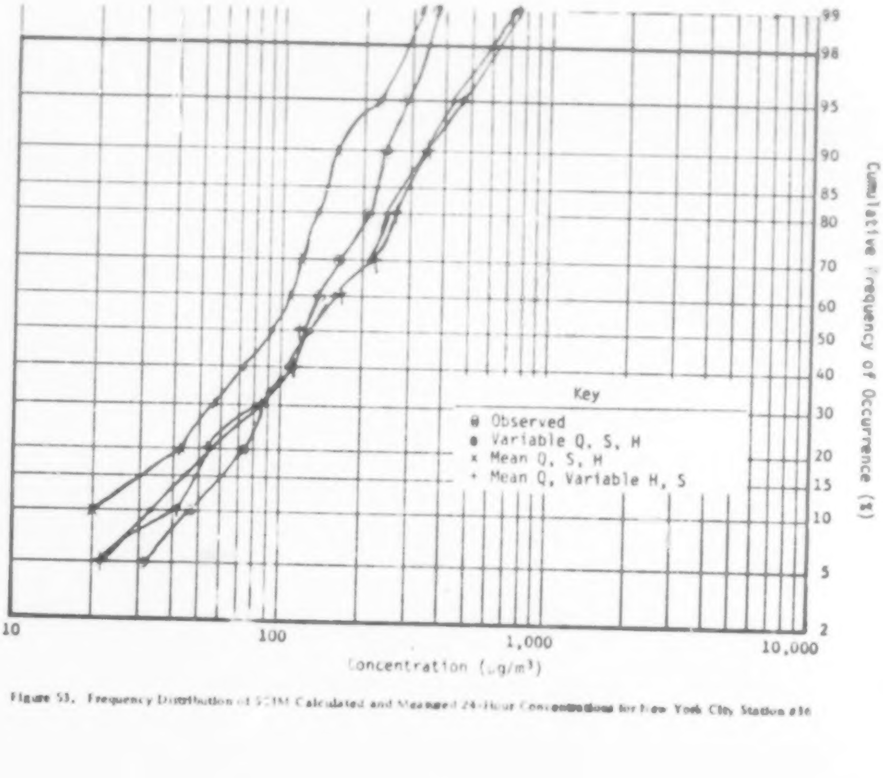

Figure 53. Frequency Distribution of SCIM Calculated and Measured 24-Hour Concentrations for New York City Station #16

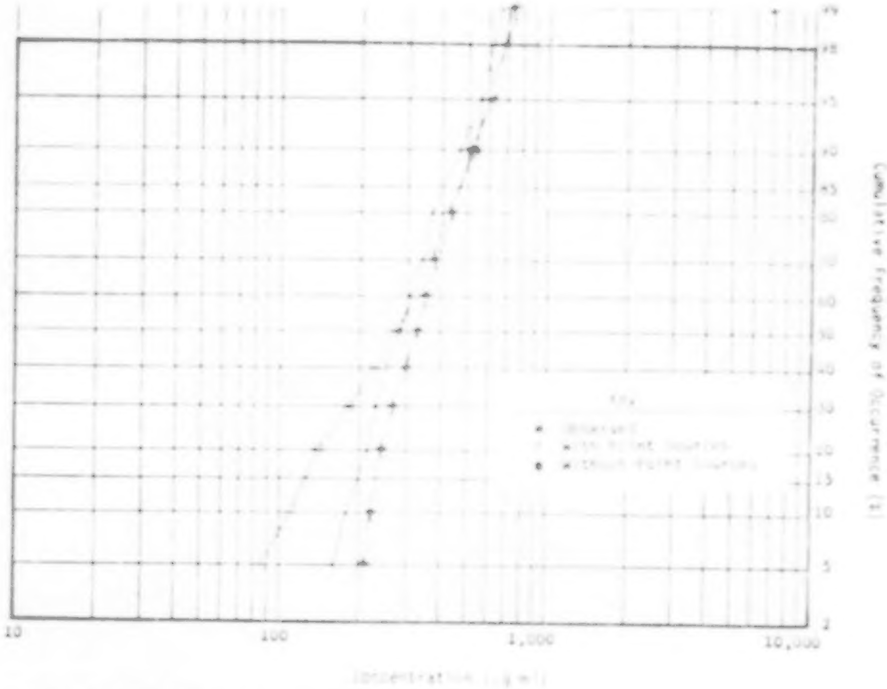

Figure 54. Frequency Distribution of CDM Calculated and Measured 24-Hour SO$_2$ Concentrations for New York City Station #0

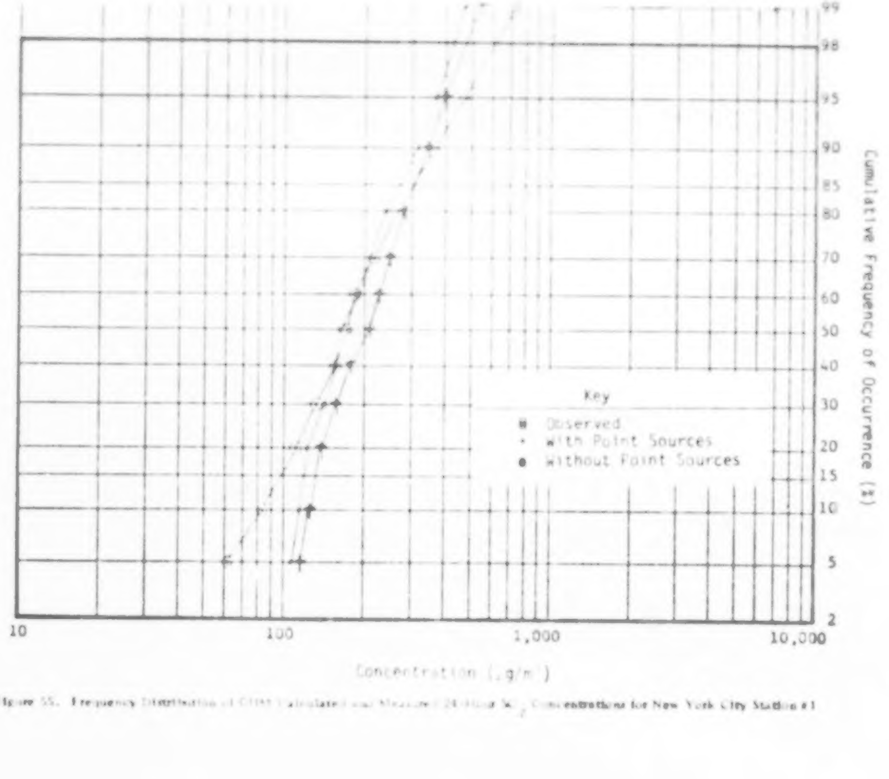

Figure 55. Frequency Distribution of CDM Calculated and Measured 24-Hour SO$_2$ Concentrations for New York City Station #1

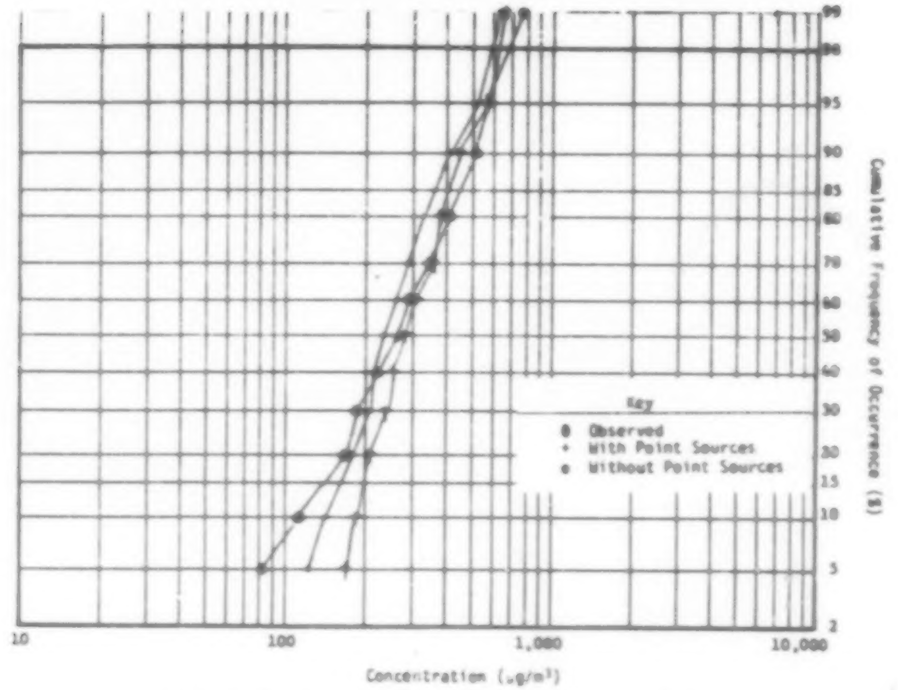

Figure 56. The Frequency Distribution of 24-Hour SO_2 Concentrations for the Two Sets of CHM Calculations and Measured Values for New York City Station #3

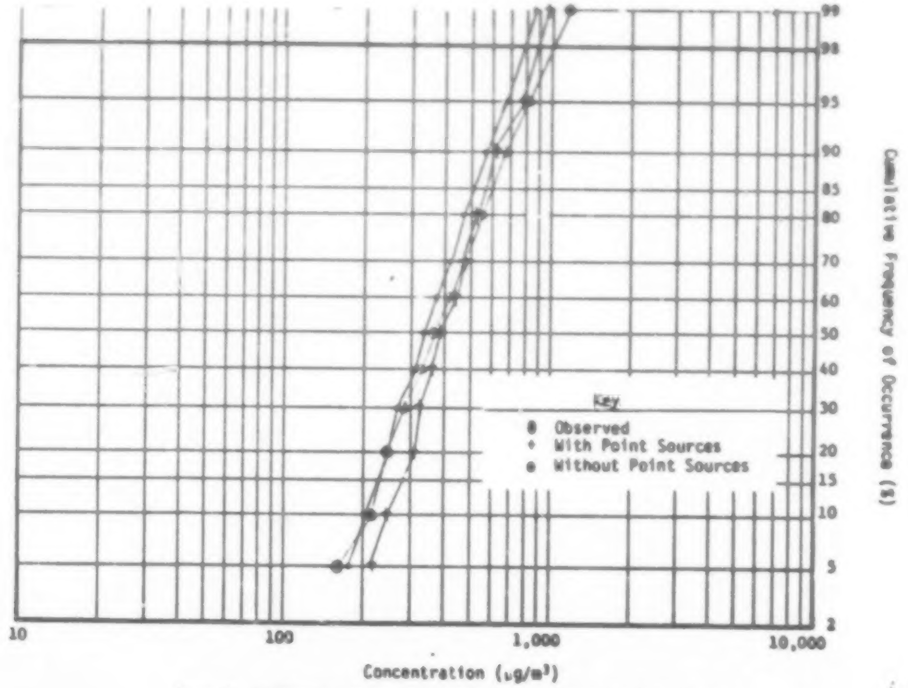

Figure 57. The Frequency Distribution of 24-Hour SO_2 Concentrations for the Two Sets of CHM Calculations and Measured Values for New York City Station #10

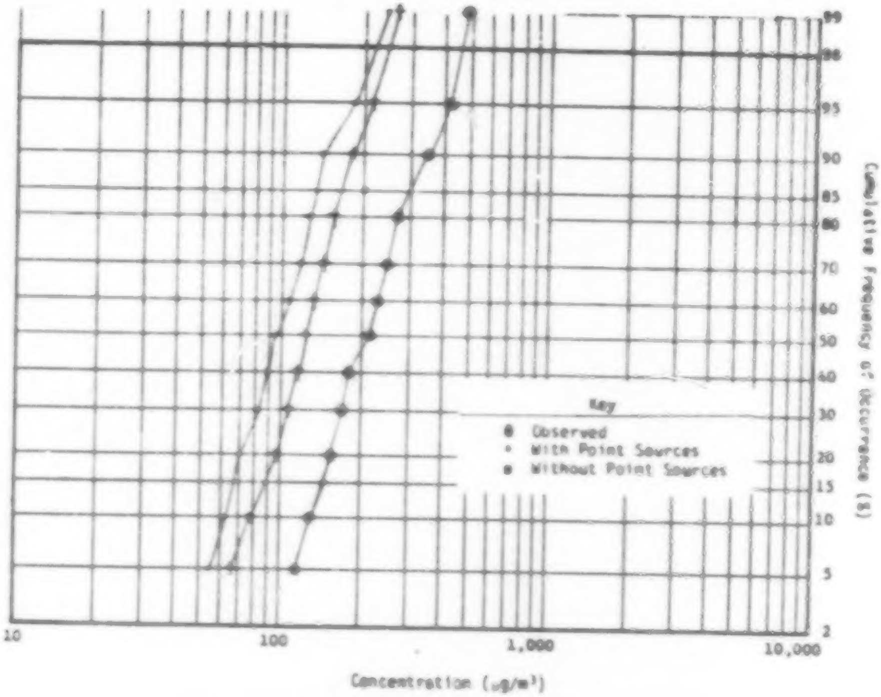

Figure 58. The Frequency Distribution of 24-Hour SO_2 Concentrations for the Two Sets of CHM Calculations and Measured Values for New York City Station #14

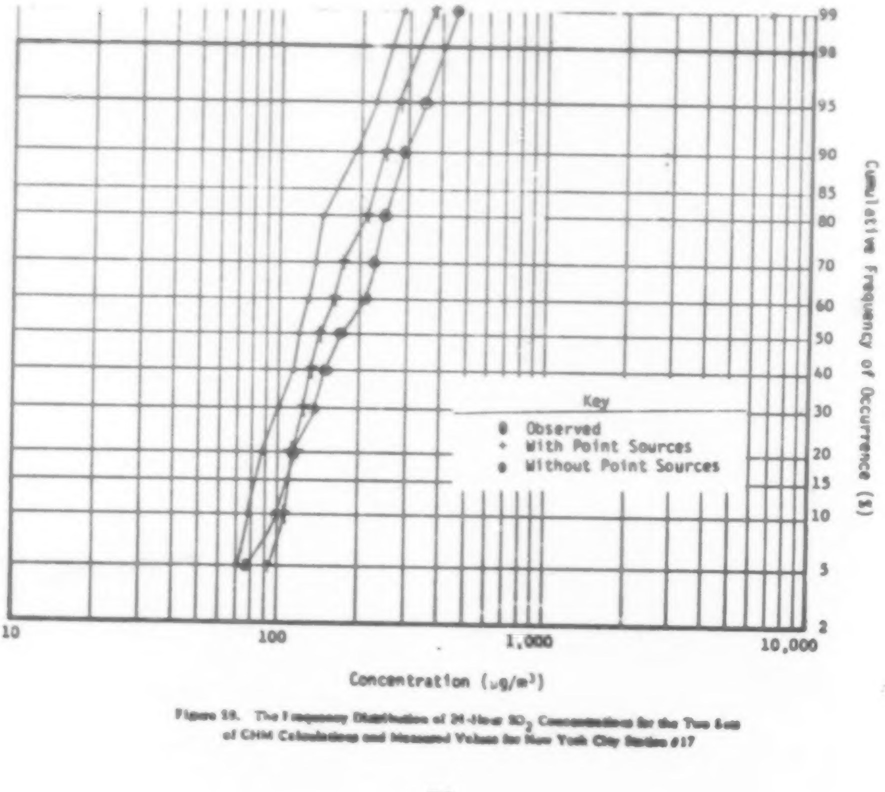

Figure 59. The Frequency Distribution of 24-Hour SO_2 Concentrations for the Two Sets of CHM Calculations and Measured Values for New York City Station #17

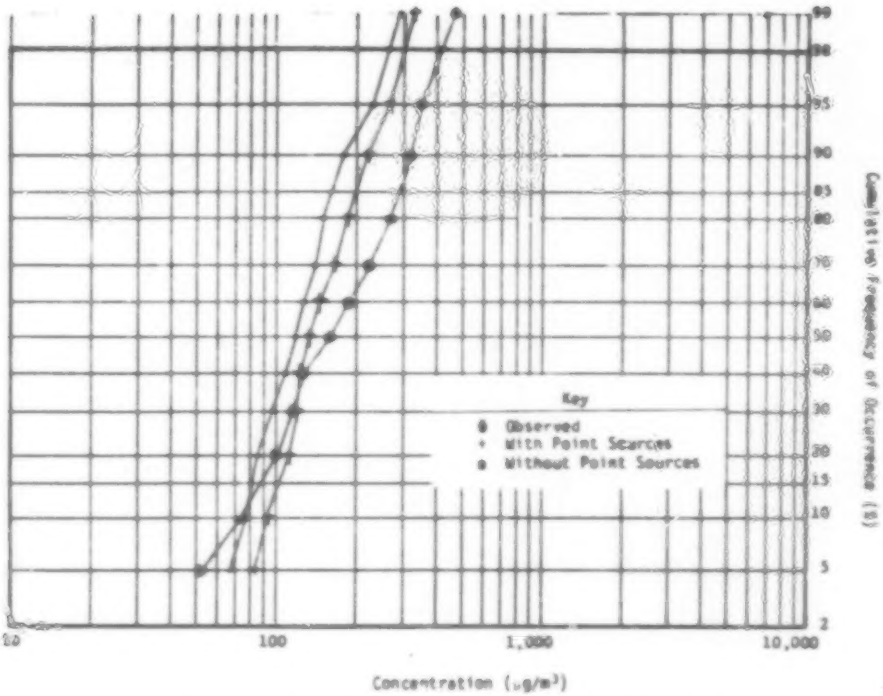

Figure 60. The Frequency Distribution of 24-Hour SO_2 Concentrations for the Two Sets of CDM Calculations and Measured Values for New York City Station #27

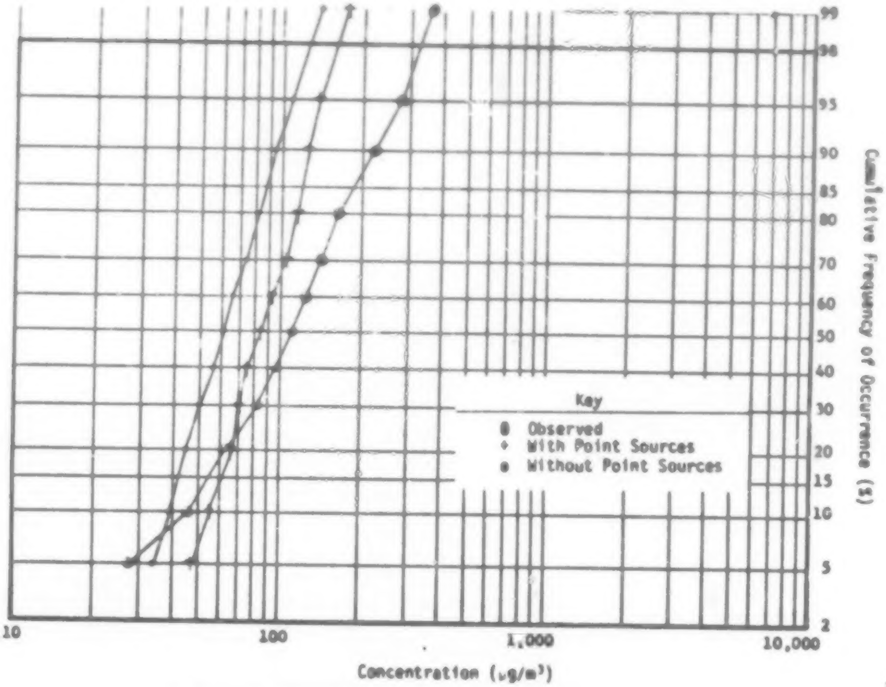

Figure 61. The Frequency Distribution of 24-Hour SO_2 Concentrations for the Two Sets of CDM Calculations and Measured Values for New York City Station #28

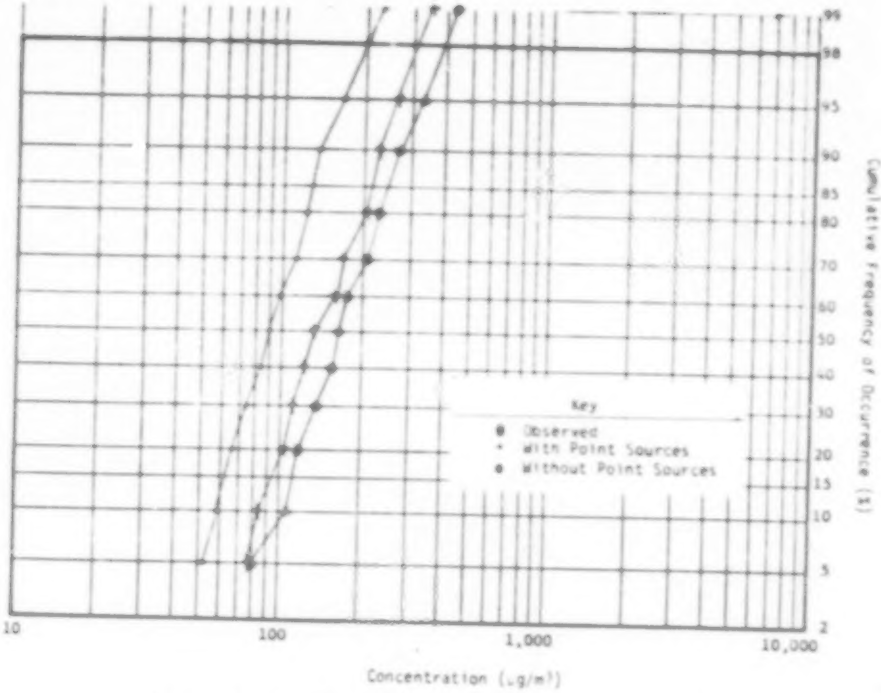

Figure 62. The Frequency Distribution of 24-Hour SO_2 Concentrations for the Two Sets of CHM Calculations and Measured Values for New York City Station #31

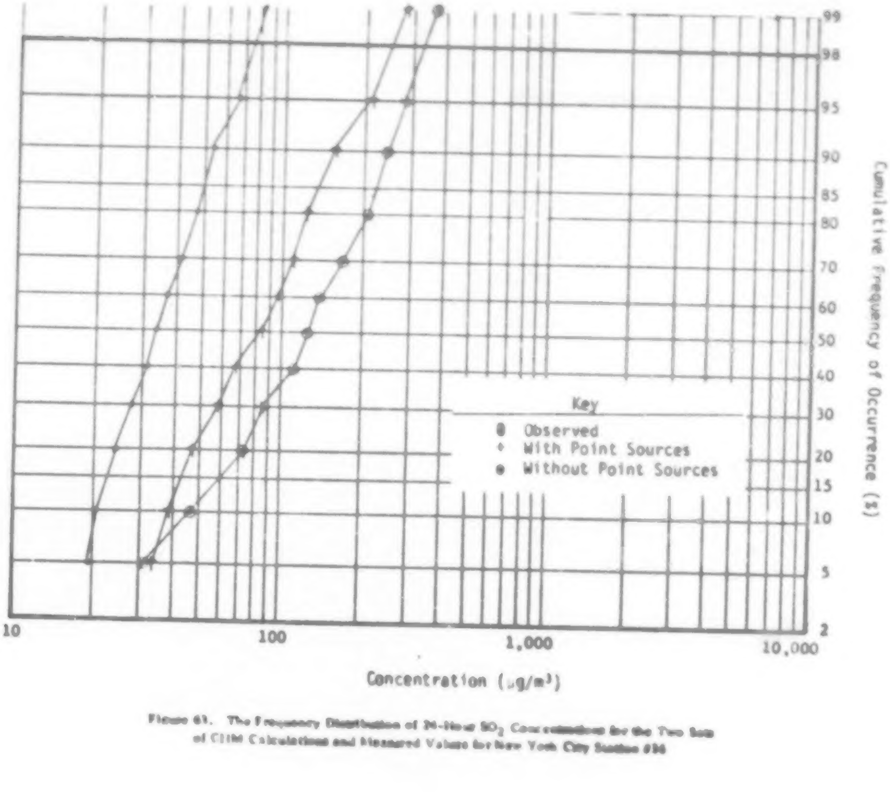

Figure 63. The Frequency Distribution of 24-Hour SO_2 Concentrations for the Two Sets of CHM Calculations and Measured Values for New York City Station #36

Table 9. Model-to-Measurement Comparisons of 24-Hour NYC SO_2 Concentrations by Mean, Standard Deviation, RMSE, MAE and Error at Maximum Measurement

		NYC Station Number									
		0	1	3	10	14	17	27	28	31	36
	Number of Comparisons	364	213	257	268	266	285	281	233	283	245
Mean (μg/m^3)	Measured	303	212	292	420	229	194	185	126	186	144
	SCIM (Variable Q, H, S)	421	281	367	314	170	193	211	99	225	169
	SCIM (Mean Q, Var. H, S)	440	289	384	324	180	197	211	102	229	178
	SCIM (Mean Q, H, S)	283	159	246	226	93	101	118	49	122	102
	GHM (without points)	307	196	268	375	106	130	128	66	99	37
	GHM (with points)	350	227	310	429	131	169	156	90	158	96
Standard Deviation (μg/m^3)	Measured	163	139	163	220	98	89	98	74	76	80
	SCIM (Variable Q, H, S)	241	276	246	188	137	150	160	115	213	141
	SCIM (Mean Q, Var. H, S)	258	276	274	186	150	148	159	110	202	156
	SCIM (Mean Q, H, S)	106	106	112	99	47	58	60	30	63	69
	GHM (without points)	119	83	111	159	43	52	52	25	40	14
	GHM (with points)	121	92	115	166	45	64	55	31	72	57
Root Mean Square (μg/m^3)	SCIM (Variable Q, H, S)	247	261	274	271	133	150	158	120	212	141
	SCIM (Mean Q, Var. H, S)	314	284	309	300	148	161	179	123	204	162
	SCIM (Mean Q, H, S)	192	164	194	313	161	137	126	108	105	100
	GHM (without points)	143	124	190	226	151	111	108	91	115	130
	GHM (with points)	150	121	184	227	126	95	95	81	87	100
Mean Absolute Error (μg/m^3)	SCIM (Variable Q, H, S)	183	164	175	196	106	112	107	84	113	94
	SCIM (Mean Q, Var. H, S)	242	199	206	224	118	115	125	90	122	106
	SCIM (Mean Q, H, S)	161	129	140	232	138	109	100	83	82	75
	GHM (without points)	113	84	135	157	126	86	83	68	96	107
	GHM (with points)	121	87	134	165	103	72	72	58	64	76
	Maximum Measured (μg/m^3)	917	933	1313	1613	607	674	547	446	474	413
Error at Maximum Measured (μg/m^3)	SCIM (Variable Q, H, S)	118	-203	-1112	-1025	-161	-451	-235	-284	-359	-301
	SCIM (Mean Q, Var. H, S)	41	-267	-1129	-1166	-142	-433	-286	-318	-375	-286
	SCIM (Mean Q, H, S)	-528	-619	-1208	-1300	-499	-605	-380	-384	-375	-308
	GHM (without points)	-555	-715	-1125	-804	-485	-520	-249	-352	-376	-326
	GHM (with points)	-443	-628	-1117	-749	-444	-480	-223	-333	-316	-314

Table 10. Model-to-Measurement Comparisons of 24-Hour NYC SO_2 Concentrations by Correlation Coefficients, Variance and Regression Coefficients

		NYC Station Number									
		0	1	3	10	14	17	27	28	31	36
	Number of Comparisons	364	213	257	268	266	285	281	233	283	245
Correlation Coefficient	SCIM (Variable Q, H, S)	0.48	0.42	0.22	0.26	0.51	0.28	0.34	0.28	0.24	0.31
	SCIM (Mean Q, Var. H, S)	0.16	0.27	0.15	0.03	0.41	0.15	0.11	0.18	0.22	0.23
	SCIM (Mean Q, H, S)	0.03	0.22	0.09	-0.05	0.36	0.11	0.14	0.09	0.28	0.27
	GHM (without points)	0.52	0.47	0.09	0.36	0.32	0.24	0.38	0.36	0.27	0.45
	GHM (with points)	0.53	0.52	0.16	0.33	0.50	0.32	0.40	0.25	0.38	0.22
Reduction of Variance by Linear Correlation	SCIM (Variable Q, H, S)	0.23	0.17	0.05	0.07	0.26	0.08	0.12	0.08	0.06	0.10
	SCIM (Mean Q, Var. H, S)	0.02	0.07	0.02	0.00	0.17	0.02	0.01	0.03	0.05	0.05
	SCIM (Mean Q, H, S)	0.00	0.05	0.01	0.00	0.13	0.01	0.02	0.01	0.08	0.07
	GHM (without points)	0.27	0.22	0.01	0.13	0.10	0.06	0.14	0.13	0.07	0.20
	GHM (with points)	0.28	0.28	0.03	0.11	0.25	0.10	0.16	0.06	0.15	0.05
Slope of Regression Line	SCIM (Variable Q, H, S)	0.32	0.21	0.14	0.30	0.34	0.17	0.21	0.18	0.08	0.17
	SCIM (Mean Q, Var. H, S)	0.10	0.14	0.09	0.03	0.25	0.09	0.06	0.12	0.08	0.12
	SCIM (Mean Q, H, S)	0.05	0.29	0.14	-0.11	0.70	0.17	0.22	0.22	0.34	0.31
	GHM (without points)	0.72	0.80	0.13	0.49	0.68	0.41	0.71	1.04	0.51	2.52
	GHM (with points)	0.71	0.80	0.23	0.44	1.00	0.44	0.72	0.59	0.40	0.30
Intercept of Regression Line	SCIM (Variable Q, H, S)	167	153	240	324	172	161	141	108	167	114
	SCIM (Mean Q, Var. H, S)	259	172	257	410	185	177	171	114	167	123
	SCIM (Mean Q, H, S)	289	165	259	444	164	177	159	115	145	112
	GHM (without points)	82	55	257	236	158	140	93	58	136	50
	GHM (with points)	53	31	220	231	98	120	72	73	122	114

of SCIM calculations, the calculations based on variable Q, S and H show the highest correlation with measured values and the closed agreement between calculated and measured means. The smallest root-mean-square errors occurred with the mean Q, S and H calculations. As with the hourly concentrations, the 24-hourly concentrates show that using variable S and H leads to a higher frequency of large overprediction errors and fewer and slightly smaller underprediction errors. The 24-hour comparisons also support the finding that using variable Q and mean Q give similar results with slightly better results (smaller errors, larger correlations) occurring with variable Q.

These results indicate that one possible approach to improving SCIM is to reexamine the means by which stability classifications and mixing layer heights are determined. The present method introduces more error (indicated by MAE and RMSE) than the use of annual mean values; however, there is some skill associated with the use of hourly determinations indicated by the better correlation with measured values. Some improvement in overall results might be expected from using variable Q and mean S and H input. This combination was not tested.

A statistical summary of the model-to-measurement comparisons for 24-hour mean GHM concentrations is given in Tables 9 and 10 for calculation without and with point source contributions. As with the 1-hour concentrations, the 24-hour concentrations show that calculations with point source concentration give slightly but consistently better results over the 10 stations. The calculations with point sources have larger correlation coefficients at 7 stations, smaller RMSE's at 8 stations, and calculated means closer to measured means at 8 stations.

As with the 1-hour comparisons, the 24-hour comparisons show that the variable Q, S and H version of SCIM and the GHM with point sources produced the best results. When these two are compared the results are mixed. The means, mean errors and correlation coefficients are similar for both models. SCIM produced smaller errors in estimating the maximum measured concentration, and GHM produced smaller RMSE's and better regression line characteristics. Favorable regression line characteristics include a slope near unity and an intercept near zero.

3.2.4.3 Selection of a Sampling Interval for Calculating Annual Mean Concentrations with SCIM

It was previously found that many characteristics of the frequency distribution of hourly concentrations over a long-term period can be estimated by calculations for a small sample of the hourly periods included in the long-term period (Koch and Thayer 1971). The annual mean is a characteristic which is particularly well-suited to statistical sampling. A sampling procedure found to be successful is one in which one hour out of a set sampling interval is selected. However, the selection procedure is set up so that all hours of the day are equally represented in the selected sample. The success with which the annual frequency distribution can be represented by various size sampling intervals is shown for 10 New York City locations in Appendix D. With input data available for every 3 hours, Table 11 shows the mean error and root-mean-square error in estimating an annual mean concentration with various size sampling intervals. The error is based on results obtained for 10 New York City locations. An error is defined as the annual mean calculated using a stated sampling interval less the annual mean calculated using all available input data (one set every three hours). On the basis of the results shown in Table 11 it was decided to use a sampling interval of 39 hours in estimating annual mean concentrations with SCIM for New York City. It may be noted that between a sampling interval of 36 hours and 48 hours, the results in Table 11 suggest a sharp upturn in the RMSE associated with the use of proportionate stratified sampling as described here.

Table 11. Summary of Mean Error and RMSE Associated with Various Sampling Intervals for Proportionate Stratified Sampling in SCIM

Sampling Interval (Hours)	Mean Error ($\mu g/m^3$)	Root-Mean-Square Error ($\mu g/m^3$)
3	0.0	0.0
6	-4.8	5.5
9	4.3	4.8
12	-0.1	5.0
18	-2.1	5.5
24	-3.8	5.7
36	1.8	6.1
48	-6.7	11.6
72	6.0	16.5
96	-7.9	29.7

3.2.4.4 Annual Mean SO_2 Concentrations Using Ten Model and Data Conditioning Combinations

The 10 model and input data combinations being compared were described in Section 3.2.1. Each combination was used to calculate annual mean SO_2 concentrations for 75 sampler locations in the New York - New Jersey - Connecticut AQCR for the year 1969; however, the four combinations using the GHM were only used to calculate concentrations at

71 sampler locations. Although the four omitted locations are located near the perphery of the AQCR, it is estimated that their omission does not have an important bearing on the overall evaluation.

A statistical summary of the results obtained for each model and data conditioning combination is given in Table 12. The mean errors vary from -62 $\mu g/m^3$ for the GHM, using mean emission rates and wind speed and without point sources, to 76 $\mu g/m^3$ for the AQDM. The smallest mean error of 3 $\mu g/m^3$ occurred for the CDM with variable stability and mixing layer height. The CDM also produced the smallest root-mean-square error (RMSE) and mean absolute error (MAE). Two of the combinations, CDM with mean stability and mixing layer height and AQDM, had mean errors, RMSE's and MAE's which were notably higher than any of the others. Next to CDM, the GHM combinations with point sources and the two SCIM combinations with variable stability and mixing layer height produced very similar RMSE's and MAE's, which are slightly larger than those for CDM. It may be noted that GHM combinations underestimated while the SCIM combinations overestimated, on the average. All combinations produced high correlations with the measured concentrations; however, the 0.89 value for AQDM led the rest by a slight amount. A desirable regression relationship of measured on calculated values would have a slope of unity and an intercept of zero. No one combination is clearly superior to the others. It may be noted that the smallest intercepts and slope closest to unity occur for different SCIM combinations. The error for the maximum measured value shows best results occurred for two of the GHM combinations and one CDM combination.

Table 12. Model Comparisons for Annual Mean SO_2 Concentrations Using New York City Data

Statistic	SCIM	SCIM $(\overline{Q})$	SCIM $(\overline{Q},\overline{S},\overline{H}_m)$	GHM $(\overline{Q},\overline{U})$	GHM	GHM $(\overline{Q},\overline{U})$ + Points	GHM + Points	AQDM	CDM	CDM $(\overline{S},\overline{H}_m)$
Number of Comparisons	75	75	75	71	71	71	71	75	75	75
Mean Measured ($\mu g/m^3$)	135	135	135	140	140	140	140	135	135	135
Mean Calculated ($\mu g/m^3$)	163	162	88	78	94	107	123	211	138	206
Mean Error ($\mu g/m^3$)	28	27	-47	-62	-46	-33	-17	76	3	71
Root-Mean-Square Error ($\mu g/m^3$)	59	59	65	78	70	58	59	121	52	124
Mean Absolute Error ($\mu g/m^3$)	46	47	50	67	59	46	44	92	37	89
Largest Negative Error ($\mu g/m^3$)	-112	-106	-149	-171	-170	-139	-133	-87	-118	-112
Largest Positive Error ($\mu g/m^3$)	169	162	50	104	162	151	209	310	166	332
Error Range ($\mu g/m^3$)	281	268	200	274	332	290	342	397	284	444
Correlation Coefficient	0.84	0.83	0.82	0.82	0.82	0.83	0.83	0.89	0.84	0.84
Reduction of Variance (%)	71	69	68	67	67	70	69	79	70	71
Slope of Regression Line	0.70	0.70	0.98	0.85	0.70	0.76	0.64	0.45	0.66	0.41
Intercept of Regression Line	20	21	48	74	74	59	61	31	35	40
Maximum Measured ($\mu g/m^3$)	385	385	385	385	385	385	385	350	350	350
Error for Maximum Measured ($\mu g/m^3$)	-47	-58	-149	-75	-11	-10	53	112	-101	13

3.2.4.5 Annual Mean Particulate Concentrations Using Ten Model and Data Conditioning Combinations

Annual mean particulate concentrations were calculated for about 113 sampling locations in the New York - New Jersey - Connecticut AQCR using each of the 10 model and data conditioning combinations described in Section 3.2.1. A statistical summary of the model-to-measurement comparisons obtained for each combination is given in Table 13. A background concentration of 35 $\mu g/m^3$ was added to all model calculations.

The smallest mean errors were produced by the two CDM combinations. However, the mean errors were small for all 10 combinations, varying from -24 to 22 $\mu g/m^3$ compared to a measured mean of 82 $\mu g/m^3$. The same relatively small RMSE and MAE were obtained for the two SCIM combinations and the CDM combination which use variable stability and mixing layer height. The largest positive error was notably lower for the SCIM and SCIM ($\overline{Q}$) combinations than for any of the others. This resulted in a notably smaller error range. Except for the SCIM ($\overline{Q}, \overline{S}, \overline{H}_m$) combination, for which correlation coefficient was low, all the correlation coefficients were similar. The highest correlation coefficients occurred for the SCIM and SCIM ($\overline{Q}$) combinations. The SCIM and SCIM ($\overline{Q}$) also produced the best regression of measured on calculated values, having both the smallest intercepts and the slopes most nearest to unity. The smallest errors for the maximum measured concentration occurred for the AQDM and CDM ($\overline{S}, \overline{H}_m$) combinations.

Table 13. Model Comparisons for Annual Mean Particulate Concentrations Using New York City Data

Statistic	SCIM	SCIM $(\bar{Q})$	SCIM $(\bar{Q},\bar{S},\bar{H}_m)$	GHM $(\bar{Q},\bar{U})$	GHM	GHM $(\bar{Q},\bar{U})$ + Points	GHM + Points	AQDM	CDM	CDM $(\bar{S},\bar{H}_m)$
Number of Comparisons	114	114	114	112	112	112	112	113	113	113
Mean Measured ($\mu g/m^3$)	81	81	81	82	82	82	82	82	82	82
Mean Calculated ($\mu g/m^3$)	69	69	58	92	104	101	113	102	74	88
Mean Error ($\mu g/m^3$)	-12	-13	-24	11	22	19	31	20	-8	6
Root-Mean-Square Error ($\mu g/m^3$)	22	22	55	60	77	64	82	36	22	28
Mean Absolute Error ($\mu g/m^3$)	16	16	33	36	44	38	47	28	16	21
Largest Negative Error ($\mu g/m^3$)	-68	-66	-83	-66	-63	-61	-57	-51	-63	-60
Largest Positive Error ($\mu g/m^3$)	-43	39	463	325	405	338	419	115	68	98
Error Range ($\mu g/m^3$)	110	106	546	391	468	400	475	166	131	158
Correlation Coefficient	0.68	0.68	0.30	0.66	0.66	0.67	0.67	0.62	0.61	0.64
Reduction of Variance (%)	46	46	9	43	43	45	45	39	37	41
Slope of Regression Line	0.78	0.80	0.13	0.21	0.18	0.21	0.17	0.38	0.63	0.42
Intercept of Regression Line	28	26	74	62	63	61	62	43	35	45
Maximum Measured ($\mu g/m^3$)	169	169	169	169	169	169	169	169	169	169
Error for Maximum Measured ($\mu g/m^3$)	-54	-52	-83	150	208	161	219	5	-48	-6

Section 4.0

CONCLUSIONS

Conclusions (1-5) regarding the use of the Sampled Chronological Input Model (SCIM), a multiple-source Gaussian plume model, to estimate short-term SO_2 concentrations (e.g., 1-hour and 24-hour concentrations) are based on model-to-measurement comparisons for 1 month of Chicago, 3 months of St. Louis and 1 year of New York City (NYC) data. The model was analyzed using NYC data for three types of inputs, including: (1) variable emission rates, stability classifications and mixing heights (variable Q, S, H), (2) mean emission rates and variable stability classifications and mixing heights (mean Q, variable S, H), and (3) mean emission rates, stability classifications and mixing heights (mean Q, S, H). The model was analyzed using St. Louis and Chicago data for the first two types of input. For comparison purposes, an analysis was also made of the use of the simplified Gifford-Hanna Model (GHM).

1. Comparing the results for the three types of input to SCIM, it is concluded that:

- Use of a mean, rather than a variable, emission rate may either increase or decrease the root-mean-square error (RMSE) at a receptor but will decrease the correlation with measurements (observed at 10 of 10 St. Louis receptors for 2-hour concentrations, 5 of 8 Chicago receptors for 1-hour concentrations, and 10 of 10 NYC receptors for 1-hour and 24-hour concentrations).
- Based on comparisons using NYC data and mean emission rates, the use of a neutral stability classification and a mean mixing height will decrease the RMSE at a receptor (observed at 9 of 10 receptors for 1-hour concentrations and 8 of 10 receptors for 24-hour concentrations).

- Based on NYC comparisons, the combined use of a mean emission rate and mixing height and a neutral stability classification will decrease the correlation with measurements but will also decrease the RMSE (observed at 10 of 10 receptors for 1-hour concentrations and 7 of 10 receptors for 24-hour concentrations).

2. In evaluating GHM, it was concluded that adding point source contributions (i.e., calculated using SCIM) to GHM calculations improved the results for this model. The RMSE was smaller at 6 of 10 NYC receptors, the correlation coefficient was higher at 6 of 10 receptors, and the standard deviation of calculated concentrations was closer to the standard deviation of measured concentrations at all 10 receptors.

3. Comparing SCIM and GHM based on NYC data, SCIM produced the least annual mean error at 6 of 10 receptors, the closer agreement between standard deviations of calculated and measured concentrations at 5 of 10 receptors, the least error in estimating the maximum measured concentration at 6 of 10 receptors, and the highest correlation coefficient at 3 of 10 receptors; GHM produced the least RMSE at all 10 receptors.

4. There is a need to improve the input data used with the multiple-source Gaussian plume type of model, particularly atmospheric stability information, since the model is very sensitive to the rather gross changes in stability which are routinely introduced. SCIM calculations on the average, greatly overestimated concentrations associated with Turner-Pasquill stability classes 2 and 5.

5. Calculations based on a NYC emission algorithm developed in this report, particularly when applied with GHM, generally agree with diurnal and temperature dependent trends in measured SO_2 concentrations. Further improvements in this algorithm are desirable but require more detailed information.

Conclusions (6-8) regarding the use of several versions of the multiple-source Gaussian plume model and GHM to estimate long-term mean concentrations of SO_2 and particulates are based on model-to-measurement comparisons for the same data periods and locations.

6. The use of variable emission rates for SCIM and GHM are not able to demonstrate any conclusive improvement in model validity over the use of mean emission rates. It is inferred that this result is due to the failure to properly treat other causes of variance, such as those associated with atmospheric stability.

7. Based on results for NYC, the Climatological Dispersion Model (CDM) and SCIM versions of the multiple-source Gaussian plume model produce a smaller station-to-station RMSE than the Air Quality Display Model (AQDM) version (i.e., RMSE's of 52 and 59, respectively, compared to 92, with an overall mean of 135 $\mu g/m^3$ of SO_2; RMSE's of 22 and 22 compared to 36 with a overall mean of 82 $\mu g/m^3$ of particulates).

8. Although the NYC validation statistics for GHM, CDM, and SCIM are similar for SO_2, GHM results for particulates have a much higher station-to-station RMSE than do CDM and SCIM (i.e., RMSE of 60 compared to 22, with an overall mean of 82 $\mu g/m^3$).

Section 5.0

REFERENCES

Blade, E. and E.F. Ferrand. 1969. Sulfur Dioxide Air Pollution on New York City: Statistical Analysis of Twelve Years. Journal of the Air Pollution Control Association, Volume 19, Number 11, pp. 873-878.

Briggs, G.A. 1969. Plume Rise. AEC Critical Review Series. U.S. Atomic Energy Commission, Division of Technical Information. (Available as TID-25075 from NTIS.)

Calder, Kenneth L. 1970. "Some Miscellaneous Aspects of Current Urban Pollution Models" from Stern (ed.), Proceedings of Symposium on Multiple-Source Urban Diffusion Models. U.S. Environmental Protection Agency, Air Pollution Control Office, Research Triangle Park, North Carolina.

Calder, K.L. 1971. A Climatological Model for Multiple Source Urban Air Pollution. Proceeding 2nd Meeting of the Expert Panel on Air Pollution Modeling. NATO Committee on the Challenges of Modern Society, Paris, France.

Chamot, C. et al. 1970. A Computerized Air Pollution Data Management System APICS. ANL/ES-CC-006, Argonne National Laboratory, Argronne, Illinois.

Gifford, F.A. 1972. Applications of a Simple Urban Pollution Model. Preprints Conference on Urban Environment and Second Conference on Biometeorology, Philadelphia, October 31-November 2, 1972. pp. 62-63. American Meteorological Society. Boston, Massachusetts.

Gifford, F.A. and S.R. Hanna. 1973. Modeling Urban Air Pollution. Atmospheric Environment 7, pp. 131-136.

Haltiner, G.J. and F.L. Martin. 1957. Dynamical and Physical Meteorology. McGraw-Hill, New York.

Hanna, S.R. 1971. A Simple Method of Calculating Dispersion from Urban Area Sources. Journal of the Air Pollution Control Association, Volume 21, Number 12, pp. 774-777.

Holzworth, G.C. 1972. Mixing Heights, Wind Speeds, and Potential for Urban Air Pollution Throughout the Contiguous United States. AP-101, U.S. Environmental Protection Agency, Office of Air Programs, Research Triangle Park, North Carolina. (Available from GPO.)

Koch, R.C. and S.D. Thayer. 1971. Validation and Sensitivity Analysis of the Gaussian Plume Multiple-Source Urban Diffusion Model. GEOMET Report Number EF-60. GEOMET, Inc., Rockville, Maryland.

Martin, Delance O. and Joseph A. Tikvart. 1968. A General Atmospheric Diffusion Model for Estimatimating the Effects of One or More Sources on Air Quality. Presented at 61st Annual Meeting of the Air Pollution Control Association, St. Paul, Minnesota. June 1968. APCA-68-148.

McElroy, J.L. 1969. A Comparative Study of Urban and Rural Dispersion. Journal Applied Meteorology 8, pp. 19-31.

Roberts, J.J. et al. 1970. Chicago Air Pollution Systems Analysis Program: A Multiple-Source Urban Atmospheric Dispersion Model, ANL/ES-CC-007, Argonne National Laboratory, Argonne, Illinois.

NOAA Environmental Data Service, 1968. Climatic Atlas of the United States, U.S. GPO, Washington, D. C.

Singer, I.A., Y.B. Lee, C.M. Nagle and D.H. Slade. 1970. Comparative Studies of Urban and Rural Wind Climatology. Proceedings of Seminar Wind Loads on Structures, ed. A.N.L. Chiu, Held at University of Hawaii, Honolulu, Hawaii, October 19-24, 1970, pp. 39-53. (Available from NTIS, PB203449.)

Saucier, W.J. 1955. Principles of Meteorological Analysis. The University of Chicago Press, Chicago, Illinois.

TRW Systems Group. 1969. Air Quality Display Model. Contract Number PH 22-68-60. Prepared for Department of HEW, Public Health Service Consumer Protection and Environmental Health Service, National Air Pollution Control Administration, Washington, D. C. (Available from CFSTI as PB189194.)

Turner, D.B. 1964. A Diffusion Model for an Urban Area. Journal Applied Meteorology 3, pp. 83-91.

Turner, D.B. 1968. The Diurnal and Day-to-Day Variations of Fuel Usage for Space Heating in St. Louis, Missouri. Atmospheric Environment, Volume 2, pp. 339-351.

Turner, D.B., J.R. Zimmerman, and A.D. Busse. 1972. An Evaluation of Some Climatological Dispersion Models. Proceedings of the Third Meeting of the Expert Panel on Air Pollution Modeling, October 2-3, 1972, Paris, France. Published by Air Pollution Technical Information Center, Office of Air and Water Programs, Environmental Protection Agency, Research Triangle Park, North Carolina, 27711.

Appendix A

AN ALGORITHM FOR ESTIMATING AREA SOURCE SO_2 EMISSION RATES

A.1 BASIS FOR NEW YORK CITY HOURLY SO_2 EMISSION RATE ALGORITHM

An algorithm has been developed for estimating SO_2 emissions in New York City from area sources. It is designed to use the emissions data prepared for the Air Quality Implementation Planning Program (IPP). The IPP area source data consists of a single annual source emission rate for each grid square. The area source algorithm developed here is cast in a general framework so that it can be applied to any large city where IPP area source data, or its equivalent, are available. The area source emissions are assumed to be due primarily to residential and commercial space heating requirements and to be functions of the ambient air temperature and of hour of the day.

It is recognized that annual emissions occur as a function of both diurnal and seasonal influences resulting from climate and weather, and from patterns of human activities. The weakness of previous attempts to estimate these effects directly from emission information is illustrated in Table 4 of the main body of this report. Another source of data, namely SO_2 concentration measurements from centralized downtown sampling stations, was used in this study to describe the annual distribution of emissions. The obvious disadvantage of using this data to model emissions is that systematic variations due to meteorological effects such as atmospheric stability and wind speed will be included both in the emissions estimates and in the diffusion model. However, the double effect may be small since it is only the consistent long-term effects which are being represented in the emissions. For instance, the average wind speed in summer (8 mph) is only slightly less than the average wind speed in winter (11 mph) (NOAA Environmental Data Service 1968). Also, the consistent diurnal variation in atmospheric stability from unstable in the afternoon to stable in the early morning is reduced in the city by increased roughness and thermal emissions.

Data from a study by Blade and Ferrand (1969) of the SO_2 concentrations in New York City were used to formulate an emission algorithm. They analyzed a large set (12 years of almost continuous hourly observations) of SO_2 concentrations. They summarized the data by hour of the day, day of the week, and week and month of the year. They also investigated the functional relationship between normal temperature and SO_2 concentration. Blade and Ferrand present diurnal curves of the mean hourly SO_2 levels for each calendar month. There are peaks in the concentrations at 7 a.m. and 7 p.m.; these peaks being most pronounced in the winter season. The area source algorithm described here is based on values extracted from these 12 diurnal curves. No discrimination is made between weekdays and weekends since only a small difference was found in Blade and Ferrand's study.

The first step in the formulation of the algorithm was to find the mean hourly SO_2 concentration and temperature for each hour of the day for each month of the year. Climatological temperature data from LaGuardia Airport for the period 1962-1971 were used to obtain mean hourly temperatures for each month. A graph was prepared for each hour of the day of the 12 mean monthly SO_2 concentrations versus the respective climatological temperatures. As examples, the two graphs for Hours 0 and 9 are shown together in Figure A-1.

Excluding the values for the four warm season months (June-September), the SO_2 concentrations closely approximate a linear function of temperature. A mean of the hourly concentrations for the four warm season months was used to represent a "base" level. A straight line was fitted to the remaining eight data points. The temperature at which the line intersected the base level was taken to be the "threshold" temperature at which space heating would just be required for that hour. The slopes of the straight lines, the base levels, and the threshold temperatures were plotted as a function of hour of the day and fitted by smooth curves. The adjusted values of base level, threshold temperature and slope read from the curves for each hour of the day are shown in Table A-1. The base level values have been normalized by dividing by the sum of the 24 values. Each slope value gives the rate of change of SO_2 concentration with temperature. This is assumed to be equal to the rate of change of space heating emissions with temperature. The base level concentration is assumed to be proportional to the non-temperature dependent emissions. For the present, the units of the emission rates (both space heating and non-temperature dependent sources) are undefined and will be designated as index values. The index values were determined in terms of measured SO_2 concentrations but will be multiplied by an appropriate scaling factor later. The 24-hour threshold temperatures are shown in Figure A-2, where for comparison two climatologically normal days are included, one representing a fall or spring day with a mean temperature of 65°F and the other

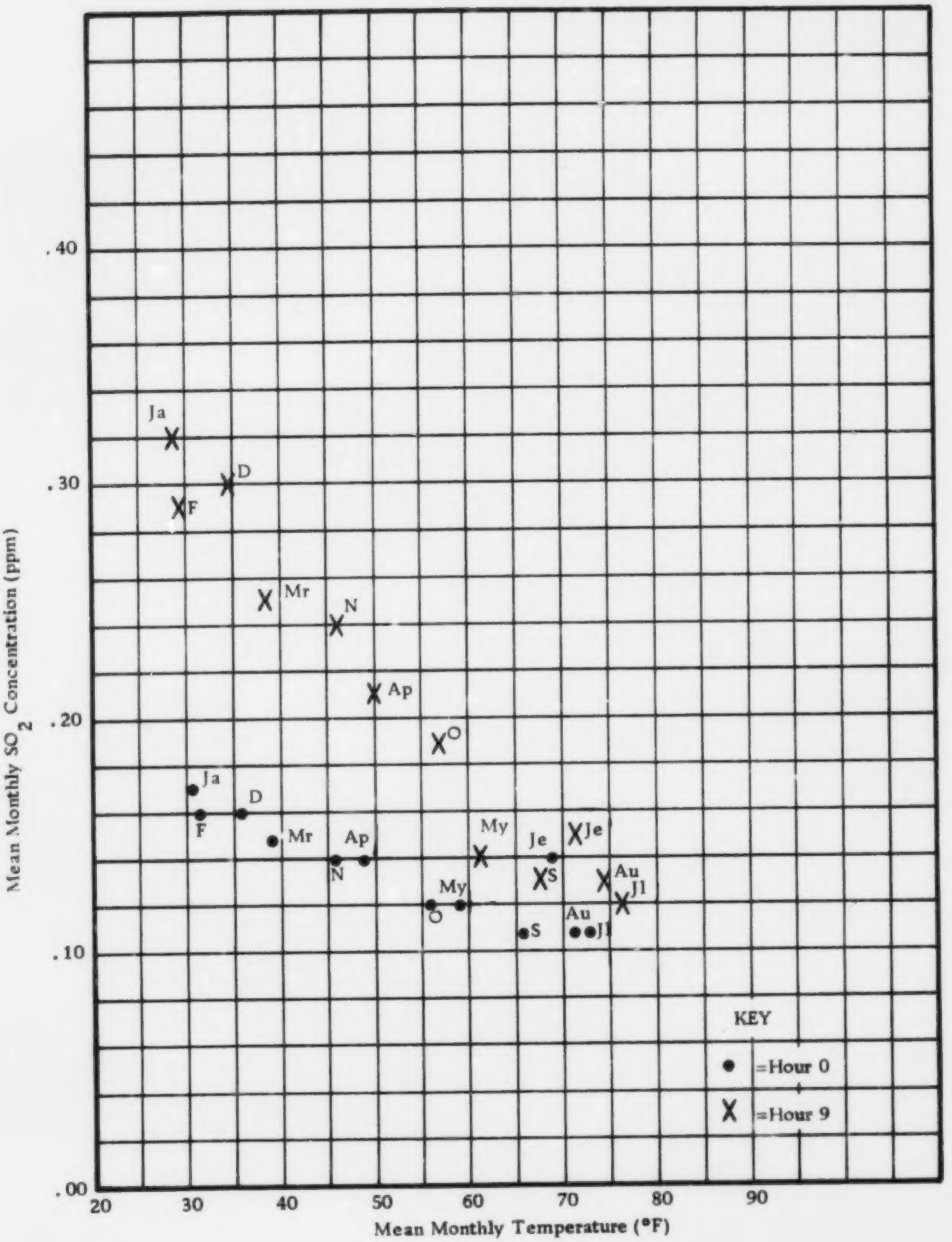

Figure A-1. Relation Between Mean Monthly Concentrations of SO_2 and Temperature for Hours 0 and 9

Table A-1. Numerical Values for Constants in the New York City Emission Algorithm

Hour	Base Level Emission Factor (J_i) (day/hr)	Temperature Sensitivity Threshold (T_i) (°F)	Temperature Sensitivity Factor I_i (Index/°F)
0	0.0428	56	0.0161
1	0.0417	55	0.0137
2	0.0399	55	0.0137
3	0.0399	55	0.0143
4	0.0431	56	0.0181
5	0.0491	58	0.0350
6	0.0543	59	0.0590
7	0.0550	61	0.0702
8	0.0526	63	0.0593
9	0.0484	64	0.0477
10	0.0421	65	0.0436
11	0.0389	65	0.0411
12	0.0365	65	0.0411
13	0.0343	65	0.0416
14	0.0340	65	0.0418
15	0.0340	65	0.0433
16	0.0343	65	0.0480
17	0.0351	65	0.0518
18	0.0368	65	0.0547
19	0.0386	65	0.0558
20	0.0406	65	0.0544
21	0.0421	64	0.0500
22	0.0428	62	0.0340
23	0.0431	60	0.0203

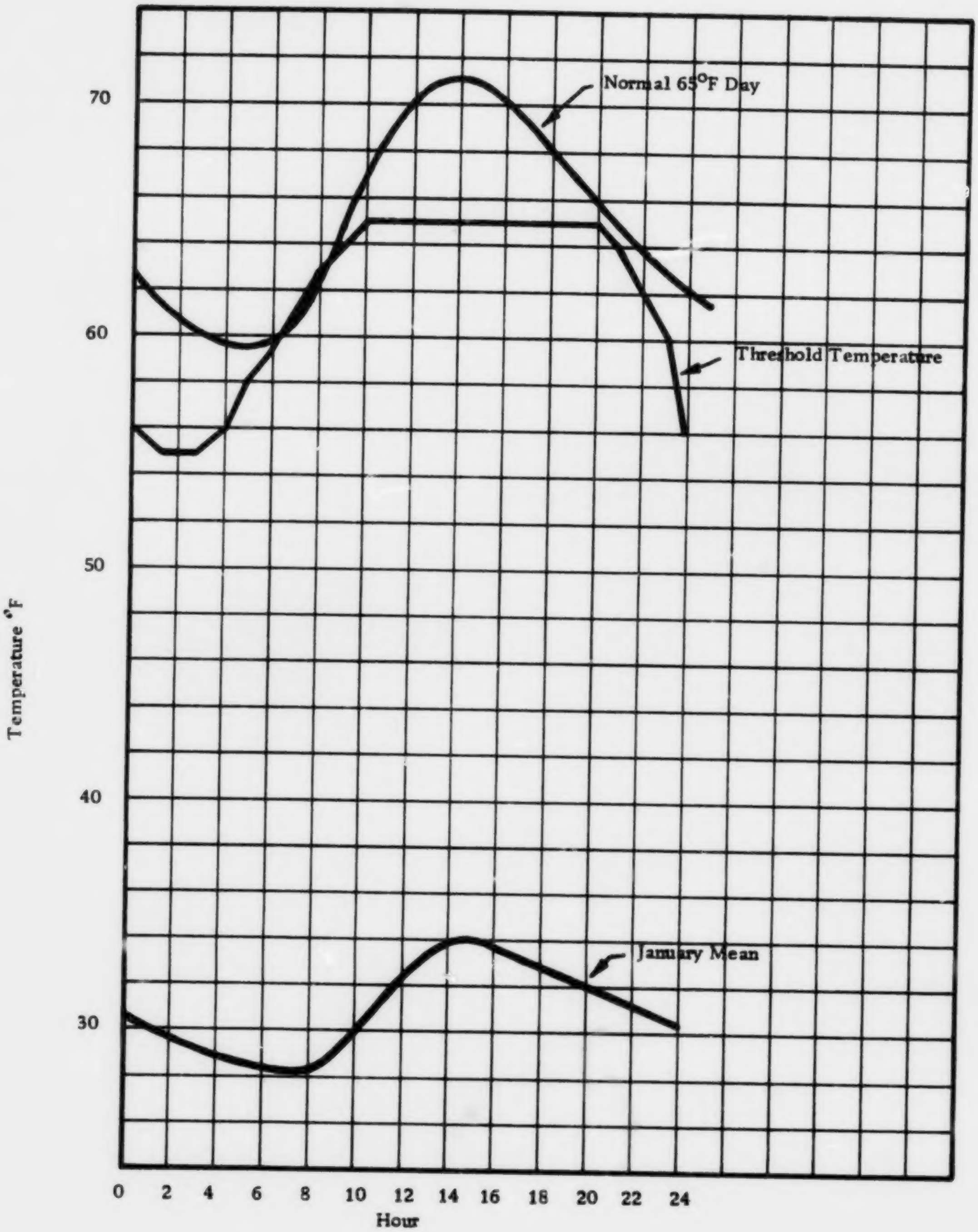

Figure A-2. Threshold Temperature Profile and Representative Diurnal Temperature Profiles a January day with a mean temperature of 31°F. For a typical spring or fall day requiring minimum space heating (e.g., a mean daily temperature of 63°F), the 65°F line in Figure A-2 may be lowered by 2°F. This would indicate that space heating would be required for the morning hours 0600 to 1000 and for the evening hours 1900 to 2200. For progressively colder days, the space heating requirement will gradually extend to all hours of the day.

The relationship between SO_2 concentrations and temperature which is illustrated in Figure A-1 is assumed to relate area source emissions from space heating and temperature. The temperature dependent emissions have the following form:

$$\left.\begin{array}{ll} (Q_H)_{i,j} = Q_A\, F_H\, (T_i - T_{i,j})\, I_i K, & T_i > T_{i,j} \\ (Q_H)_{i,j} = 0 & , T_i \leq T_{i,j} \end{array}\right\} \qquad (A\text{-}1)$$

where

$(Q_H)_{i,j}$ = area source emission rate for hour i, day of year j, due to space heating (lb/hr)

Q_A = total annual area source emission (lb/yr)

F_H = fraction of the total area source emission which is temperature dependent

T_i = threshold temperature for hour i (°F) (refer to Table A-1)

$T_{i,j}$ = observed temperature for hour i, day of year j (°F)

I_i = temperature sensitivity of emissions for hour i (Index/°F) (refer to Table A-1), and

K = index scaling factor (yr/Index hr).

The parameter F_H represents the fraction of the annual emissions which are temperature dependent. Presumably, these emissions are primarily due to space heating requirements. The constant K is a scaling factor which, for a specific set of I_i values and the climatological mean hourly temperatures for each month, is defined as

$$K = 1 \Bigg/ \left[\sum_{i=1}^{24} I_i \sum_{k=1}^{12} N_k \left(T_i - \overline{T}_{i,k}\right) \right] \qquad \text{(A-2)}$$

where

N_k = number of days in month k, and

$\overline{T}_{i,k}$ = mean temperature for hour i, month k.

The base level area source emissions, assumed the same for each day of the year, show a diurnal variation which is incorporated into the following non-temperature dependent portion of the algorithm.

$$Q_{B_i} = Q_A \left(1 - F_H\right) J_i/365 \qquad \text{(A-3)}$$

where

Q_{B_i} = base level area source emission rate for hour i (lb/hr), and

J_i = base level emission factor for hour i (day/hr) (refer to Table A-1).

The J_i values taken from Table A-1 already have been scaled. They represent the ratio of emissions during the ith hour to a total day's emissions.

The complete form of the algorithm for the area source emission rate is then

$$\left.\begin{aligned} Q_{i,j} &= Q_{B_i} + Q_{H_{i,j}} = Q_A \left[\frac{(1-F_H)J_i}{365} + F_H \, (T_i - T_{i,j}) I_i \, K\right], \ (\text{For } T_i > T_{i,j}) \\ Q_{i,j} &= Q_{B_i} + Q_{H_{i,j}} = Q_A \, (1 - F_H) \, J_i/365, \ (\text{For } T_i \le T_{i,j}) \end{aligned}\right\} \text{(A-4)}$$

where

$Q_{i,j}$ = area source emission rate for hour i, day of the year j (lb/hr).

The numerical values of J_i, T_i, and I_i are given in Table A-1. Using the climatological data for LaGuardia Airport, the constant K is equal to 0.0002337 yr/Index hr.

To complete the algorithm in a completely objective manner, the F_H factor can be derived from the same 12-year data sample used to derive the parameters J_i, T_i, and I_i. The temperature-dependent portion of the sum of all SO_2 concentration observations can be evaluated using the monthly mean hourly temperatures derived from LaGuardia; the average annual sum for the 12-year period is exactly the value of 1/K, or 4278.64 Index hr/yr.

The non-temperature-dependent portion of the SO_2 concentration observations is the remainder, which is an average of 10,413.45 Index hr/yr. Therefore, the F_H factor is defined as

$$F_H = \frac{4278.64}{4278.64 + 10{,}413.45} = 0.29.$$

It may be noted that this differs greatly from 0.80 which was previously judged to be appropriate (Roberts et al. 1970).

The sources which contribute to F_H are difficult to identify since many effects are represented, including space heating of residences, space heating of commercial establishments, industrial temperature-dependent operations, hot water requirements, etc. This value of $F_H = 0.29$ is used in all applications of the algorithm to the New York City experiments. For comparison purposes, GHM calculations using variable wind speeds and emission rates were made with emissions based on $F_H = 0.29$ and a previously assumed value of 0.80. The resulting calculations are plotted as a function of temperature intervals along with measured values in Figure A-3. The results suggest that the use of $F_H = 0.29$ gives a slope (and a resulting temperature sensitivity) which is very nearly parallel to the measured values.

A.2 COMPARISONS WITH OTHER HOURLY EMISSION RATE ALGORITHMS

It is informative to compare the preceding area source emission algorithm with the area source algorithms used in the application of the GEOMET diffusion model to the St. Louis and Chicago sites (Koch and Thayer 1971). Each of the three algorithms are tailored to the New York City climate (LaGuardia), and put in the form

$$Q_i = Q_T K_i \tag{A-5}$$

where

Q_i = area source emission rate for hour i (lb/hr)
Q_T = annual area source emission (lb/yr)

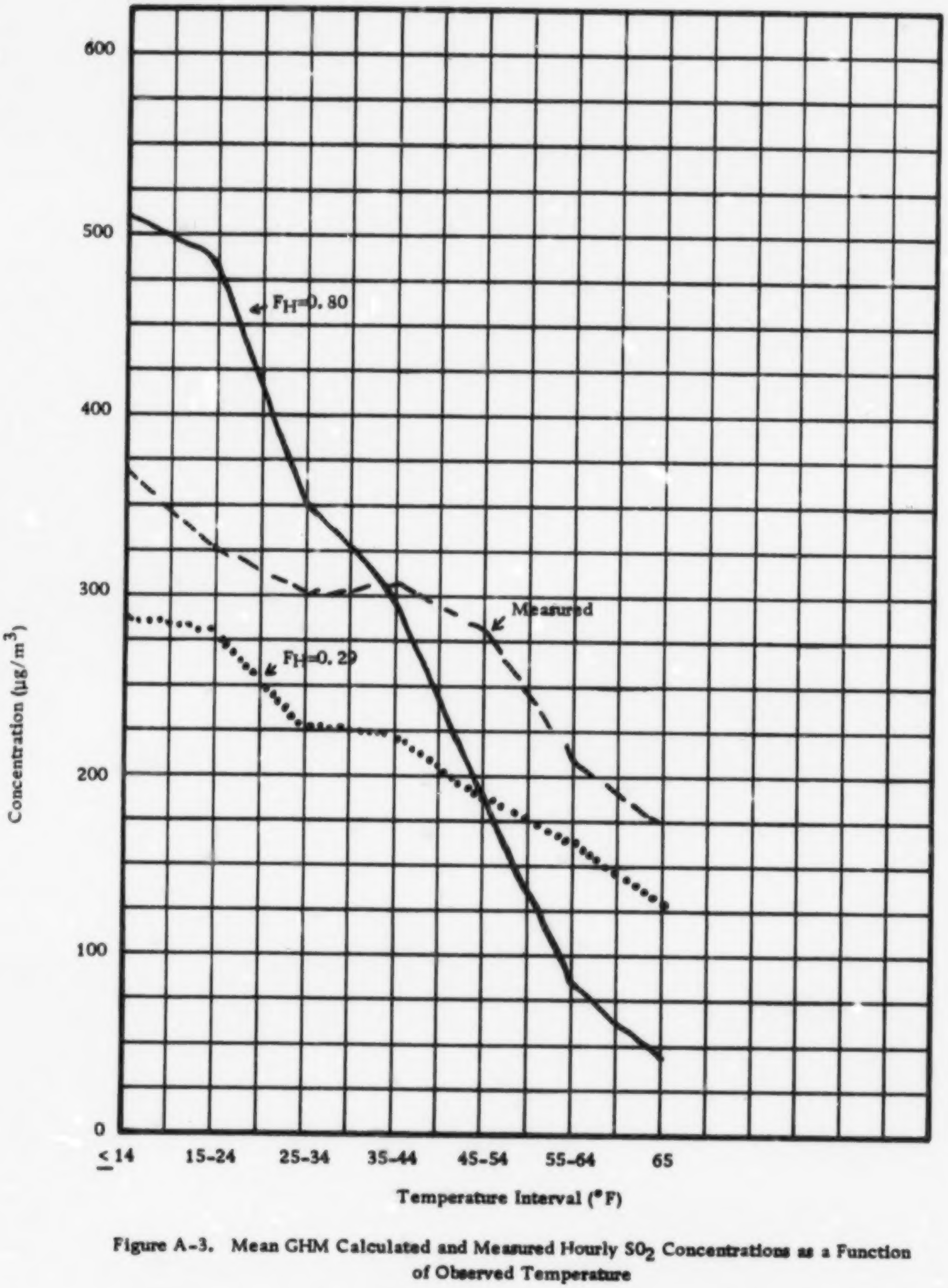

Figure A-3. Mean GHM Calculated and Measured Hourly SO_2 Concentrations as a Function of Observed Temperature

K_i = algorithm coefficient for hour i which can be a function of temperature, hour of the day, and climatological variables (yr/hr).

The three algorithms are evaluated for days of three different daily mean temperatures having diurnal temperature ranges typical of New York City. The three daily mean temperatures considered are 70°, 50°, and 30°F. The variable K_i's, plotted against hour of the day, are compared for each of the three algorithms and for each of the three types of days.

For the St. Louis experiment, detailed information was available for the area source emissions. The complex algorithm included the contributions from residential, commercial, river vessel, automotive, railroad, backyard burning, and industrial sources. For comparison purposes, only two components of the algorithm are examined here - the residential and commercial sources. These two components are based primarily on the study by Turner (1968) of the fuel usage for space heating in St. Louis during a winter season. Turner developed methods to determine the rate of fuel use from residential and commercial space heating sources as a function of temperature, hour of the day, and day of the week.

The residential component of the algorithm is composed of a constant Base Residential SO_2 Emission Rate, and a Residential Heating SO_2 Emission Rate which is a function of temperature and time of day

$$Q_R = Q_{RT} \left[\frac{F_R D_W}{24(365\ D_W F_R + D(1-F_R))} + \frac{D_r(t)\ (1 - F_R)}{24(365\ D_W F_R + D(1-F_R))} \right] \qquad \text{(A-6)}$$

where

Q_R = residential SO_2 emission rate (lb/hr)

Q_{RT} = annual residential SO_2 emission (lb)

F_R = 0.2 = summer day fuel consumption as fraction of average winter day fuel consumption

D_W = average winter degree day (= 32.9°F day/day)

$D_r(t) = 65 - T(t) - \Delta_r(t)$ (°F)

$T(t)$ = temperature at time t (°F)

$\Delta_r(t)$ = residential correction factor (Table A-2)

D = annual degree days (= 4977 degree days).

The commercial component of the St. Louis algorithm is composed of a Base Commercial SO_2 Emission Rate which is a function of hour of the day, and a Commercial Heating SO_2 Emission Rate which is a function of temperature and hour of the day.

$$Q_c = Q_{ct}\left[\frac{F_S D_W F_c(t)}{24(365\ D_W F_S + D(F_W - F_S))} + \frac{D_c(t)\ (F_W - F_S)}{24(365\ D_W F_S + D(F_W - F_S))}\right] \qquad \text{(A-7)}$$

where

Q_c = commercial SO_2 emission rate (lb/hr)

Q_{ct} = annual commercial SO_2 emission (lb)

F_S = fraction of annual fuel consumption used in summer

F_W = fraction of annual fuel consumption used in winter

$F_c(t)$ = commercial diurnal variation factor (Table A-2)

$D_c(t) = 65 - T(t) - \Delta_c(t)$ (°F)

$\Delta_c(t)$ = commercial correction factor (Table A-2).

Table A-2. Numerical Values for Constants in the St. Louis Algorithm

Hour Ending	$\Delta_c(t)$ (Weekday)	$\Delta_r(t)$ (Weekday)	$F_c(t)$
0	13.19	9.11	0.20
1	13.32	11.11	
2	13.23	10.61	0.20
3	12.54	9.69	
4	10.43	8.54	0.20
5	5.64	7.08	
6	-1.75	3.13	0.20
7	-8.04	-2.15	
8	-11.69	-7.32	1.96
9	-13.91	-7.61	
10	-12.94	-8.85	1.82
11	-12.43	-8.44	
12	-12.53	-7.46	1.75
13	-12.39	-6.73	
14	-11.19	-6.25	1.69
15	-9.62	-5.11	
16	-7.88	-4.08	1.62
17	-4.37	-3.17	
18	0.56	-2.41	1.48
19	4.55	-0.77	
20	6.62	-0.01	0.68
21	9.08	2.56	
22	10.41	3.22	0.20
23	11.53	5.33	

Values for F_S and F_W are determined as follows:

Twenty percent of the annual commercial fuel usage is attributed to hot water requirements and is distributed uniformly throughout the year. Therefore, F_{HW}, the fuel required for hot water in a three-month season, is defined as

$$F_{HW} = 0.2\ (1/4 \text{ years}) = 0.05.$$

Assuming that the summer season requires no space heating

$$F_S = F_{HW} = 0.05.$$

The remaining 80 percent of the fuel usage is used for space heating; the amount of this used in the winter season is proportional to the ratio of the number of degree days in the winter to the total annual degree days, so

$$F_W = 0.05 + 0.80 \frac{D_W}{D}$$

where

D_W = degree days for the winter season = 2886, therefore,

$$F_W = 0.05 + 0.80 \left(\frac{2886}{4977}\right) = 0.514.$$

For the Chicago study, an estimate of the annual SO_2 emission rate was obtained for each of three classes of emitters. These include:

- Low-rise residential structures consisting of 19 or less dwelling units (Class I)
- High-rise residential structures consisting of 20 or more dwelling units, and commercial and institutional buildings (Class II)
- Industrial plants not large enough to be treated as individual point emitters (Class III).

In addition to the annual emission rates, estimates regarding diurnal variations in emission rates were generated in Argonne's extensive study of Chicago emission data (Roberts et al. 1970, Chamot et al. 1970). Algorithms for estimating diurnal variations in emission rates are given by Equations (A-8), (A-9), and (A-10). In the equations below, Turner's temperature correction factors have been incorporated into the Argonne algorithms as proposed by Koch and Thayer (1970).

1. Residential or commercial low-rise (Class I)

$$Q_1 = \left[\frac{F_H}{8760} + \frac{(1 - F_H)\ (65 - T - \Delta_R)\ U_i}{DH_j}\right] Q_{1T} \qquad \text{(A-8)}$$

2. Residential or commercial high-rise (Class II)

$$Q_2 = \left[\frac{F_H}{8760} + \frac{(1 - F_H)\ (65 - T - \Delta_c)}{24D}\right] Q_{2T} \qquad \text{(A-9)}$$

3. Industrial (Class III)

$$Q_3 = \frac{Q_{3T}}{8760} \qquad \text{(A-10)}$$

where

Q_1 = emission rate of SO_2 for Class I emitters (lb/hr)

Q_2 = emission rate of SO_2 for Class II emitters (lb/hr)

Q_3 = emission rate of SO_2 for Class III emitters (lb/hr)

Q_{1T} = annual SO_2 emission for Class I emitters (lb/yr)

Q_{2T} = annual SO_2 emission for Class II emitters (lb/yr)

Q_{3T} = annual SO_2 emission for Class III emitters (lb/yr)

F_H = 0.2 = fraction of annual residential/commercial fuel usage attributed to hot water requirements

U_i = fraction average hourly fuel usage associated with ith hour

H_j = hours of fuel usage per day (hr/day)

U_i = 1.5 ($T < 5°F$, hours 4 and 5),($5°F < T < 65°F$, hours 6 and 7)

U_i = 1.0 ($T \leq 5°F$, hours 6 to 22),($5°F < T < 65°F$, hours 8 to 22)

U_i = 0 ($T \leq 5°F$, hours 0 to 3 and 23),($5°F < T < 65°F$, hours 0 to 5 and 23),($T \geq 65°F$, all hours)

H_j = 19 ($T \leq 5°F$)

H_j = 17 ($T > 5°F$).

In Equations (A-8) and (A-9), 20 percent of the annual emissions are attributed to hot water requirements and distributed evenly over the year. The remaining emissions for Classes I and II are attributed to space heating requirements and are allocated on the basis of outside air temperature deficit below 65°F. Only the first term is applicable in these equations when the outside air temperature is over 65°F. Equation (A-8) includes a "janitor" factor U_h to account for "hold fire" periods after 10 p.m. and for a 50 percent increase in the burn rate during the first two early morning start-up hours (starting at 4 a.m. when temperature is $\leq$ 5°F and 6 a.m. otherwise).

The three sets of algorithms represented by equation sets (A-4), (A-6 and A-7), and (A-8, A-9, and A-10) and referred to as the "New York City," "St. Louis," and "Chicago" algorithms respectively, were evaluated for New York City climate on three days of different mean temperature. For the purpose of comparison, the F_H factor in equation set (A-4) was assigned a value of 0.8. Values of K_i in Equation (A-5) for each of the three algorithms are presented in Figures A-4 through A-6. Numbers in parentheses refer to 24-hour summations of K_i values. The two New York City K_i values may be added together to give the total K_i representing both base level and space heating emissions. The curves of K_i for St. Louis and Chicago cannot be added together since the K_i's are coefficients of different emission rates (Q_T). The general shapes of the K_i profiles are similar for the three algorithms, each having a minimum value during the pre-dawn hours, and a maximum value between the hours of 6 and 10 a.m. The New York City algorithm is closely approximated by the Chicago (Argonne) Residential or Commercial Low-Rise Profile. The space heating profile for New York City has a second, weaker maximum in the K_i profile in the early evening hours.

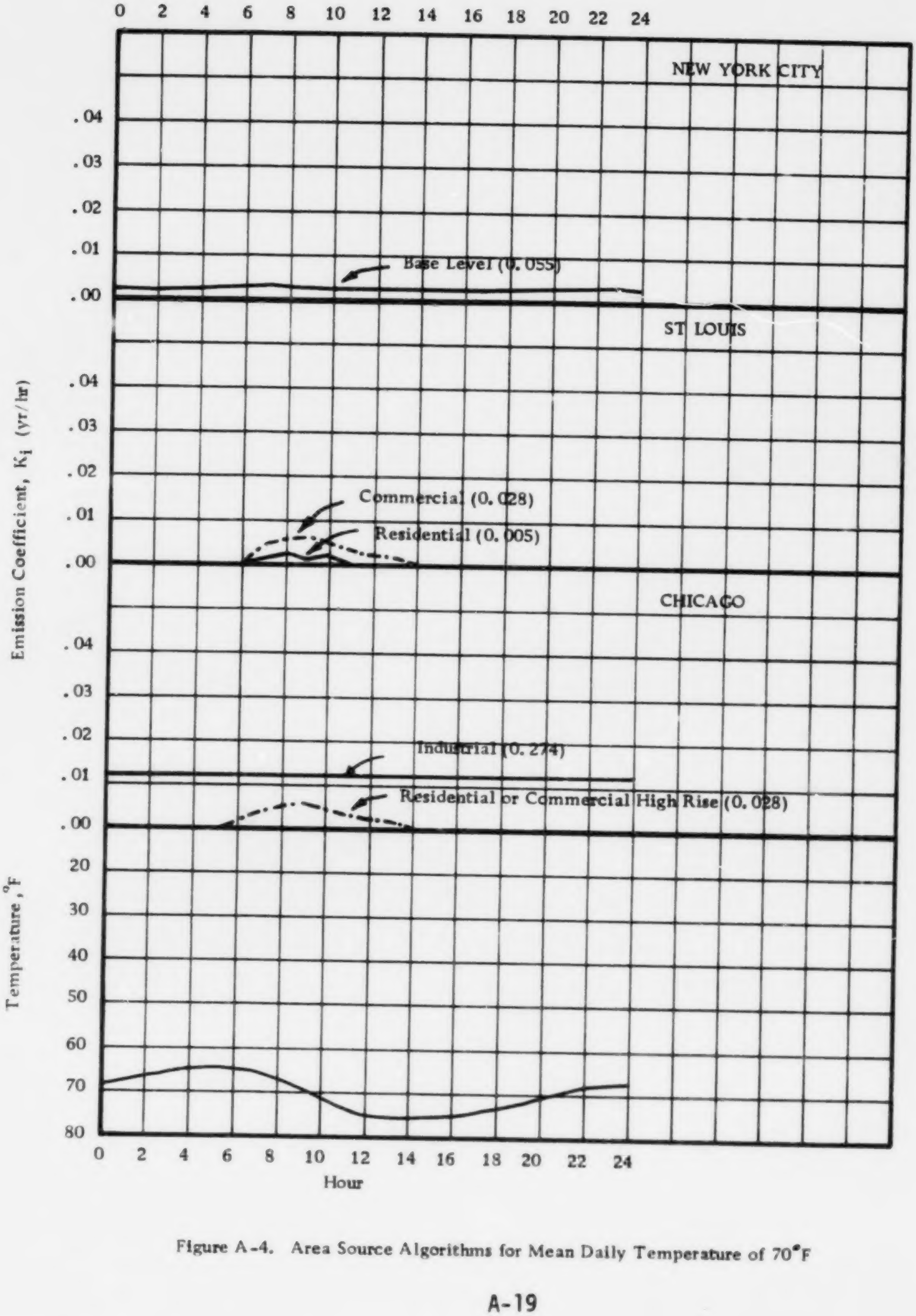

Figure A-4. Area Source Algorithms for Mean Daily Temperature of 70°F

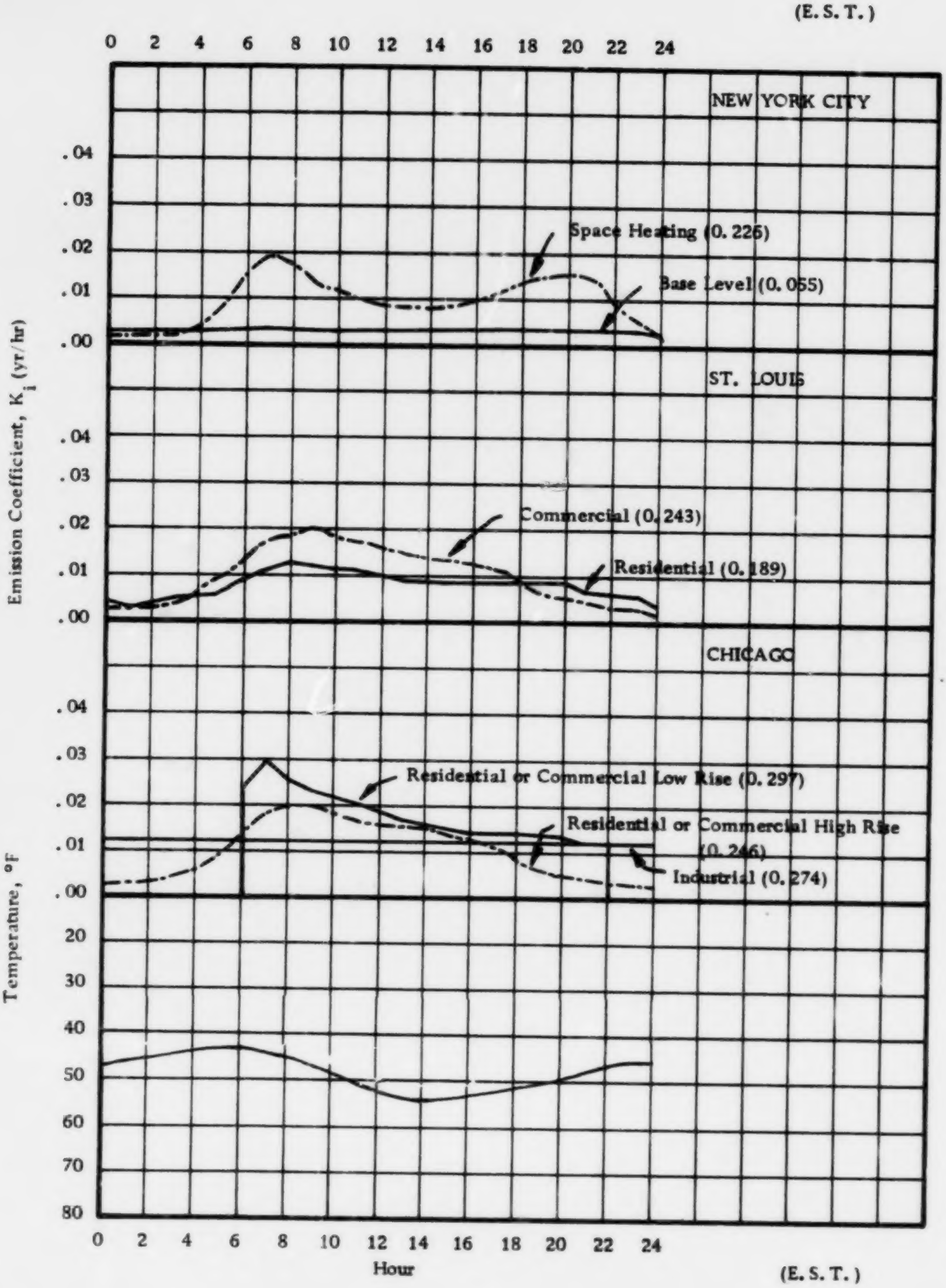

Figure A-5. Area Source Algorithms for Mean Daily Temperature of 50°F

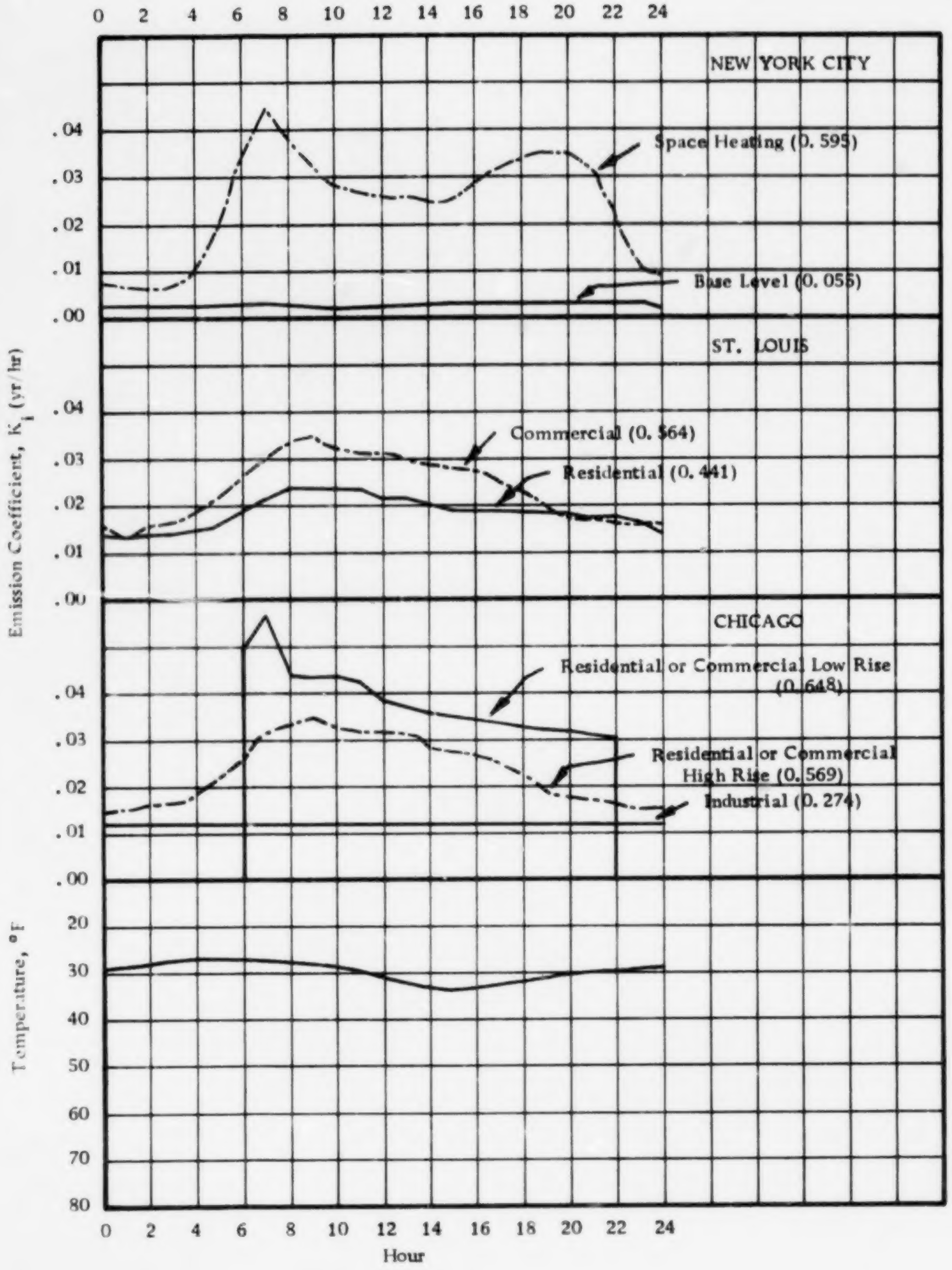

Figure A-6. Area Source Algorithms for Mean Daily Temperature of 30°F

Appendix B

METHOD OF ESTIMATING THE HEIGHT OF THE MIXING LAYER

Mixing layer heights were estimated for New York City using radiosonde data collected at Kennedy Airport in New York City. The data were obtained from the NOAA National Weather Records Center in Asheville, North Carolina on two magnetic tapes. One tape contained standard level data (height, temperature, and relative humidity for 50 mb intervals starting with 1000 mb). The other tape contained significant level data (height, pressure, temperature, and relative humidity of significant points identified by the radiosonde observers). These two data sets were merged to form a single chronological file of height-ordered measurements. The following seven steps were used to determine the mixing layer height for each observation time.

1. Read and store the height, pressure, temperature, and relative humidity of each data level.

2. Convert all relative humidities to mixing ratios using the following equations (Saucier 1955):

$$M = 0.01\ U\ S \qquad \text{(B-1)}$$

$$S = \frac{0.62197\ f\ E}{P - f\ E} \approx 0.622\ \frac{E}{P} \qquad \text{(B-2)}$$

$$E = 6.11\ (10)^{\frac{7.5\ T}{T + 237.3}} \qquad \text{(B-3)}$$

where

M = mixing ratio

U = reported relative humidity (percent)

S = saturation mixing ratio

$f \approx 1$ = correction factor for departure from ideal gas laws

E = saturation vapor pressure of water (mb)

P = reported pressure (mb)

T = reported temperature (°C).

3. Find the maximum mixing ratio for the observation time (M_x).

4. Find the mixing condensation level by the following equations (Saucier 1955):

$$Z_c = \frac{1000}{8.2} (T_o - D_o) \qquad \text{(B-4)}$$

where

Z_c = mixing condensation level (m)

T_o = ground level temperature (°C)

D_o = ground level dewpoint (°C).

In order to account for evaporation of dew during the early morning, it is assumed that the mixed atmosphere will contain moisture equal to that indicated by M_x. D_o is determined from M_x by means of Equations B-2 and B-3 using $S = M_x$ and $T = D_o$:

$$D_o = \frac{237.3 \log_{10} \left[\frac{M_x P_o}{6.11 (0.622)}\right]}{7.5 - \log_{10} \left[\frac{M_x P_o}{6.11 (0.622)}\right]} \qquad \text{(B-5)}$$

where

P_o = ground level pressure.

5. Using the reported data levels to define layers, find the layer (Z_{i-1} to Z_i) containing the top of the mixing layer. The top of the mixing layer is identified by the parcel method. When the reported vertical temperature profile exceeds the temperature of a parcel lifted from the surface by 1°C, this is assumed to be the top of the mixing layer (Z_m). The layer containing the mixing layer height is identified by testing if

$$T_i \geq T_i' + 1 \tag{B-6}$$

where

T_i = temperature of ith level (°C)

T_i' = temperature of parcel lifted to ith level (°C).

The parcel temperature is calculated as follows:

$$T_i' = T_{i-1}' + \gamma' \left(Z_i - Z_{i-1}\right) \tag{B-6}$$

$$\gamma' = \begin{cases} -0.0098, & Z_i \leq Z_c \\ -0.0098 \dfrac{1 + \dfrac{L\, S_{i-1}'}{R_d \left(T_{i-1}' + 273\right)}}{1 + \dfrac{L^2\, S_{i-1}'}{c_p\, R_v \left(T_{i-1}' + 273\right)^2}}, & Z_i > Z_c \end{cases} \tag{B-7}$$

where

γ' = temperature lapse rate (°C/m, Haltiner and Martin 1957)

L = 2500 = latent heat of vaporization (joules/g)

S'_{i-1} = saturation mixing ratio of parcel lifted to (i-1)th level, estimated from Equations B-2 and B-3 using P_{i-1} and T'_{i-1}

R_d = 0.287 = gas constant for dry air (joule/g/°C)

c_p = 1.003 = specific heat of dry air at constant pressure (joule/g/°C)

R_v = 0.461 = gas constant for water vapor (joule/g/°C).

6. Estimate the height of the mixing layer by linear interpolation as follows:

$$Z_m = Z_{i-1} + \frac{[1 - (T_{i-1} - T'_{i-1})]\,(Z_i - Z_{i-1})}{(T_i - T'_i) - (T_{i-1} - T'_{i-1})} \quad .$$

7. Enter Z_m on the output data file.

Appendix C

DEVELOPMENT OF A METHOD OF ESTIMATING EMISSION RATES FOR USE IN THE SIMPLIFIED GIFFORD-HANNA MODEL

The mean area source emission rate used in the Gifford-Hanna model (GHM) is to be a mean value over n by n 1 km grid cells centered on the grid cell containing the receptor. An appropriate value for n is required.

On the average, the New York City receptors considered in this study are located in areas of relatively high area source emissions of both SO_2 and particulates. The mean SO_2 emission decreases steadily from an average maximum value of 0.747 tons/km^2/year for the 1 km grid cell containing the receptor to 0.319 tons/km^2/year for a square with sides of 79 km (maximum size considered). Likewise, for particulates a value of 0.136 tons/km^2/year is obtained for the average 1 x 1 km square, and a value of 0.059 tons/km^2/year for the 79 x 79 km averaging area. Clearly then the mean value of the calculated concentrations will vary by a factor of 2 depending on the choice of the averaging area.

In a forthcoming paper, Turner et al. (1972) in applying GHM used a 10 km radius for determining $\overline{Q^*}$ for both SO_2 and particulate emissions. They considered circles of 3, 5, 10, 20, 30, and 40 km radii centered over the receptor location. If the center of a 1 km^2 grid cell was within the circle, it was included in the average; if the center was outside, it was not included. Their selection was based on the best linear correlation of the measured annual concentration at the receptor with the mean annual emissions over the different sized circles.

The GEOMET analysis based on squares instead of circles confirms Turner's findings. Forty different squares were tested, ranging from 1 x 1 km to 79 x 79 km.

A maximum correlation of 0.84 was obtained between SO_2 concentration measurements and a 31 x 31 km square emission averaging area; for particulate concentration measurements, a maximum correlation of 0.65 was obtained for all squares with sides ranging from 15 to 57 km.

A second analysis of the area source emission data was made after dividing the receptors into subsets of low and high measured concentration. Mean values of 135 $\mu g/m^3$ for SO_2 and 82 $\mu g/m^3$ for particulates were used to divide the sample. The correlations between measured concentrations and Q* as a function of the size of the averaging square were markedly different for the two data subsets. The correlation coefficients and the Q* values for 1 to 73 km squares are plotted in Figures C-1 and C-2, for SO_2 and particulates, respectively. Correlations for those receptors measuring large concentrations were maximum for small averaging areas based on emissions near the receptor and fell off rapidly with increasing size of the averaging area. The receptors with low concentrations, however, tended to have a maximum correlation with emission means computed from large-sized squares. Also, the cases of low concentration had mean emission values which either increased or remained constant with increasing area size. These results indicate that large measured concentrations are primarily due to nearby sources, and that low measured concentrations are affected by sources at large distances from the receptor. It might also be hypothesized that the pattern of correlation coefficients shown for the divided sets is associated with selecting

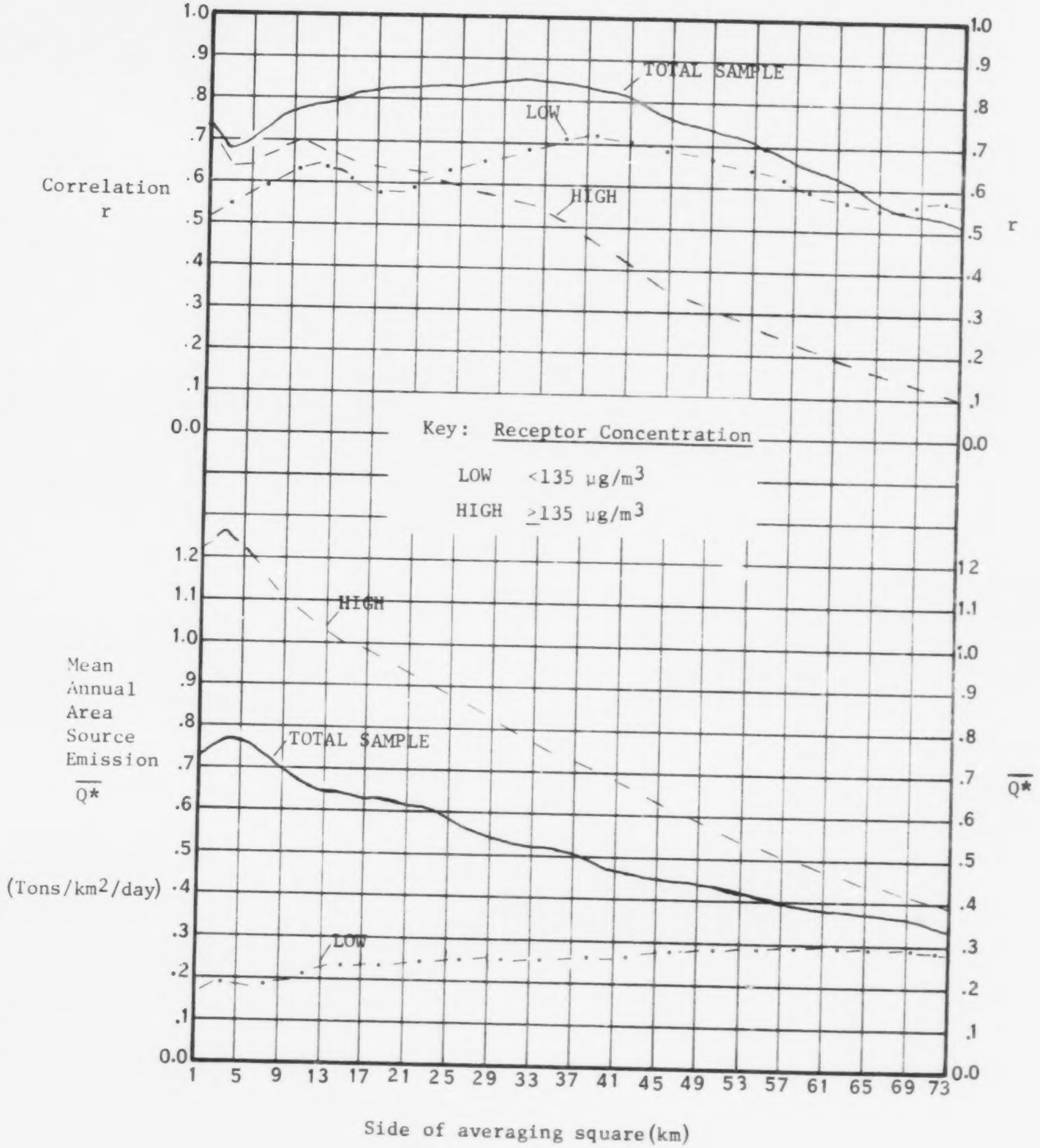

Figure C-1. Mean SO_2 Area Source Emissions

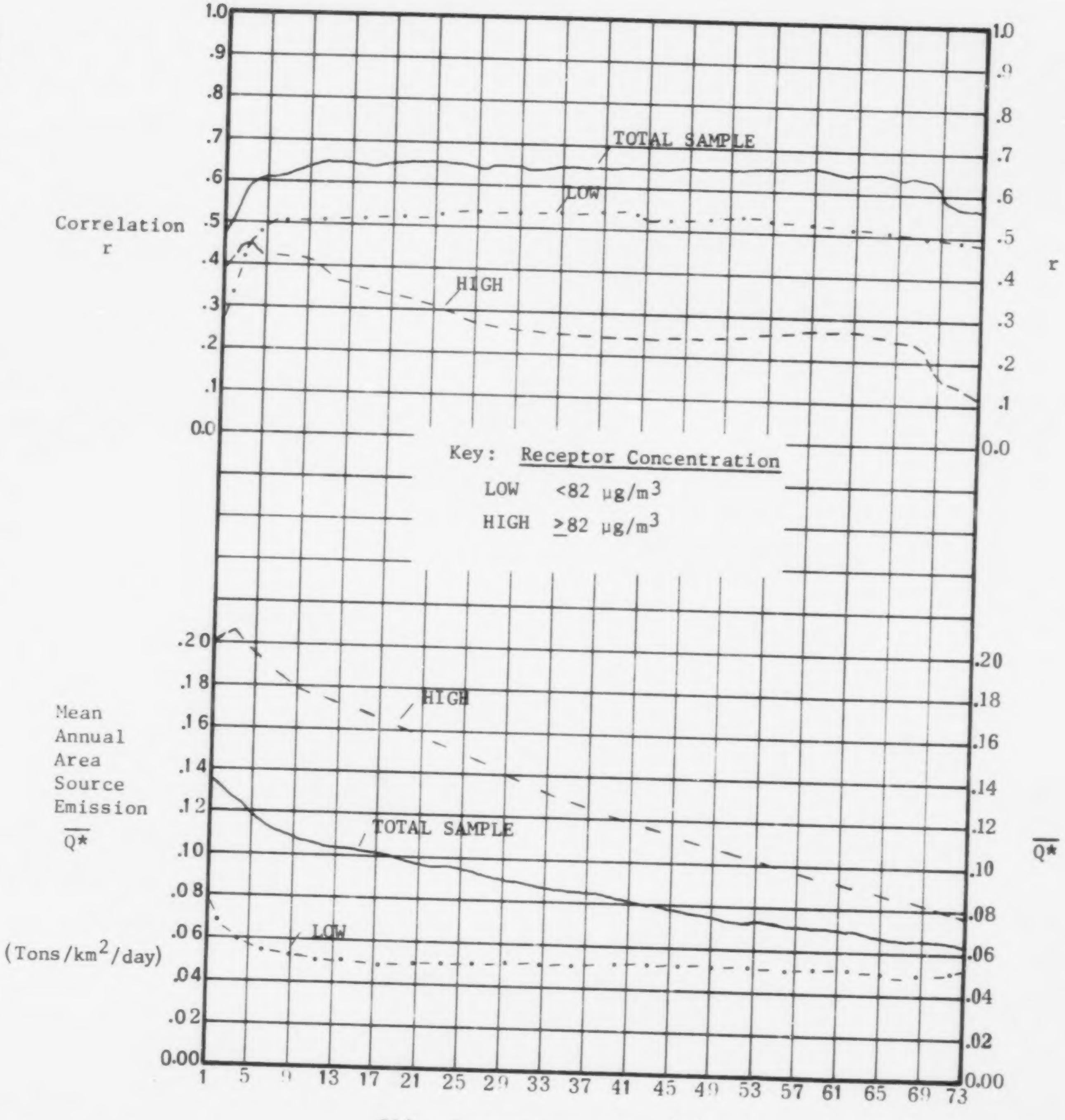

Figure C-2. Mean Particulate Area Source Emissions averaging square sizes which yield the highest values of mean emission rates.

Based on the preceding analysis, the following five different averaging routines for the area source emissions were defined and tested:

1. Use only the single area source emission value for the 1 km^2 grid cell containing the receptor (designated 1 x 1 in Tables C-1 and C-2).

2. Use an averaging area approximating the 10 km radius used by Turner, i.e., 19 x 19 km square centered on the grid cell containing the receptor (designated 19 x 19 in Tables C-1 and C-2).

3. Use the area for which the highest linear correlation was obtained, i.e., 31 x 31 km for SO_2 and 19 x 19 km for particulates (designated 31 x 31 in Table C-1 and 19 x 19 in Table C-2).

4. Search increasingly large squares until the maximum area source emission value is obtained (designated Q^*_A in Tables C-1 and C-2).

5. Use the following Q* magnitude and pollutant oriented criteria (designated Q^*_B in Tables C-1 and C-2):

Pollutant	Criteria[1]	Averaging Square
SO_2	(a) $Q^*_9 > 0.701$ ton/km^2/day and $Q^*_{37} > 0.512$ ton/km^2/day	(a) 9 x 9 km
	(b) $Q^*_9 < 0.701$ ton/km^2/day and $Q^*_{37} < 0.512$ ton/km^2/day	(b) 37 x 37 km
	(c) Neither (a) nor (b)	(c) 31 x 31 km
Particulates	(a) $Q^*_3 > 0.128$ ton/km^2/day and $Q^*_{28} > 0.082$ ton/km^2/day	(a) 3 x 3 km
	(b) $Q^*_3 < 0.128$ ton/km^2/day and $Q^*_{28} < 0.082$ ton/km^2/day	(b) 39 x 39 km
	(c) Neither (a) nor (b)	(c) 19 x 19 km

(1) Q^*_s is the average emission rate from the s^2 grid squares whose center grid square contains the receptor (s must be an odd integer).

Each of the five above procedures has been evaluated by comparing GHM calculations with corresponding measured values. For the particulates there would only be four procedures since the procedures (2) and (3) above yield

Table C-1. SO_2 Experiments

Statistic	Experiment				
	1 x 1	19 x 19	31 x 31	$\overline{\varphi^{*}_{A}}$	$\overline{Q^{*}_{B}}$
Number Cases	68	68	68	68	68
Mean Measured	142.31	142.31	142.31	142.31	142.31
Mean Calculated	75.62	65.06	56.43	96.99	80.30
RMSE	98.69	90.13	100.45	90.13	77.98
Mean Error	-66.69	-77.25	-85.88	-45.32	-62.01
Mean Absolute Error	84.80	78.63	86.40	70.09	67.28
Largest Negative Error	-199.91	-208.29	-273.60	-171.57	-170.71
Largest Positive Error	174.76	46.71	17.76	350.41	103.58
Error Range	374.67	255.00	291.36	521.98	274.29
Least Error	-4.07	-9.77	-16.25	-4.60	-4.02
Linear Correlation	0.733	0.817	0.831	0.738	0.815
Reduction of Variance	0.537	0.667	0.690	0.545	0.665
Slope, Least Squares	0.539	1.186	1.766	0.504	0.832
Intercept, Least Squares	101.58	65.14	42.63	93.44	75.46
Max. Measurement	385.00	385.00	385.00	385.00	385.00
Error at Max. Measurement	146.55	-208.29	-273.60	95.36	-74.61
Skewness	0.96	-0.36	-0.84	2.31	0.38
Kurtosis	1.59	0.02	1.07	9.28	1.36
Frequency Distribution of Calculated Minus Measured By Percentiles					
100.0	174.76	46.71	17.76	350.41	103.58
99.5	174.76	46.71	17.76	350.41	103.58
99.0	174.76	46.71	17.76	350.41	103.58

(Continued)

Table C-1. SO_2 Experiments (Concluded)

Statistic	Experiment				
	1 x 1	19 x 19	31 x 31	$\overline{Q}^*_A$	$\overline{Q}^*_B$
Frequency Distribution of Calculated Minus Measured By Percentiles					
95.0	100.47	-19.27	-21.51	74.98	-4.02
90.0	9.61	-26.69	-26.22	21.71	-14.36
80.0	-24.99	-37.15	-37.47	-20.30	-27.36
70.0	-38.11	-46.06	-51.13	-31.39	-37.36
60.0	-46.93	-53.83	-65.75	-38.84	-46.97
50.0	-61.65	-65.30	-78.13	-42.68	-56.04
40.0	-92.33	-85.18	-97.74	-55.00	-70.19
30.0	-111.38	-103.42	-109.36	-77.61	-85.93
20.0	-122.15	-119.90	-122.83	-107.24	-105.29
10.0	-151.52	-138.50	-156.51	-123.48	-122.83
5.0	-169.96	-160.95	-186.22	-146.90	-135.25
1.0	-199.91	-208.29	-273.60	-171.57	-170.71
0.5	-199.91	-208.29	-273.60	-171.57	-170.71
0.0	-199.91	-208.29	-273.60	-171.57	-170.71

Table C-2. Particulate Experiments

Statistic	Experiment				
	1 x 1	19 x 19	31 x 31	$\overline{Q^*_A}$	$\overline{Q^*_B}$
Number Cases	101	101	101	101	101
Mean Measured	83.73	83.73	83.73	83.73	83.73
Mean Calculated	97.07	83.46	78.00	105.21	97.34
RMSE	73.37	33.44	26.77	66.65	63.23
Mean Error	13.34	-0.27	-5.73	21.48	13.60
Mean Absolute Error	47.04	27.53	22.14	42.65	38.55
Largest Negative Error	-81.44	-79.67	-72.41	-66.49	-66.49
Largest Positive Error	319.38	75.35	41.27	324.85	324.85
Error Range	400.83	155.02	113.68	391.34	391.34
Least Error	-0.33	-0.16	0.07	1.54	0.25
Linear Correlation	0.486	0.632	0.603	0.640	0.642
Reduction of Variance	0.236	0.399	0.364	0.410	0.412
Slope, Least Squares	0.138	0.338	0.425	0.195	0.199
Intercept, Least Squares	70.30	55.52	50.61	63.24	64.38
Max. Measurement	169.00	169.00	169.00	169.00	169.00
Error at Max. Measurement	148.48	-10.68	-47.63	150.00	150.00
Skewness	1.99	0.37	-0.12	2.14	2.51
Kurtosis	4.62	-0.37	-0.65	6.45	8.33
Frequency Distribution of Calculated Minus Measured By Percentiles					
100.0	319.38	75.35	41.27	324.85	324.85
99.5	319.38	75.35	41.27	324.85	324.85
99.0	300.60	71.52	40.06	281.42	281.42

(Continued)

Table C-2. Particulate Experiments (Concluded)

Statistic	Experiment				
	1 x 1	19 x 19	31 x 31	$\overline{Q}^*_A$	$\overline{Q}^*_B$
Frequency Distribution of Calculated Minus Measured By Percentiles					
95.0	148.48	63.90	35.64	129.57	122.85
90.0	111.91	54.50	30.70	95.09	80.70
80.0	42.79	24.01	22.37	54.80	38.88
70.0	16.67	16.39	8.45	37.31	18.84
60.0	3.56	5.22	1.32	14.70	7.92
50.0	-7.99	-7.42	-6.70	5.41	-5.79
40.0	-19.22	-14.01	-13.31	-7.89	-12.00
30.0	-24.89	-21.55	-19.95	-16.16	-18.09
20.0	-31.89	-26.40	-26.14	-23.50	-25.18
10.0	-42.44	-36.38	-37.68	-32.31	-35.13
5.0	-64.4[illegible]	-40.32	-47.63	-36.38	-42.40
1.0	-76.44	-65.25	-59.94	-59.40	-59.40
0.5	-81.44	-79.67	-72.41	-66.49	-66.49
0.0	-81.44	-79.67	-72.41	-66.49	-66.49

the same averaging area of 19 x 19 km; however, a 31 x 31 km area was added for comparison purposes.

C.1 EVALUATION USING ANNUAL MEAN EMISSION RATES AND WIND SPEEDS

The annual concentrations in $\mu g/m^3$ calculated with the GHM using annual mean emissions and wind speed for each of the five averaging procedures are listed in Tables C-1 and C-2 for SO_2 and particulates, respectively. The analysis was limited to receptors in areas in which detailed 1 x 1 km area source emission data were available, including 68 SO_2 receptors and 101 particulate receptors. The annual mean wind speed for LaGuardia for 1969 is 5.1852 m/sec. Statistics comparing the calculations with measured values are presented in Tables C-1 and C-2.

Of the five SO_2 experiments, the use of the 19 x 19 km averaging square and the $\overline{Q_A^*}$ and $\overline{Q_B^*}$ routine produce the better results. The large 31 x 31 km averaging area tends to reduce the magnitude of the calculated mean emission values; it therefore leads to underprediction of the SO_2 concentrations.

The results of the particulate experiments show that the 19 x 19 km and the 31 x 31 km averaging areas produce the better calculated concentrations. The remaining three experiments, in addition to having large errors, overpredict the concentration. The skill of these three procedures is further reduced when the contribution from the point sources are added to the calculated values.

C.2 EVALUATION USING HOURLY ESTIMATES OF EMISSION RATES AND WIND SPEED

The Gifford-Hanna model was used to calculate hourly SO_2 concentrations using emission rates multiplied by the K_i values defined by Equations A-4 and A-5 in Appendix A.

Three-hourly wind speed and temperature observations for LaGuardia Airport were used to evaluate K_i and to define the wind speed. Calculations were made for 10 stations located within the New York City area (listed in Table 5 of the main body of the report) using each of the five previously described procedures for estimating annual area source emission values. Verification statistics were calculated separately for each of the five averaging procedures.

Comparisons are presented both with and without the concentrations from point sources, as calculated by SCIM using hourly varying mixing layer height and atmospheric stability (see main body of report for a description of this model), added to the Gifford-Hanna area source calculations.

The results of these calculations are shown in Tables C-3 through C-22. Tables C-3 through C-7 present results for 1-hour SO_2 concentrations without point sources; Tables C-8 through C-12, for 24-hour concentrations without point sources; Tables C-13 through C-17, for 1-hour concentrations with point sources; and Tables C-18 through C-22, for 24-hour concentrations with point sources.

A few comments can be made on the calculations using both area and point source emissions (Tables C-13 through C-22).

- Averaging procedure $\overline{Q}^*_B$ generally produces calculations closest to measured values.

Table C-3. One Hourly Calculation, 1 x 1 Area Source Mean

Statistic	Station										
	0	1	3	10	14	17	27	28	31	36	All
Number Cases	2892	1213	1489	1670	1641	1768	1702	1381	1783	1475	17014
Mean Measured	303.77	212.38	295.89	419.87	229.56	192.82	187.56	127.21	187.39	145.07	237.36
Mean Calculated	562.89	324.69	362.03	631.71	98.92	87.78	147.78	4.70	15.19	16.05	249.33
Root-Mean-Square Error	419.22	241.47	283.85	492.17	180.35	158.43	141.38	150.55	202.35	164.79	284.76
Mean Error	259.12	112.31	66.15	211.84	-130.65	-105.04	-39.78	-122.51	-172.19	-129.02	11.96
Mean Absolute Error	290.87	168.08	199.24	314.62	141.01	119.09	100.52	122.55	172.28	129.20	184.98
Largest Negative Error	-710.74	-992.05	-1410.08	-6228.51	-1063.06	-840.25	-933.54	-832.24	-1061.79	-879.68	-6228.51
Largest Positive Error	2781.62	1363.32	1643.84	2545.36	497.42	384.37	707.55	6.70	16.07	31.05	2781.62
Error Range	3492.36	2355.37	3053.92	8773.87	1560.48	1224.62	1641.09	838.93	1077.87	910.72	9010.13
Least Error	0.05	-0.08	0.01	0.09	-0.71	-0.02	-0.03	3.30	-1.60	-0.11	0.01
Linear Correlation	0.459	0.336	0.163	0.276	0.286	0.242	0.294	0.189	0.208	0.326	0.475
Reduction of Variance	0.210	0.113	0.027	0.076	0.082	0.059	0.087	0.036	0.043	0.106	0.225
Slope, Least Squares	0.276	0.254	0.135	0.223	0.686	0.513	0.406	5.687	2.380	3.458	0.290
Intercept, Least Squares	148.57	129.93	247.02	278.94	173.38	147.83	127.61	100.46	151.23	89.55	165.15
Max. Measurement	2242.48	1349.53	1723.04	6710.64	1345.49	1009.12	1178.08	835.76	1071.59	902.68	6710.64
Error at Max. Measurement	-651.24	-992.05	-1410.08	-6228.51	-1063.06	-754.24	-933.54	-832.24	-1061.79	-879.68	-6228.51
Skewness of Error Dist.	2.04	0.74	0.60	-1.50	-1.17	-1.22	-0.27	-2.05	-1.89	-1.71	1.16
Kurtosis of Error Dist.	8.08	4.72	3.95	32.20	5.19	4.59	3.84	9.10	7.14	5.83	24.29

Table C-4. One Hourly Calculation, 19 x 19 Area Source Mean

Statistic	Station										
	0	1	3	10	14	17	27	28	31	36	All
Number Cases	2892	1213	1489	1670	1641	1768	1702	1381	1783	1475	17014
Mean Measured	303.77	212.38	295.89	419.87	229.56	192.82	187.56	127.21	187.39	145.07	237.36
Mean Calculated	195.21	124.19	162.64	210.01	77.88	121.64	116.35	25.08	67.05	46.24	121.74
Root-Mean-Square Error	225.27	174.01	242.87	380.33	194.69	144.19	147.14	133.79	161.16	140.41	209.79
Mean Error	-108.56	-88.19	-133.25	-209.86	-151.68	-71.19	-71.21	-102.13	-120.33	-98.83	-115.62
Mean Absolute Error	160.01	117.44	174.64	240.42	156.69	104.85	106.06	103.30	126.01	104.11	141.69
Largest Negative Error	-1690.64	-1212.79	-1582.45	-6550.36	-1123.13	-780.13	-985.55	-816.97	-1028.34	-836.42	-6550.36
Largest Positive Error	740.57	430.87	613.78	645.66	379.47	576.52	532.86	51.80	264.43	141.11	740.57
Error Range	2431.21	1643.66	2196.23	7096.02	1502.60	1356.64	1518.41	868.77	1292.77	977.54	7290.93
Least Error	0.09	-0.25	-0.05	0.11	-0.31	0.05	-0.16	0.16	0.01	0.01	0.01
Linear Correlation	0.459	0.336	0.163	0.276	0.286	0.242	0.294	0.189	0.208	0.326	0.450
Reduction of Variance	0.210	0.113	0.027	0.076	0.082	0.059	0.087	0.036	0.043	0.106	0.202
Slope, Least Squares	0.795	0.664	0.300	0.671	0.721	0.370	0.515	1.066	0.539	1.201	0.829
Intercept, Least Squares	148.57	129.93	247.02	278.94	173.38	147.83	127.61	100.46	151.23	89.55	136.42
Max. Measurement	2242.48	1349.53	1723.04	6710.64	1345.49	1009.12	1178.08	835.76	1071.59	902.68	6710.64
Error at Max. Measurement	-1690.64	-1212.79	-1582.45	-6550.36	-1123.13	-655.95	-985.55	-816.97	-1028.34	-836.42	-6550.36
Skewness of Error Dist.	-1.16	-1.92	-1.12	-7.13	-1.47	-0.66	-0.82	-2.03	-1.56	-1.55	-5.33
Kurtosis of Error Dist.	5.48	8.58	4.53	111.71	5.85	3.96	4.09	9.40	6.55	8.43	132.76

Table C-5. One Hourly Calculation, 31 x 31 Area Source Mean

Statistic	Station										
	0	1	3	10	14	17	27	28	31	36	All
Number Cases	2892	1213	1489	1670	1641	1768	1702	1381	1783	1475	17014
Mean Measured	303.77	212.38	295.89	419.87	229.56	192.82	187.56	127.21	187.39	145.07	237.36
Mean Calculated	126.52	92.99	112.52	132.39	105.46	107.50	107.87	65.44	73.64	36.91	99.34
Root-Mean-Square Error	264.66	189.98	266.83	425.83	176.37	148.99	150.24	108.91	156.86	147.47	226.94
Mean Error	-177.25	-119.39	-183.36	-287.48	-124.11	-85.32	-79.70	-61.77	-113.75	-108.16	-138.03
Mean Absolute Error	192.35	131.93	199.46	294.19	136.70	109.68	108.75	78.89	121.32	111.10	152.64
Largest Negative Error	-1884.81	-1247.15	-1625.77	-6609.59	-1044.38	-805.23	-999.59	-786.74	-1024.10	-849.80	-6609.59
Largest Positive Error	426.35	315.97	416.51	324.17	534.10	496.27	485.70	186.80	301.55	107.07	534.10
Error Range	2311.16	1563.11	2042.28	6933.76	1578.48	1301.50	1485.29	973.55	1325.65	956.87	7143.69
Least Error	0.08	0.16	-0.03	0.34	0.01	-0.35	-0.06	0.02	0.05	0.16	0.01
Linear Correlation	0.459	0.336	0.163	0.276	0.286	0.242	0.294	0.189	0.208	0.326	0.383
Reduction of Variance	0.210	0.113	0.027	0.076	0.082	0.059	0.087	0.036	0.043	0.106	0.146
Slope, Least Squares	1.227	0.887	0.434	1.065	0.533	0.419	0.556	0.409	0.491	1.504	1.041
Intercept, Least Squares	148.57	129.93	247.02	278.94	173.38	147.83	127.61	100.46	151.23	89.55	133.94
Max. Measurement	2242.48	1349.53	1723.04	6710.64	1345.49	1009.12	1178.08	835.76	1071.59	902.68	6710.64
Error at Max. Measurement	-1834.81	-1247.15	-1625.77	-6609.59	-1044.38	-697.00	-999.59	-786.74	-1024.10	-849.80	-6609.59
Skewness of Error Dist.	-1.78	-2.26	-1.50	-7.46	-1.07	-0.90	-0.97	-1.58	-1.48	-1.62	-5.53
Kurtosis of Error Dist.	7.13	9.52	5.26	115.53	5.01	4.16	4.25	7.97	6.37	5.60	123.87

Table C-6. One Hourly Calculation, $\overline{Q^{\cdot}_{A}}$ Area Source Mean

Statistic	Station										
	0	1	3	10	14	17	27	28	31	36	All
Number Cases	2892	1213	1489	1670	1641	1768	1702	1381	1783	1475	17014
Mean Measured	303.77	212.38	295.89	419.87	229.56	192.82	187.56	127.21	187.39	145.07	237.36
Mean Calculated	442.81	222.82	370.54	570.88	83.62	130.50	131.58	72.82	109.35	88.03	239.41
Root-Mean-Square Error	304.32	172.99	289.80	444.08	190.55	142.11	143.17	106.04	138.86	116.51	237.37
Mean Error	139.04	10.43	74.65	151.00	-145.94	-62.32	-55.99	-54.39	-78.03	-57.04	2.04
Mean Absolute Error	207.73	117.22	203.36	276.63	152.19	102.76	102.37	76.63	102.67	84.06	148.48
Largest Negative Error	-990.69	-1104.21	-1402.73	-6274.94	-1106.73	-764.38	-960.35	-781.21	-1001.06	-776.55	-6274.94
Largest Positive Error	2115.05	846.31	1691.18	2271.32	411.66	626.85	617.50	216.83	503.00	327.69	2271.32
Error Range	3105.74	1950.52	3093.91	8546.25	1518.39	1391.23	1577.85	998.04	1504.06	1104.24	8546.25
Least Error	-0.07	0.01	-0.27	0.01	-0.64	0.04	0.18	-0.12	-0.05	-0.20	0.01
Linear Correlation	0.459	0.336	0.163	0.276	0.286	0.242	0.294	0.189	0.208	0.326	0.478
Reduction of Variance	0.210	0.113	0.027	0.076	0.082	0.059	0.087	0.036	0.043	0.106	0.228
Slope, Least Squares	0.350	0.370	0.132	0.247	0.672	0.345	0.456	0.367	0.331	0.631	0.362
Intercept, Least Squares	148.57	129.93	247.02	278.94	173.38	147.83	127.61	100.46	151.23	89.55	150.77
Max. Measurement	2242.48	1349.53	1723.04	6710.64	1345.49	1009.12	1178.08	835.76	1071.59	902.68	6710.64
Error at Max. Measurement	-990.69	-1104.21	-1402.73	-6274.94	-1106.73	-630.20	-960.35	-781.21	-1001.06	-776.55	-6274.94
Skewness of Error Dist.	1.48	-0.46	0.65	-2.18	-1.40	-0.50	-0.56	-1.44	-0.93	-1.04	0.18
Kurtosis of Error Dist.	6.43	5.50	4.00	39.90	5.66	3.89	3.90	7.54	5.43	4.39	41.23

Table C-7. One Hourly Calculation, $\overline{Q^*_B}$ Area Source Mean

Statistic	Station										
	0	1	3	10	14	17	27	28	31	36	All
Number Cases	2892	1213	1489	1670	1641	1768	1702	1381	1783	1475	17014
Mean Measured	303.77	212.38	295.89	419.87	229.56	192.82	187.56	127.21	187.39	145.07	237.36
Mean Calculated	307.63	195.91	269.79	368.88	105.46	130.50	128.02	65.44	97.04	36.91	181.29
Root-Mean-Square Error	219.38	165.25	237.99	350.07	176.37	142.11	143.90	108.91	143.94	147.47	198.25
Mean Error	3.86	-16.48	-26.10	-50.99	-124.11	-62.32	-59.54	-61.77	-90.35	-108.16	-56.07
Mean Absolute Error	154.04	110.60	167.14	207.16	136.70	102.76	103.05	78.89	107.65	111.10	130.52
Largest Negative Error	-1372.83	-1133.84	-1489.82	-6429.10	-1044.38	-764.38	-966.24	-786.74	-1009.00	-849.80	-6429.10
Largest Positive Error	1364.64	709.75	1130.32	1361.36	534.10	626.85	597.73	186.80	433.55	107.07	1364.64
Error Range	2737.48	1843.58	2620.14	7790.46	1578.48	1391.23	1563.96	973.55	1442.55	956.87	7793.74
Least Error	0.01	-0.26	-0.19	0.03	0.01	0.04	-0.01	0.02	-0.02	0.16	0.01
Linear Correlation	0.459	0.336	0.163	0.276	0.286	0.242	0.294	0.189	0.208	0.326	0.472
Reduction of Variance	0.210	0.113	0.027	0.076	0.082	0.059	0.087	0.036	0.043	0.106	0.223
Slope, Least Squares	0.505	0.421	0.181	0.382	0.533	0.345	0.468	0.409	0.373	1.504	0.531
Intercept, Least Squares	148.57	129.93	247.02	278.94	173.38	147.83	127.61	100.46	151.23	89.55	141.13
Max. Measurement	2242.48	1349.53	1723.04	6710.64	1345.49	1009.12	1178.08	835.76	1071.59	902.68	6710.64
Error at Max. Measurement	-1372.83	-1133.84	-1489.82	-6429.10	-1044.38	-630.20	-966.24	-786.74	-1009.00	-849.80	-6429.10
Skewness of Error Dist.	0.22	-0.86	-0.13	-5.11	-1.07	-0.50	-0.62	-1.58	-1.14	-1.62	-2.92
Kurtosis of Error Dist.	4.56	6.14	3.69	79.82	5.01	3.89	3.94	7.97	5.73	5.60	91.17

Table C-8. 24 Hourly Calculations, 1 x 1 Area Source Mean

Statistic	Station										
	0	1	3	10	14	17	27	28	31	36	All
Number Cases	364	213	257	268	266	285	281	233	283	245	2695
Mean Measured	302.80	211.56	292.39	420.33	229.35	194.02	184.71	125.89	185.87	143.51	233.16
Mean Calculated	562.40	325.41	359.89	642.41	99.02	87.77	147.77	4.72	15.48	16.18	237.85
Root-Mean-Square Error	322.73	181.60	221.00	359.81	156.51	137.38	100.11	141.31	185.91	148.96	216.88
Mean Error	259.61	113.85	67.50	222.08	-130.32	-106.25	-36.94	-121.17	-170.40	-127.32	4.69
Mean Absolute Error	268.82	146.38	169.85	279.20	132.21	111.35	77.10	121.17	170.40	127.32	164.65
Largest Negative Error	-255.35	-572.19	-1060.97	-1075.69	-492.39	-570.78	-305.33	-439.51	-458.64	-374.91	-1075.69
Largest Positive Error	1393.01	632.39	691.86	1322.99	77.20	116.86	313.26	-19.57	-16.07	-0.90	1393.01
Error Range	1648.36	1204.58	1752.83	2398.68	569.59	687.65	618.59	419.94	442.57	374.01	2468.70
Least Error	-1.00	0.32	3.73	1.54	0.28	0.38	0.33	-19.57	-16.07	-0.90	0.28
Linear Correlation	0.524	0.474	0.090	0.355	0.317	0.243	0.378	0.360	0.269	0.451	0.574
Reduction of Variance	0.274	0.225	0.008	0.126	0.101	0.059	0.143	0.130	0.073	0.203	0.329
Slope, Least Squares	0.392	0.482	0.098	0.286	0.721	0.614	0.618	14.500	3.244	5.805	0.333
Intercept, Least Squares	82.44	54.87	257.10	236.41	157.98	140.14	93.46	57.50	135.66	49.55	153.98
Max. Measurement	916.65	932.63	1313.45	1612.87	607.10	674.30	546.97	446.26	474.04	412.70	1612.87
Error at Max. Measurement	-255.35	-572.19	-1060.97	-228.04	-492.39	-570.78	-202.47	-439.51	-458.64	-374.91	-228.04
Skewness of Error Dist.	0.88	-0.48	-0.58	0.04	-1.01	-1.03	-0.12	-1.23	-1.03	-0.70	1.08
Kurtosis of Error Dist.	3.37	3.53	2.94	3.51	1.77	3.06	0.45	2.18	1.70	0.07	3.08

Table C-9. 24 Hourly Calculations, 19 x 19 Area Source Mean

Statistic	Station										
	0	1	3	10	14	17	27	28	31	36	All
Number Cases	364	213	257	268	266	285	281	233	283	245	2695
Mean Measured	302.80	211.56	292.39	420.33	229.35	194.02	184.71	125.89	185.87	143.51	233.16
Mean Calculated	195.04	124.47	161.67	213.57	77.96	121.61	116.34	25.16	68.32	46.62	119.11
Root-Mean-Square Error	175.92	150.83	214.54	291.91	174.10	115.66	113.63	122.91	138.56	121.68	171.06
Mean Error	-107.75	-87.09	-130.71	-206.76	-151.38	-72.41	-68.37	-100.73	-117.55	-96.89	-114.05
Mean Absolute Error	133.04	101.00	155.00	216.89	151.90	89.87	88.47	100.89	120.00	98.58	126.31
Largest Negative Error	-687.32	-794.76	-1200.03	-1342.87	-516.78	-530.86	-345.54	-410.23	-406.06	-332.90	-1342.87
Largest Positive Error	254.67	152.58	267.07	311.08	34.59	216.99	218.25	9.38	58.73	47.05	311.08
Error Range	941.98	947.34	1467.10	1653.94	551.37	747.85	563.79	419.61	464.79	379.96	1653.94
Least Error	-0.18	-0.09	-0.88	2.27	-1.24	0.37	-1.11	0.25	0.08	-0.96	0.08
Linear Correlation	0.524	0.474	0.090	0.355	0.317	0.243	0.378	0.360	0.269	0.451	0.559
Reduction of Variance	0.274	0.225	0.008	0.126	0.101	0.059	0.143	0.130	0.073	0.203	0.313
Slope, Least Squares	1.130	1.259	0.218	0.861	0.915	0.443	0.784	2.719	0.735	2.015	1.070
Intercept, Least Squares	82.44	54.87	257.10	236.41	157.98	140.14	93.46	57.50	135.66	49.55	105.76
Max. Measurement	916.65	932.63	1313.45	1612.87	607.10	674.30	546.97	446.26	474.04	412.70	1612.87
Error at Max. Measurement	-687.32	-794.76	-1200.03	-1152.49	-516.78	-530.86	-275.73	-410.23	-406.06	-303.86	-1152.49
Skewness of Error Dist.	-0.73	-2.08	-1.55	-1.94	-1.12	-0.72	-0.34	-1.23	-0.76	-0.59	-2.07
Kurtosis of Error Dist.	0.74	6.79	5.78	7.09	1.81	2.59	0.22	2.26	1.78	-0.10	11.73

Table C-10. 24 Hourly Calculations, 31 x 31 Area Source Mean

Statistic	Station										
	0	1	3	10	14	17	27	28	31	36	All
Number Cases	364	213	257	268	266	285	281	233	283	245	2695
Mean Measured	302.80	211.56	292.39	420.33	229.35	194.02	184.71	125.89	185.87	143.51	233.16
Mean Calculated	126.41	93.19	111.86	134.63	105.57	107.48	107.86	65.62	75.03	37.21	98.46
Root-Mean-Square Error	227.31	172.35	244.53	352.65	151.32	123.89	118.69	91.18	133.10	129.85	191.99
Mean Error	-176.38	-118.36	-180.53	-285.70	-123.77	-86.54	-76.85	-60.27	-110.84	-106.30	-134.70
Mean Absolute Error	180.05	123.31	188.51	287.14	126.38	97.91	92.75	68.10	114.18	107.06	140.70
Largest Negative Error	-768.01	-829.40	-1234.97	-1392.04	-484.80	-547.53	-356.39	-352.27	-399.39	-341.61	-1392.04
Largest Positive Error	74.25	98.74	176.62	161.46	90.63	175.18	192.60	66.70	78.41	32.22	192.60
Error Range	842.27	928.14	1411.60	1553.50	575.43	722.71	548.99	418.98	477.80	373.84	1584.64
Least Error	-0.72	-2.16	-0.31	3.29	0.15	0.24	-0.03	0.14	-0.97	0.05	-0.03
Linear Correlation	0.524	0.474	0.090	0.355	0.317	0.243	0.378	0.360	0.269	0.451	0.481
Reduction of Variance	0.274	0.225	0.008	0.126	0.101	0.059	0.143	0.130	0.073	0.203	0.231
Slope, Least Squares	1.743	1.681	0.315	1.366	0.676	0.501	0.846	1.042	0.669	2.525	1.482
Intercept, Least Squares	82.44	54.87	257.10	236.41	157.98	140.14	93.46	57.50	135.66	49.55	87.28
Max. Measurement	916.65	932.63	1313.45	1612.87	607.10	674.30	546.97	446.26	474.04	412.70	1612.87
Error at Max. Measurement	-768.01	-829.40	-1234.97	-1322.64	-484.80	-547.53	-295.51	-352.27	-399.39	-325.83	-1322.64
Skewness of Error Dist.	-0.86	-2.20	-1.67	-2.04	-0.97	-0.86	-0.39	-1.15	-0.70	-0.63	-2.27
Kurtosis of Error Dist.	0.83	7.05	6.25	7.14	1.75	2.78	0.18	2.16	1.79	-0.05	11.24

Table C-11. 24 Hourly Calculations, $\overline{Q'_A}$ Area Source Mean

Statistic	Station										
	0	1	3	10	14	17	27	28	31	36	All
Number Cases	364	213	257	268	266	285	281	233	283	245	2695
Mean Measured	302.80	211.56	292.39	420.33	229.35	194.02	184.71	125.89	185.87	143.51	233.16
Mean Calculated	442.43	223.31	368.34	580.54	83.71	130.48	131.57	73.03	111.42	88.74	232.12
Root-Mean-Square Error	214.76	126.11	225.85	310.31	169.18	111.24	105.95	86.48	107.19	89.95	172.68
Mean Error	139.63	11.75	75.96	160.21	-145.63	-63.54	-53.14	-52.86	-74.45	-54.76	-1.04
Mean Absolute Error	173.20	88.81	174.12	235.19	146.44	85.51	81.95	63.90	87.09	69.81	123.46
Largest Negative Error	-396.42	-685.28	-1055.04	-1114.23	-510.12	-520.40	-326.06	-341.67	-366.17	-293.92	-1114.23
Largest Positive Error	1021.25	358.35	712.28	1137.87	45.81	243.22	264.28	77.19	185.18	113.43	1137.87
Error Range	1417.67	1043.63	1767.32	2252.10	555.93	763.62	590.34	418.86	551.35	407.35	2252.10
Least Error	-0.55	-0.82	-0.21	0.33	1.54	0.64	-0.33	0.08	-0.05	-0.31	-0.05
Linear Correlation	0.524	0.474	0.090	0.355	0.317	0.243	0.378	0.360	0.269	0.451	0.584
Reduction of Variance	0.274	0.225	0.008	0.126	0.101	0.059	0.143	0.130	0.073	0.203	0.341
Slope, Least Squares	0.498	0.702	0.096	0.317	0.853	0.413	0.694	0.937	0.451	1.059	0.429
Intercept, Least Squares	82.44	54.87	257.10	236.41	157.98	140.14	93.46	57.50	135.66	49.55	133.61
Max. Measurement	916.65	932.63	1313.45	1612.87	607.10	674.30	546.97	446.26	474.04	412.70	1612.87
Error at Max. Measurement	-396.42	-685.28	-1055.04	-361.40	-510.12	-520.40	-240.24	-341.67	-363.18	-205.50	-361.40
Skewness of Error Dist.	0.40	-1.37	-0.54	-0.23	-1.09	-0.63	-0.23	-1.11	-0.34	-0.39	0.85
Kurtosis of Error Dist.	2.20	5.20	2.85	3.76	1.80	2.48	0.31	2.10	1.89	-0.18	4.94

Table C-12. 24 Hourly Calculations, $\overline{Q_B^{\prime}}$ Area Source Mean

Statistic	Station										
	0	1	3	10	14	17	27	28	31	36	All
Number Cases	364	213	257	268	266	285	281	233	283	245	2695
Mean Measured	302.80	211.56	292.39	420.33	229.35	194.02	184.71	125.89	185.87	143.51	233.16
Mean Calculated	307.37	196.34	268.19	375.13	105.57	130.48	128.01	65.62	98.87	37.21	176.92
Root-Mean-Square Error	142.81	124.46	189.99	225.67	151.32	111.24	107.57	91.18	115.27	129.85	144.60
Mean Error	4.57	-15.22	-24.19	-45.20	-123.77	-63.54	-56.70	-60.27	-87.00	-106.30	-56.25
Mean Absolute Error	113.09	83.59	135.29	156.87	126.38	85.51	83.33	68.10	95.85	107.06	106.27
Largest Negative Error	-555.24	-715.15	-1125.30	-1242.21	-484.80	-520.40	-330.61	-352.27	-376.48	-341.61	-1242.21
Largest Positive Error	602.72	285.96	470.37	617.31	90.63	243.22	253.53	66.70	148.37	32.22	617.31
Error Range	1157.96	1001.12	1595.67	1859.52	575.43	763.62	584.14	418.98	524.86	373.84	1859.52
Least Error	-0.15	-0.01	1.57	-0.46	0.15	0.64	-0.86	0.14	1.86	0.05	-0.01
Linear Correlation	0.524	0.474	0.090	0.355	0.317	0.243	0.378	0.360	0.269	0.451	0.584
Reduction of Variance	0.274	0.225	0.008	0.126	0.101	0.059	0.143	0.130	0.073	0.203	0.341
Slope, Least Squares	0.717	0.798	0.132	0.490	0.676	0.413	0.713	1.042	0.508	2.525	0.657
Intercept, Least Squares	82.44	54.87	257.10	236.41	157.98	140.14	93.46	57.50	135.66	49.55	116.90
Max. Measurement	916.65	932.63	1313.45	1612.87	607.10	674.30	546.97	446.26	474.04	412.70	1612.87
Error at Max. Measurement	-555.24	-715.15	-1125.30	-804.21	-484.80	-520.40	-248.53	-352.27	-375.66	-325.83	-804.21
Skewness of Error Dist.	-0.29	-1.60	-1.07	-1.30	-0.97	-0.63	-0.26	-1.15	-0.47	-0.63	-0.77
Kurtosis of Error Dist.	0.96	5.71	4.16	5.56	1.75	2.48	0.29	2.16	1.84	-0.05	7.64

Table C-13. One Hourly Calculation, 1 x 1 Area Source Mean, with Point Source Emissions

Statistic	Station										
	0	1	3	10	14	17	27	28	31	36	All
Number Cases	2892	1213	1489	1670	1641	1768	1702	1381	1783	1475	17014
Mean Measured	303.77	212.38	295.89	419.87	229.56	192.82	187.56	127.21	187.39	145.07	237.36
Mean Calculated	605.77	354.44	404.78	686.38	124.90	125.90	176.14	29.03	74.22	72.96	290.24
Root-Mean-Square Error	448.96	259.77	295.23	523.14	159.64	141.92	138.61	136.36	175.15	155.28	294.70
Mean Error	302.00	142.06	108.89	266.50	-104.66	-66.92	-11.42	-98.18	-113.17	-72.11	52.88
Mean Absolute Error	322.65	183.91	207.01	350.33	121.30	103.63	97.94	106.13	136.58	115.11	185.63
Largest Negative Error	-666.12	-895.21	-1392.94	-6157.38	-1040.47	-837.24	-868.92	-832.22	-963.76	-774.96	-6157.38
Largest Positive Error	2799.54	1370.43	1658.35	2664.25	516.27	473.44	730.56	225.88	1174.61	714.66	2799.54
Error Range	3465.66	2265.64	3051.29	8821.63	1556.73	1310.68	1599.48	1058.10	2138.37	1489.62	8956.92
Least Error	0.55	0.44	-0.07	-0.01	-0.10	0.09	0.06	0.35	-0.47	0.31	-0.01
Linear Correlation	0.465	0.361	0.199	0.272	0.367	0.258	0.308	0.008	0.182	0.089	0.482
Slope, Least Squares	0.276	0.260	0.161	0.216	0.641	0.383	0.389	0.020	0.195	0.096	0.286
Reduction of Variance	0.216	0.131	0.040	0.074	0.134	0.067	0.095	0.000	0.033	0.008	0.232
Intercept, Least Squares	136.77	120.17	230.80	271.30	149.53	144.66	119.12	126.64	172.95	138.08	154.32
Max. Measurement	2242.48	1349.53	1723.04	6710.64	1345.49	1009.12	1178.06	835.76	1071.59	902.68	6710.64
Error at Max. Measurement	-400.97	-749.75	-1392.94	-6157.38	-1040.47	-753.40	-868.92	-832.22	-963.76	-744.28	-6157.38
Skewness of Error Dist.	2.10	0.90	0.75	-1.41	-1.09	-0.69	-0.10	-1.49	1.09	0.50	1.22
Kurtosis of Error Dist.	8.14	4.22	4.36	30.34	5.97	3.74	3.64	7.11	15.81	4.86	22.67

Table C-14. One Hourly Calculation, 19 x 19 Area Source Mean, with Point Source Emissions

Statistic	Station										
	0	1	3	10	14	17	27	28	31	36	All
Number Cases	2892	1213	1489	1670	1641	1768	1702	1381	1783	1475	17014
Mean Measured	303.77	212.38	295.89	419.87	229.56	192.82	187.56	127.21	187.39	145.07	237.36
Mean Calculated	238.09	153.94	205.38	264.68	103.87	159.75	144.72	49.41	126.08	103.15	162.66
Root-Mean-Square Error	210.87	163.67	221.36	359.97	172.58	136.52	137.94	121.75	149.74	143.67	196.29
Mean Error	-65.68	-58.44	-90.51	-155.19	-125.70	-33.07	-42.85	-77.80	-61.31	-41.92	-74.70
Mean Absolute Error	149.09	110.52	159.15	217.84	134.95	97.88	98.10	91.06	106.17	100.86	128.79
Largest Negative Error	-1453.38	-1088.21	-1565.31	-6479.23	-1100.53	-777.12	-920.93	-816.96	-930.31	-701.03	-6479.23
Largest Positive Error	975.34	542.08	652.30	828.25	398.32	609.92	555.87	269.18	1285.49	840.57	1285.49
Error Range	2428.71	1630.29	2217.61	7307.47	1498.85	1387.04	1476.80	1086.14	2215.80	1541.60	7764.72
Least Error	0.01	0.17	0.10	0.10	-0.11	-0.10	0.08	-0.15	-0.00	0.04	-0.00
Linear Correlation	0.452	0.357	0.224	0.246	0.372	0.266	0.305	0.069	0.225	0.142	0.427
Reduction of Variance	0.204	0.128	0.050	0.060	0.138	0.071	0.093	0.005	0.051	0.020	0.182
Slope, Least Squares	0.714	0.559	0.361	0.528	0.773	0.323	0.468	0.157	0.218	0.143	0.658
Intercept, Least Squares	133.75	126.25	221.67	280.10	149.29	141.26	119.77	119.46	159.95	130.27	130.27
Max. Measurement	2242.48	1349.53	1723.04	6710.64	1345.49	1009.12	1178.08	835.76	1071.59	902.68	6710.64
Error at Max. Measurement	-1440.37	-970.49	-1565.31	-6479.23	-1100.53	-655.11	-920.93	-816.96	-930.31	-701.03	-6479.23
Skewness of Error Dist.	-0.84	-1.33	-0.88	-6.56	-1.41	-0.21	-0.62	-1.45	1.44	0.74	-4.38
Kurtosis of Error Dist.	4.51	6.94	4.88	100.78	6.72	3.40	3.83	7.42	16.63	5.16	113.25

Table C-15. One Hourly Calculation, 31 x 31 Area Source Mean, with Point Source Emissions

Statistic	Station										
	0	1	3	10	14	17	27	28	31	36	All
Number Cases	2892	1213	1489	1670	1641	1768	1702	1381	1783	1475	17014
Mean Measured	303.77	212.38	295.89	419.87	229.56	192.82	187.56	127.21	187.39	145.07	237.36
Mean Calculated	169.41	122.74	155.27	187.06	131.44	145.61	136.23	89.76	132.66	93.81	140.25
Root-Mean-Square Error	240.36	175.01	238.85	397.11	156.22	137.38	139.47	103.68	148.02	146.44	209.20
Mean Error	-134.36	-89.64	-140.62	-232.81	-98.12	-47.21	-51.33	-37.45	-54.72	-51.26	-97.11
Mean Absolute Error	170.42	120.68	176.37	257.52	117.72	99.22	99.46	74.56	103.81	104.45	135.88
Largest Negative Error	-1690.71	-1118.24	-1608.63	-6538.46	-1021.79	-802.23	-934.97	-786.73	-926.06	-722.88	-6538.46
Largest Positive Error	669.75	462.08	455.04	622.58	552.94	552.92	508.70	354.92	1299.57	801.64	1299.57
Error Range	2360.48	1580.32	2063.66	7161.04	1574.73	1355.15	1443.67	1141.65	2225.63	1524.51	7838.03
Least Error	0.22	-0.14	0.27	-0.02	-0.02	0.01	0.05	0.02	0.05	-0.03	0.01
Linear Correlation	0.426	0.344	0.230	0.215	0.365	0.264	0.303	0.137	0.229	0.127	0.347
Reduction of Variance	0.181	0.118	0.053	0.046	0.133	0.070	0.092	0.019	0.052	0.016	0.120
Slope, Least Squares	0.938	0.638	0.478	0.635	0.606	0.347	0.494	0.224	0.217	0.131	0.694
Intercept, Least Squares	144.79	134.07	221.71	301.03	149.89	142.29	120.23	107.11	158.54	132.79	140.10
Max. Measurement	2242.48	1349.53	1723.04	6710.64	1345.49	1009.12	1178.08	835.76	1071.59	902.68	6710.64
Error at Max. Measurement	-1634.54	-1004.85	-1608.63	-6538.46	-1021.79	-696.16	-934.97	-786.73	-926.06	-714.40	-6538.46
Skewness of Error Dist.	-1.44	-1.65	-1.24	-6.87	-0.98	-0.42	-0.75	-1.10	1.47	0.67	-4.70
Kurtosis of Error Dist.	5.66	7.71	5.52	104.19	5.76	3.48	3.96	6.70	16.50	5.08	109.01

Table C-16. One Hourly Calculation, $\overline{Q}_A$ Area Source Mean, with Point Source Emissions

Statistic	Station										
	0	1	3	10	14	17	27	28	31	36	All
Number Cases	2892	1213	1489	1670	1641	1768	1702	1381	1783	1475	17014
Mean Measured	303.77	212.38	295.89	419.87	229.56	192.82	187.56	127.21	187.39	145.07	237.36
Mean Calculated	485.69	252.57	413.28	625.54	109.61	168.62	159.94	97.14	168.38	144.94	280.32
Root-Mean-Square Error	328.55	180.73	302.13	471.11	168.78	137.03	137.01	102.44	145.64	141.41	248.67
Mean Error	181.92	40.18	117.39	205.67	-119.96	-24.20	-27.62	-30.07	-19.01	-0.13	42.96
Mean Absolute Error	229.79	124.45	211.93	307.33	130.89	97.90	97.11	73.73	97.73	95.49	153.66
Largest Negative Error	-762.15	-993.27	-1385.59	-6203.81	-1084.14	-761.37	-895.73	-781.20	-903.03	-641.16	-6203.81
Largest Positive Error	2132.97	853.42	1705.69	2390.21	430.51	645.68	640.50	370.61	1375.93	1014.86	2390.21
Error Range	2895.11	1846.70	3091.28	8594.01	1514.65	1407.05	1536.24	1151.81	2278.95	1656.02	8594.01
Least Error	-0.25	0.18	-0.02	-0.67	-0.30	-0.14	-0.03	0.04	0.09	0.08	-0.02
Linear Correlation	0.465	0.365	0.199	0.271	0.371	0.267	0.306	0.144	0.243	0.198	0.481
Reduction of Variance	0.216	0.133	0.039	0.074	0.138	0.071	0.094	0.021	0.059	0.039	0.231
Slope, Least Squares	0.348	0.367	0.157	0.238	0.734	0.308	0.427	0.220	0.209	0.178	0.348
Intercept, Least Squares	134.83	119.80	231.09	271.02	149.16	140.81	119.29	105.81	152.26	119.31	139.75
Max. Measurement	2242.48	1349.53	1723.04	6710.64	1345.49	1009.12	1178.08	835.76	1071.59	902.68	6710.64
Error at Max. Measurement	-740.42	-861.91	-1385.59	-6203.81	-1084.14	-629.36	-895.73	-781.20	-903.03	-641.16	-6203.81
Skewness of Error Dist.	1.58	-0.09	0.80	-2.05	-1.33	-0.08	-0.37	-1.00	1.61	1.02	0.38
Kurtosis of Error Dist.	6.50	4.63	4.41	37.35	6.51	3.39	3.67	6.45	15.20	5.43	36.39

Table C-17. One Hourly Calculation, $\overline{\dot{Q}}_B$ Area Source Mean, with Point Source Emissions

Statistic	Station									
	0	1	3	10	14	17	27	28	31	36	All
Number Cases	2892	1213	1489	1670	1641	1768	1702	1381	1783	1475	17014
Mean Measured	303.77	212.38	295.89	419.87	229.56	192.82	187.56	127.21	187.39	145.07	237.36
Mean Calculated	350.51	225.66	312.53	423.55	131.44	168.62	156.39	89.76	156.08	93.81	222.21
Root-Mean-Square Error	227.29	168.36	235.71	353.55	156.22	137.03	137.01	103.68	145.09	146.44	197.62
Mean Error	46.74	13.27	16.65	3.68	-98.12	-24.20	-31.18	-37.45	-31.32	-51.26	-15.15
Mean Absolute Error	160.08	114.38	165.89	212.58	117.72	97.90	97.13	74.56	98.57	104.45	127.43
Largest Negative Error	-1122.57	-1019.18	-1472.68	-6357.97	-1021.79	-761.37	-901.62	-786.73	-910.97	-722.88	-6357.97
Largest Positive Error	1475.49	725.96	1144.83	1480.25	552.94	645.68	620.73	354.92	1349.60	801.64	1480.25
Error Range	2598.06	1745.13	2617.50	7838.22	1574.73	1407.05	1522.35	1141.65	2260.57	1524.51	7838.22
Least Error	0.05	-0.02	0.10	0.03	-0.02	-0.14	-0.02	0.02	-0.01	-0.03	-0.01
Linear Correlation	0.463	0.365	0.208	0.265	0.365	0.267	0.306	0.137	0.239	0.127	0.470
Reduction of Variance	0.214	0.133	0.043	0.070	0.133	0.071	0.094	0.019	0.057	0.016	0.221
Slope, Least Squares	0.489	0.408	0.220	0.351	0.606	0.308	0.436	0.224	0.213	0.131	0.488
Intercept, Least Squares	132.54	120.29	226.99	271.24	149.89	140.81	119.37	107.11	154.16	132.79	128.94
Max. Measurement	2242.48	1349.53	1723.04	6710.64	1345.49	1009.12	1178.08	835.76	1071.59	902.68	6710.64
Error at Max. Measurement	-1122.57	-891.54	-1472.68	-6357.97	-1021.79	-629.36	-901.62	-786.73	-910.97	-714.40	-6357.97
Skewness of Error Dist.	0.43	-0.42	0.06	-4.74	-0.98	-0.08	-0.43	-1.10	1.56	0.67	-2.29
Kurtosis of Error Dist.	4.37	5.09	4.11	72.94	5.76	3.39	3.70	6.70	15.74	5.08	78.33

Table C-18. 24 Hourly Calculations, 1 x 1 Area Source Mean, with Point Source Emissions

Statistic	Station										
	0	1	3	10	14	17	27	28	31	36	All
Number Cases	364	213	257	268	266	285	281	233	283	245	2695
Mean Measured	302.80	211.56	292.39	420.33	229.35	194.02	184.71	125.89	185.87	143.51	233.16
Mean Calculated	605.35	355.91	401.55	696.33	124.69	126.66	176.11	28.91	74.47	75.03	278.63
Root-Mean-Square Error	357.52	200.66	232.20	399.25	130.73	109.94	92.32	123.47	136.40	112.74	222.98
Mean Error	302.55	144.35	109.16	276.00	-104.65	-67.36	-8.60	-96.98	-111.40	-63.48	45.47
Mean Absolute Error	305.64	166.14	181.45	319.17	107.94	83.47	70.31	98.37	116.55	88.67	159.06
Largest Negative Error	-142.85	-485.34	-1052.60	-1046.09	-451.78	-530.08	-276.14	-420.55	-398.89	-362.98	-1052.60
Largest Positive Error	1424.36	638.12	770.52	1331.82	84.19	230.71	327.71	59.05	202.76	214.80	1424.36
Error Range	1567.21	1123.46	1823.12	2377.91	535.97	760.79	603.84	479.60	601.65	577.78	2476.96
Least Error	-0.27	2.22	-3.56	3.24	-0.02	-0.07	0.12	-0.23	-0.95	-0.94	-0.02
Linear Correlation	0.532	0.514	0.148	0.344	0.504	0.320	0.406	-0.049	0.323	0.160	0.585
Reduction of Variance	0.283	0.264	0.022	0.119	0.254	0.102	0.164	0.002	0.104	0.025	0.343
Slope, Least Squares	0.397	0.498	0.159	0.273	1.066	0.562	0.635	-0.200	0.430	0.231	0.334
Intercept, Least Squares	62.39	34.48	228.55	230.01	96.37	122.84	72.95	131.68	153.82	126.15	140.09
Max. Measurement	916.65	932.63	1313.45	1612.87	607.10	674.30	546.97	446.26	474.04	412.70	1612.87
Error at Max. Measurement	-142.85	-485.34	-1052.60	-173.10	-451.78	-530.08	-177.19	-420.55	-398.89	-362.98	-173.10
Skewness of Error Dist.	0.92	-0.17	-0.48	0.05	-1.00	-0.78	-0.05	-1.12	-0.43	-0.12	1.15
Kurtosis of Error Dist.	3.17	2.68	3.79	3.27	2.11	2.90	0.46	1.92	2.68	0.83	3.19

Table C-19. 24 Hourly Calculations, 19 x 19 Area Source Mean, with Point Source Emissions

Statistic	Station										
	0	1	3	10	14	17	27	28	31	36	All
Number Cases	364	213	257	268	266	285	281	233	283	245	2695
Mean Measured	302.80	211.56	292.39	420.33	229.35	194.02	184.71	125.89	185.87	143.51	233.16
Mean Calculated	237.98	154.97	203.33	267.49	103.63	160.50	144.68	49.34	127.32	105.46	159.89
Root-Mean-Square Error	153.51	131.47	187.51	261.44	147.89	96.39	98.30	106.61	98.51	94.94	147.20
Mean Error	-64.81	-56.59	-89.06	-152.84	-125.71	-33.51	-40.02	-76.54	-58.56	-38.05	-73.27
Mean Absolute Error	118.19	89.03	133.48	183.77	126.62	73.09	75.03	81.72	76.97	71.38	103.69
Largest Negative Error	-574.81	-707.91	-1191.65	-1313.26	-476.18	-490.16	-304.18	-391.28	-353.18	-291.93	-1313.26
Largest Positive Error	286.03	193.17	382.36	340.83	41.01	294.66	232.70	83.01	287.52	242.48	382.36
Error Range	860.83	901.09	1574.01	1654.10	517.19	784.82	536.88	474.28	640.70	534.41	1695.62
Least Error	-0.30	-0.31	-0.84	-0.91	0.11	-0.00	0.34	0.70	0.35	0.56	-0.00
Linear Correlation	0.520	0.524	0.199	0.306	0.529	0.317	0.405	0.096	0.373	0.240	0.557
Reduction of Variance	0.270	0.275	0.039	0.094	0.280	0.100	0.164	0.009	0.139	0.058	0.310
Slope, Least Squares	1.061	1.133	0.428	0.667	1.341	0.459	0.781	0.347	0.437	0.328	0.942
Intercept, Least Squares	50.22	35.98	205.31	241.98	90.38	120.28	71.77	108.78	130.29	108.91	82.47
Max. Measurement	916.65	932.63	1313.45	1612.87	607.10	674.30	546.97	446.26	474.04	412.70	1612.87
Error at Max. Measurement	-574.81	-707.91	-1191.65	-1097.55	-476.18	-490.16	-250.45	-391.28	-346.31	-291.93	-1097.55
Skewness of Error Dist.	-0.55	-1.59	-1.45	-1.75	-1.12	-0.48	-0.26	-1.11	0.07	0.06	-1.81
Kurtosis of Error Dist.	0.20	5.03	7.13	6.31	2.13	2.53	0.23	2.00	3.23	0.85	11.23

Table C-20. 24 Hourly Calculations, 31 x 31 Area Source Mean, with Point Source Emissions

Statistic	Station										
	0	1	3	10	14	17	27	28	31	36	All
Number Cases	364	213	257	268	266	285	281	233	283	245	2695
Mean Measured	302.80	211.56	292.39	420.33	229.35	194.02	184.71	125.89	185.87	143.51	233.16
Mean Calculated	169.36	123.70	153.52	186.56	131.24	146.37	136.20	89.81	134.02	96.05	139.24
Root-Mean-Square Error	196.19	149.18	211.94	314.48	125.75	100.68	101.80	80.73	95.08	99.65	164.93
Mean Error	-133.44	-87.86	-138.87	-231.77	-98.10	-47.65	-48.51	-36.08	-31.85	-47.46	-93.92
Mean Absolute Error	150.22	104.12	159.33	239.82	102.64	76.50	77.99	58.39	73.35	76.07	113.58
Largest Negative Error	-655.51	-742.55	-1226.60	-1362.44	-444.19	-506.83	-311.75	-336.72	-347.67	-313.90	-1362.44
Largest Positive Error	153.86	161.29	291.91	191.22	101.41	267.95	207.05	130.44	298.27	233.92	298.27
Error Range	809.37	903.84	1518.51	1553.66	545.60	774.78	518.80	467.17	645.94	547.82	1660.71
Least Error	-0.11	-0.24	-0.74	-2.24	0.39	-0.04	0.97	-0.02	0.86	-0.26	-0.02
Linear Correlation	0.491	0.514	0.222	0.265	0.497	0.319	0.404	0.246	0.376	0.217	0.475
Reduction of Variance	0.241	0.265	0.049	0.070	0.247	0.102	0.163	0.061	0.141	0.047	0.226
Slope, Least Squares	1.424	1.337	0.611	0.813	0.998	0.500	0.829	0.587	0.431	0.303	1.167
Intercept, Least Squares	61.71	46.15	198.52	267.05	98.43	120.85	71.75	73.19	128.16	114.38	70.65
Max. Measurement	916.65	932.63	1313.45	1612.87	607.10	674.30	546.97	446.26	474.04	412.70	1612.87
Error at Max. Measurement	-655.51	-742.55	-1226.60	-1267.70	-444.19	-506.83	-270.23	-333.32	-339.64	-313.90	-1267.70
Skewness of Error Dist.	-0.68	-1.72	-1.57	-1.84	-0.96	-0.61	-0.32	-1.03	0.14	0.00	-2.11
Kurtosis of Error Dist.	0.22	5.25	7.64	6.35	2.10	2.68	0.19	1.96	3.28	0.84	11.14

Table C-21. 24 Hourly Calculations, $\overline{Q}^*_A$ Area Source Mean, with Point Source Emissions

Statistic	Station										
	0	1	3	10	14	17	27	28	31	36	All
Number Cases	364	213	257	268	266	285	281	233	283	245	2695
Mean Measured	302.80	211.56	292.39	420.33	229.35	194.02	184.71	125.89	185.87	143.51	233.16
Mean Calculated	485.37	253.81	410.00	634.47	109.38	169.37	159.91	97.21	170.41	147.59	272.91
Root-Mean-Square Error	244.24	129.27	238.25	345.65	143.05	94.86	93.93	77.70	85.23	86.05	180.34
Mean Error	182.58	42.25	117.61	214.14	-119.96	-24.65	-24.80	-28.67	-15.46	4.08	39.75
Mean Aboslute Error	201.60	95.98	186.60	272.23	121.32	71.88	71.34	56.31	60.90	63.34	123.72
Largest Negative Error	-283.92	-598.43	-1046.67	-1084.63	-469.52	-479.70	-290.59	-329.99	-317.74	-222.30	-1084.63
Largest Positive Error	1052.60	364.08	790.94	1146.69	52.80	311.41	278.73	139.12	356.64	291.42	1146.69
Error Range	1336.52	962.51	1837.61	2231.32	522.31	791.11	569.32	469.11	674.39	513.72	2231.32
Least Error	-0.05	-0.13	0.08	-0.40	0.20	0.07	0.03	-0.10	0.36	0.24	0.03
Linear Correlation	0.532	0.523	0.147	0.343	0.522	0.316	0.40[illegible]	0.280	0.344	0.321	0.592
Reduction of Variance	0.283	0.273	0.022	0.118	0.272	0.100	0.164	0.068	0.147	0.103	0.350
Slope, Least Squares	0.503	0.710	0.154	0.300	1.257	0.436	0.704	0.575	0.387	0.387	0.421
Intercept, Least Squares	58.54	31.30	229.14	229.87	91.82	120.15	72.20	69.99	119.97	86.43	118.21
Max. Measurement	916.65	932.63	1313.45	1612.87	607.10	674.30	546.97	446.26	474.04	412.70	1612.87
Error at Max. Measurement	-283.92	-598.43	-1046.67	-306.46	-469.52	-479.70	-214.96	-322.71	-303.43	-193.57	-306.46
Skewness of Error Dist.	0.48	-0.94	-0.43	-0.20	-1.09	-0.40	-0.16	-1.00	0.51	0.30	0.95
Kurtosis of Error Dist.	1.94	3.83	3.68	3.48	2.13	2.44	0.32	1.91	3.49	1.02	4.85

Table C-22. 24 Hourly Calculations, $\overline{Q}_B$: Area Source Mean, with Point Source Emissions

Statistic	Station										
	0	1	3	10	14	17	27	28	31	36	All
Number Cases	364	213	257	268	266	285	281	233	283	245	2695
Mean Measured	302.80	211.56	292.39	420.33	229.35	194.02	184.71	125.89	185.87	143.51	233.16
Mean Calculated	350.31	226.84	309.85	429.06	131.24	169.37	156.35	89.81	157.87	96.05	217.70
Root-Mean-Square Error	150.03	120.77	183.83	227.37	125.75	94.86	94.72	80.73	86.76	99.65	135.13
Mean Error	47.51	15.28	17.47	8.73	-98.10	-24.65	-28.36	-36.08	-28.01	-47.46	-15.46
Mean Absolute Error	120.98	86.67	134.46	165.49	102.64	71.88	71.97	58.39	63.53	76.07	96.34
Largest Negative Error	-442.73	-628.30	-1116.93	-1212.61	-444.19	-479.70	-293.77	-336.72	-328.06	-313.90	-1212.61
Largest Positive Error	634.08	296.07	575.77	647.07	101.41	311.41	267.98	130.44	336.52	233.92	647.07
Error Range	1076.81	924.38	1692.70	1859.68	545.60	791.11	561.74	467.17	664.58	547.82	1859.68
Least Error	-0.23	1.11	-1.12	-0.22	0.39	0.07	-0.04	-0.02	0.13	-0.26	-0.02
Linear Correlation	0.531	0.525	0.165	0.333	0.497	0.316	0.405	0.246	0.382	0.217	0.594
Reduction of Variance	0.282	0.275	0.027	0.111	0.247	0.100	0.164	0.061	0.146	0.047	0.353
Slope, Least Squares	0.713	0.796	0.233	0.441	0.998	0.436	0.720	0.587	0.403	0.303	0.635
Intercept, Least Squares	52.86	30.97	220.32	230.96	98.43	120.15	72.06	73.19	122.21	114.38	94.93
Max. Measurement	916.65	932.63	1313.45	1612.87	607.10	674.30	546.97	446.26	474.04	412.70	1612.87
Error at Max. Measurement	-442.73	-628.30	-1116.93	-749.27	-444.19	-479.70	-223.25	-333.32	-315.92	-313.90	-749.27
Skewness of Error Dist.	-0.15	-1.15	-0.97	-1.18	-0.96	-0.40	-0.19	-1.03	0.38	0.00	-0.54
Kurtosis of Error Dist.	0.58	4.20	5.25	5.01	2.10	2.44	0.30	1.96	3.43	0.84	7.45

- Averaging procedures 1 x 1, 31 x 31, and $\overline{Q}_B^*$ generally produce the highest linear correlation of calculated values to measured values.
- Averaging procedures 19 x 19 and $\overline{Q}_B^*$ generally produce the smallest RMS errors.
- Averaging procedures 19 x 19 and $\overline{Q}_B^*$ generally produce the smallest mean absolute errors.

The averaging procedure $\overline{Q}_B^*$ produced the better calculations and has been used in the validation results reported in Section 3.2.

C.3 ANALYSIS OF GHM CALCULATIONS IN TERMS OF PARAMETERS OF THE VARIABLE EMISSION RATE ALGORITHM

The hourly area source emission rates were derived from annual means on the basis of an algorithm which is a function of the hour of the day and temperature. An analysis was made of the hourly calculations obtained with GHM using this algorithm and the five averaging procedures by temperature, hour of the day, day of the week, and month of the year. The mean and RMSE of calculated concentrations, without the addition of concentrations from point sources, for all stations combined are shown in Table C-23; a summary for calculations with point source concentrations added is shown in Table C-24. Both the measured and calculated values exhibit a strong peak at 7 a.m. and a weaker peak at 7 p.m. The amplitudes of the cycles generally agree except at 7 a.m. when the calculated concentrations are relatively too large. There is no discernible variation by day of the week. Both measured and calculated values show an inverse relationship to temperature, and the amplitudes of the two distributions

Table C-23. Selected Comparisons of GHM Calculations (Without Point Sources) and Measurements of NYC Hourly SO_2 Concentrations

	CASES	MEASURED MEAN	1 x 1		19 x 19		31 x 51		$\overline{Q}_{a}^{*}$		$\overline{Q}_{b}^{*}$	
			CALCULATED MEAN	RMSE	CALCULATED MEAN	RMSE	CALCULATED MEAN	RMSE	CALCULATED MEAN	RMSE	CALCULATED MEAN	RMSE
HOUR												
1	2143	208.79	213.49	236.13	104.62	167.74	85.51	179.97	205.77	194.15	155.66	158.85
4	2116	237.02	246.49	279.86	121.36	196.99	94.64	210.35	236.22	232.50	180.53	189.90
7	2111	302.69	415.49	449.12	202.92	250.13	165.85	272.43	398.86	364.86	302.40	265.63
10	2077	258.18	259.47	316.14	126.23	276.53	102.96	294.60	249.02	276.46	186.29	257.22
13	2134	222.77	192.44	232.63	93.38	207.09	75.86	222.79	184.32	200.48	139.29	137.31
16	2146	214.18	191.94	217.17	93.45	189.92	75.92	206.14	183.47	163.44	139.94	168.25
19	2146	230.70	242.59	243.52	118.28	158.54	96.24	209.60	232.11	201.16	176.00	167.47
22	2141	226.13	235.25	233.78	114.95	181.15	93.75	199.07	225.94	191.95	171.12	161.91
DAY												
MON	1796	231.65	249.47	263.12	113.89	207.15	89.41	227.38	229.79	215.60	171.39	187.66
TUE	3191	241.80	232.66	291.23	116.49	243.78	98.75	259.70	228.96	252.36	175.10	228.25
WED	3350	232.39	219.40	250.64	111.63	199.00	92.74	214.87	216.63	211.39	165.05	192.71
THUR	3362	233.32	245.25	282.07	124.29	180.73	103.25	205.24	241.07	235.12	184.16	181.93
FRI	3193	237.88	235.36	270.36	118.49	211.08	96.34	228.15	230.14	229.76	175.97	196.19
SAT	1710	240.51	291.67	3.2.26	137.27	199.16	110.12	216.36	273.67	261.47	205.78	201.91
SUN	412	283.93	586.60	481.86	203.43	217.97	131.85	249.25	461.46	350.93	320.58	238.65
MONTH												
JAN	1338	334.06	384.49	325.24	177.98	281.88	138.83	317.40	348.86	286.22	265.57	245.98
FEB	944	331.17	391.20	373.47	176.70	240.35	130.70	280.68	348.11	247.43	260.08	228.72
MARCH	1428	318.83	243.57	251.37	117.41	281.82	96.23	307.74	231.88	224.80	170.23	236.50
APRIL	1572	294.84	217.30	316.55	108.81	332.56	89.61	352.29	212.67	294.47	161.29	301.15
MAY	1337	213.48	200.50	228.27	100.88	176.45	81.68	193.28	199.91	167.62	145.23	159.87
JUNE	1390	169.12	184.37	221.69	93.95	136.46	77.91	144.38	183.39	190.50	130.33	136.83
JULY	1549	158.78	216.91	257.06	106.40	125.33	87.32	128.45	209.99	210.21	159.48	146.11
AUGUST	1401	160.87	219.15	283.08	109.32	129.35	91.27	127.73	214.31	227.34	162.62	156.35
SEPT	1438	162.97	202.06	274.60	104.57	131.04	88.13	130.73	200.90	222.17	151.23	156.29
OCT	1701	211.91	227.06	270.15	112.90	176.63	93.35	187.44	223.11	224.43	165.57	178.50
NOV	1353	249.17	275.65	301.77	137.20	178.50	113.77	197.30	267.08	235.40	203.95	177.13
DEC	1563	279.23	287.03	309.76	141.90	198.40	116.84	213.82	277.53	242.74	211.19	190.35
TEMP												
L.E. 14	36	363.11	425.18	299.26	192.99	260.46	150.05	299.20	374.85	265.99	288.36	224.63
15 - 24	511	321.97	403.40	376.56	186.04	223.39	147.51	253.04	370.13	300.46	281.13	218.22
25 - 34	2595	299.15	327.09	296.79	153.76	224.92	122.67	254.47	302.33	234.70	224.98	196.58
35 - 44	2573	305.72	307.72	317.73	147.70	250.83	119.57	276.78	290.75	262.22	220.56	225.39
45 - 54	2401	278.56	249.51	322.73	124.38	282.20	102.47	299.68	245.71	284.52	185.26	263.53
55 - 64	3316	209.70	216.44	270.08	109.26	195.18	90.25	206.61	214.92	229.00	161.81	191.21
G.E. 65	5582	167.26	190.45	240.79	94.83	140.46	78.50	145.35	185.45	196.56	140.59	148.78

Table C-24. Selected Comparisons of GHM Calculations (With Point Sources) and Measurements of NYC Hourly SO_2 Concentrations

			1 x 1		19 x 19		31 x 31		$\overline{Q}^*_A$		$\overline{Q}^*_B$	
	CASES	MEASURED MEAN	CALCULATED MEAN	RMSE	CALCULATED MEAN	RMSE	CALCULATED MEAN	RMSE	CALCULATED MEAN	RMSE	CALCULATED MEAN	RMSE
HOUR												
1	2143	204.79	251.52	245.67	142.65	157.11	123.54	165.13	243.79	206.04	193.68	160.41
4	2116	237.02	286.68	291.29	161.55	189.16	134.84	198.12	278.42	247.57	220.73	194.92
7	2111	302.69	464.72	467.67	252.16	240.89	215.08	255.53	448.10	390.96	351.64	275.69
10	2077	258.18	307.25	323.49	174.01	258.59	150.74	272.63	296.79	265.39	230.66	251.51
13	2134	222.77	233.32	233.23	134.26	185.21	116.73	198.37	225.20	155.69	180.18	174.67
16	2146	214.18	230.29	224.66	131.80	175.77	114.27	160.75	221.67	191.03	177.29	164.02
19	2146	230.70	277.08	251.57	153.47	175.08	131.53	193.09	267.40	205.79	211.29	164.79
22	2141	226.13	273.14	245.93	152.05	167.76	131.65	181.36	263.04	204.17	209.01	161.60
DAY												
MON	1796	231.65	287.73	273.33	152.14	192.67	127.67	269.11	265.05	224.59	209.64	164.35
TUE	3191	241.80	273.02	296.41	158.85	228.56	139.11	241.17	269.32	258.56	215.47	223.40
WED	3350	232.39	259.36	257.74	151.59	184.86	132.70	197.23	258.79	220.88	205.01	150.32
THUR	3322	233.32	285.32	293.36	164.36	176.78	143.32	168.61	281.14	246.78	224.22	194.43
FRI	3193	237.88	276.49	276.05	159.63	196.41	139.48	209.85	271.28	239.33	217.11	193.68
SAT	1710	240.51	339.71	339.39	185.31	188.47	158.16	197.29	321.72	281.42	253.82	209.26
SUN	812	283.93	626.69	510.55	243.52	211.21	171.94	231.00	501.55	370.00	360.67	252.28
MONTH												
JAN	1330	334.00	422.53	336.68	216.02	262.68	176.87	294.47	388.91	295.42	303.63	240.23
FEB	944	331.17	413.15	379.53	192.73	233.24	152.65	264.96	370.06	301.66	282.03	223.93
MARCH	1428	318.83	273.33	245.90	147.17	260.77	125.99	285.77	261.64	217.76	266.09	226.32
APRIL	1572	244.64	263.34	309.86	154.85	308.07	135.65	325.74	251.71	244.49	207.32	283.41
MAY	1337	213.46	249.44	235.51	149.82	150.62	130.62	162.72	240.65	193.97	197.17	149.81
JUNE	1390	169.12	235.97	246.08	145.57	131.72	129.53	132.61	235.01	208.91	165.55	152.28
JULY	1549	158.70	264.22	283.91	156.72	128.75	137.63	121.19	266.30	250.40	209.40	166.56
AUGUST	1401	160.87	276.07	310.61	166.23	147.68	146.19	138.27	271.22	264.10	219.54	189.21
SEPT	1438	162.97	244.84	291.78	147.35	126.53	130.92	117.38	243.65	241.61	196.01	167.86
OCT	1701	211.91	265.26	279.91	151.10	168.75	131.55	172.39	261.32	236.99	200.77	180.67
NOV	1353	249.17	305.39	308.99	166.93	162.71	143.51	177.73	247.61	244.24	233.65	174.94
DEC	1563	279.23	317.76	309.26	172.63	177.10	147.57	169.94	301.26	243.65	241.92	179.48
TEMP												
L.E. 14	36	363.11	457.18	321.05	224.59	245.61	112.05	276.77	406.86	265.83	320.36	227.15
15 - 24	511	321.97	426.53	382.99	211.18	211.54	177.64	238.23	395.26	306.84	306.26	217.98
25 - 34	2595	249.15	353.52	360.75	180.19	208.75	149.10	236.40	328.76	243.42	250.41	169.32
35 - 44	2573	305.72	342.19	321.13	182.18	229.42	154.00	252.71	325.23	264.85	255.04	214.71
45 - 54	2401	278.56	287.11	324.80	161.97	263.72	140.67	278.14	283.31	280.76	222.06	254.42
55 - 64	3316	209.70	256.92	279.77	149.73	180.26	136.73	188.86	255.40	237.64	202.28	189.90
G.E. 65	5582	167.26	244.25	262.99	148.63	178.61	132.30	135.11	234.25	223.14	194.34	164.85

Reproduced from best available copy.

agree well. Overall, the $\overline{Q}_B^*$ averaging procedure with point sources added produced the best results for 20 of the possible 68 comparisons of means and RMSE's in Tables C-23 and C-24.

Appendix D

FREQUENCY DISTRIBUTIONS FOR SCIM CALCULATIONS USING 3 TO 96 HOUR SAMPLING INTERVALS

Tables D-1 through D-10 show the number of calculations, means, standard deviations, and frequency distributions of SCIM variable Q, S, and H calculations using proportionate stratified sampling for various size sampling intervals. Each table shows calculations for one of 10 sampling locations in New York City. The sampling interval was varied from 1 to 32 3-hour periods or from 3 to 96 hours.

Table D-1. Test of Sampling Intervals for Long-Term Mean, NYC Station #0

	SAMPLING INTERVAL (NO. OF 3HR. INCREMENTS)									
	1	2	3	4	6	8	12	16	24	32
NO. OF COMPARISONS	2908	1455	971	726	487	363	244	183	122	92
	421.139	427.612	415.114	418.025	420.644	426.567	424.351	430.883	434.141	439.953
STANDARD DEVIATION	420.398	428.972	413.016	396.982	431.280	407.070	477.973	364.688	555.751	407.817
DISTRIBUTION PERCENTILES										
HIGH	5149.074	3607.335	4626.227	3330.449	4626.227	3330.449	4626.227	2482.139	4626.227	1857.737
99.5	2451.900	2814.579	2451.900	2238.735	2451.900	2225.886	2451.900	1775.432	2451.900	1657.737
99.0	2106.074	2230.271	1998.935	2180.929	2230.271	1819.809	2277.839	1669.186	2451.900	1796.773
95.0	1219.814	1236.119	1209.306	1249.933	1201.319	1273.255	1273.255	1172.962	1143.462	1356.292
90.0	872.728	892.367	832.518	879.709	843.623	931.467	892.728	838.017	854.770	900.921
80.0	583.056	542.622	584.753	590.614	595.562	584.028	578.123	622.159	557.999	646.376
70.0	443.254	441.051	449.536	432.734	447.612	426.665	413.881	475.352	400.939	522.746
60.0	341.023	342.532	336.238	344.607	334.500	344.911	309.237	364.393	297.575	303.190
50.0	276.718	276.634	273.546	290.289	268.861	292.031	254.483	300.190	243.483	267.474
40.0	229.593	228.133	227.045	226.752	237.113	237.298	229.038	254.483	222.025	235.117
30.0	193.922	189.650	189.503	189.160	194.665	193.200	186.153	211.660	178.278	209.645
20.0	163.031	162.757	158.565	156.565	162.757	159.324	158.565	182.348	146.803	161.053
10.0	127.640	127.463	125.467	125.810	126.144	125.500	126.729	137.389	134.550	115.814
5.0	109.547	110.046	110.662	108.793	111.371	96.312	115.314	118.186	115.314	105.497
1.0	79.998	81.039	82.223	78.297	88.286	70.153	78.297	89.284	76.429	0.000
0.5	73.425	76.153	77.652	70.089	78.297	66.666	76.429	67.412	76.429	0.000
LOW	55.872	56.447	55.872	65.320	76.429	65.320	76.429	67.412	76.429	0.000

Table D-2. Test of Sampling Intervals for Long-Term Mean, NYC Station #1

	SAMPLING INTERVAL (NO. OF 3HR. INCREMENTS)									
	1	2	3	4	6	8	12	16	24	32
OF COMPARISONS	2908	1455	971	726	487	363	244	183	122	92
	269.704	273.881	264.008	260.606	268.503	274.938	265.852	273.144	285.129	286.376
DARD DEVIATION	402.539	386.959	399.927	353.265	399.029	382.030	435.605	296.757	532.568	355.324
RIBUTION PERCENTILES										
HIGH	7467.582	4751.422	5089.258	4751.422	5089.258	4751.422	5089.258	1872.469	5089.258	1948.530
99.5	2385.150	2453.761	2294.507	2294.507	2497.659	1872.469	2294.507	1642.852	2004.611	1948.530
99.0	2004.611	1921.719	1810.606	1575.988	1659.621	1575.988	2004.611	1575.988	2004.611	1490.062
95.0	904.645	942.149	817.009	848.517	891.978	899.085	891.978	834.205	814.049	1023.890
90.0	601.979	630.966	580.076	599.703	599.934	640.158	543.244	623.647	543.244	585.912
80.0	352.678	360.810	353.692	360.810	345.462	385.854	331.692	412.374	376.897	388.779
70.0	251.238	259.472	247.808	263.863	248.695	274.368	251.101	279.224	246.684	268.820
60.0	187.944	169.357	185.365	191.253	187.605	195.046	187.805	212.709	192.720	213.951
50.0	145.280	148.144	145.862	152.050	153.285	152.899	156.130	166.241	153.265	163.323
40.0	111.435	112.162	108.994	113.610	112.856	122.567	104.292	135.035	103.679	115.295
30.0	84.140	83.503	82.113	83.100	86.428	90.202	79.775	94.649	79.775	85.442
20.0	64.172	64.053	63.870	61.844	64.987	67.265	63.028	73.270	61.252	65.251
10.0	48.794	48.335	47.403	47.632	47.208	47.101	47.076	55.008	46.063	46.063
5.0	40.862	41.787	40.733	41.870	40.679	37.776	39.302	43.544	38.799	37.443
1.0	28.615	28.642	30.031	27.647	34.052	26.854	26.854	28.783	26.854	21.290
0.5	26.010	24.446	27.342	24.446	26.854	23.973	26.010	24.446	26.854	21.290
LOW	19.179	19.339	24.550	23.856	26.010	23.856	26.010	24.446	26.854	21.290

Table D-3. Test of Sampling Intervals for Long-Term Mean, NYC Station #3

	SAMPLING INTERVAL (NO. OF 3HR. INCREMENTS)									
	1	2	3	4	6	8	12	16	24	32
JF COMPARISONS	2908	1455	971	726	487	363	244	183	122	92
	384.116	369.620	378.000	381.411	384.548	369.709	388.773	402.279	400.276	431.782
DARD DEVIATION	402.656	400.104	395.460	373.038	404.767	389.575	453.314	344.356	532.446	440.460
IBUTION PERCENTILES										
HIGH	6126.133	3933.947	3833.253	3933.947	3765.376	3933.947	3765.376	1826.472	3765.376	2182.103
99.5	2398.468	2361.104	2427.404	1894.918	2475.771	1846.258	2955.959	1554.963	2955.959	2182.103
99.0	1947.038	1941.958	1941.958	1861.367	2087.770	1630.647	2475.771	1551.863	2955.959	2065.358
95.0	1104.334	1111.152	1038.472	1104.334	1097.055	1166.930	1086.295	1132.993	1078.254	1431.749
90.0	813.581	832.661	765.339	803.728	746.112	806.199	828.929	902.777	824.779	944.519
80.0	536.900	544.816	529.222	539.638	530.248	536.140	515.263	595.006	507.301	573.252
70.0	393.043	397.732	398.515	393.247	393.247	394.077	376.114	436.862	350.938	436.862
60.0	309.755	317.562	306.613	315.663	317.064	320.589	290.710	341.776	292.578	339.370
50.0	246.424	252.672	248.446	253.956	251.800	265.609	234.032	291.353	232.359	251.269
40.0	204.762	206.772	200.423	207.304	209.905	210.081	198.589	224.825	190.729	229.204
30.0	170.587	169.296	165.154	170.573	168.395	174.842	165.255	193.977	156.908	184.283
20.0	139.351	136.690	136.680	134.518	139.351	139.084	134.518	146.797	131.794	144.531
10.0	110.699	109.348	108.238	109.274	109.777	105.646	112.396	116.438	112.396	103.970
5.0	92.422	92.540	96.451	91.784	97.668	89.557	99.793	102.238	98.468	86.036
1.0	69.266	70.635	72.785	66.987	77.771	60.048	77.771	70.635	71.118	53.314
0.5	61.517	61.625	61.790	60.048	71.118	57.743	71.118	67.725	71.118	53.314
LOW	45.963	57.509	45.963	57.509	62.314	57.509	71.118	67.725	71.118	53.314

Table D-4. Test of Sampling Intervals for Long-Term Mean, NYC Station #10

	SAMPLING INTERVAL (NO. OF 3HR. INCREMENTS)									
	1	2	3	4	6	8	12	16	24	32
IF COMPARISONS	2908	1455	971	726	487	363	244	183	122	92
	322.792	326.956	317.691	319.484	322.286	327.280	324.374	319.781	309.440	335.211
ARD DEVIATION	347.240	360.699	312.086	335.981	312.708	334.722	351.508	287.885	338.912	291.415
IBUTION PERCENTILES										
HIGH	6379.121	4630.617	3221.789	3069.072	2532.067	3024.574	2532.067	2670.137	2038.297	2158.390
99.5	2266.228	2670.137	2070.985	2081.748	2070.985	1765.745	2070.985	1765.745	2019.175	2158.390
99.0	1725.424	1817.322	1533.179	1765.745	1675.852	1675.852	2038.297	1089.835	2019.175	1054.146
95.0	839.938	891.735	874.631	900.692	959.317	1015.633	1015.633	785.786	1155.223	800.593
90.0	590.801	600.554	590.801	578.462	600.554	618.565	640.473	556.860	578.462	623.779
80.0	431.975	433.696	432.171	421.943	440.660	420.112	433.696	450.588	386.542	470.388
70.0	332.179	327.181	324.291	317.369	324.291	310.130	310.219	360.244	304.620	372.232
60.0	272.034	266.258	266.194	264.788	271.869	269.200	259.314	294.157	229.627	311.823
50.0	229.220	226.220	226.681	229.627	221.901	231.913	203.417	240.718	190.400	255.533
40.0	191.643	193.244	191.271	193.002	188.890	197.661	173.412	214.150	163.788	213.599
30.0	163.216	162.036	160.612	159.593	160.612	166.044	140.312	176.365	134.232	175.751
20.0	132.213	129.079	125.815	125.034	127.557	129.049	120.429	136.230	110.638	139.632
10.0	99.342	97.935	96.604	95.055	98.770	99.387	98.202	91.059	89.946	99.911
5.0	80.988	80.988	80.014	79.721	80.014	80.014	80.014	76.656	76.120	78.058
1.0	58.391	58.630	61.728	57.707	69.013	57.400	69.013	63.610	66.532	43.131
0.5	51.747	52.795	58.289	54.140	59.312	54.140	66.532	58.476	66.532	43.131
LOW	37.680	40.922	37.680	42.711	54.140	51.747	66.532	58.476	66.532	43.131

Table D-5. Test of Sampling Intervals for Long-Term Mean, NYC Station #14

	SAMPLING INTERVAL (NO. OF 3HR. INCREMENTS)									
	1	2	3	4	6	8	12	16	24	32
NO. OF COMPARISONS	2908	1455	971	726	487	363	244	183	122	92
	184.416	188.157	182.402	187.750	186.816	191.278	173.589	210.501	174.469	226.637
STANDARD DEVIATION	253.957	274.348	260.508	266.113	292.157	272.792	242.684	261.391	262.902	287.883
DISTRIBUTION PERCENTILES										
HIGH	3588.174	3588.174	3588.174	2675.094	3588.174	2675.094	1617.148	1561.398	1617.148	1510.684
99.5	1559.057	1612.886	1612.886	1510.684	1617.148	1490.309	1612.886	1510.684	1612.886	1510.684
99.0	1388.928	1440.759	1388.928	1424.497	1408.403	1424.497	1490.309	1424.497	1612.886	1490.309
95.0	600.443	584.055	591.083	597.847	595.558	600.443	625.339	772.459	721.900	716.795
90.0	418.380	419.598	418.300	439.045	418.380	411.140	391.570	514.031	407.858	599.838
80.0	253.506	257.062	248.263	260.466	247.586	257.758	214.676	297.227	201.113	342.929
70.0	176.377	174.947	174.030	181.722	170.936	181.722	149.764	197.144	145.759	226.529
60.0	132.087	134.347	128.391	127.562	124.699	133.890	113.938	149.764	102.657	153.495
50.0	103.746	103.746	102.154	99.144	101.629	101.406	95.752	116.815	94.204	100.934
40.0	81.630	80.999	79.322	75.298	80.716	78.812	79.487	88.925	75.039	80.502
30.0	61.406	60.683	61.326	58.771	61.326	60.436	56.509	65.615	49.025	51.704
20.0	43.419	42.971	41.904	42.137	41.721	43.419	39.587	45.694	36.650	35.287
10.0	30.880	29.940	29.273	30.650	29.768	31.050	29.797	35.311	29.187	28.395
5.0	24.486	24.149	23.451	23.072	23.530	22.026	23.662	26.800	23.051	20.834
1.0	16.825	16.825	16.158	14.571	18.405	13.323	17.591	17.184	14.855	14.571
0.5	14.113	13.295	13.323	13.080	16.841	12.893	14.855	16.841	14.855	14.571
LOW	9.201	9.201	9.424	9.201	14.855	9.201	14.855	16.841	14.855	14.571

Table D-6. Test of Sampling Intervals for Long-Term Mean, NYC Station #17

	SAMPLING INTERVAL (NO. OF 3HR. INCREMENTS)									
	1	2	3	4	6	8	12	16	24	32
OF COMPARISONS	2908	1455	971	726	487	363	244	183	122	92
	205.553	206.702	203.168	202.008	201.095	202.081	203.407	200.670	196.176	192.765
DARD DEVIATION	297.001	297.243	263.677	271.239	251.265	271.046	265.776	233.772	266.302	250.197
TRIBUTION PERCENTILES										
HIGH	6094.626	4465.957	2164.647	2906.021	1965.792	2906.021	1965.792	2019.698	1965.792	2075.194
99.5	1771.217	1906.690	1719.839	1694.731	1391.034	1408.395	1380.828	1041.761	1241.604	2075.194
99.0	1349.187	1406.002	1349.197	1408.395	1241.604	1057.183	1241.604	857.310	1241.604	723.134
95.0	665.767	697.362	699.962	666.850	663.569	666.860	743.322	648.106	663.569	461.061
90.0	465.682	479.477	484.593	464.617	461.061	489.565	497.547	474.921	484.321	395.385
80.0	295.851	296.133	283.593	278.527	294.485	296.133	272.042	311.019	272.042	287.883
70.0	209.302	265.306	212.796	209.026	209.697	203.549	203.680	239.917	182.314	206.240
60.0	146.968	143.670	156.107	149.092	196.522	149.092	149.353	165.673	149.353	176.968
50.0	107.800	106.496	110.792	110.621	110.792	110.821	101.274	110.761	105.663	116.173
40.0	83.935	82.401	82.125	78.674	85.716	83.273	74.072	89.074	76.600	90.414
30.0	61.897	61.284	59.568	59.160	59.603	60.098	57.133	58.951	53.647	67.792
20.0	45.693	44.419	43.935	43.513	43.944	44.156	42.015	44.005	41.969	42.876
10.0	30.887	30.363	29.981	29.843	30.257	29.843	29.243	32.846	29.243	27.003
5.0	23.125	23.738	22.262	23.579	22.845	23.738	21.794	23.076	19.771	19.970
1.0	14.609	14.016	14.016	12.312	15.413	11.825	14.249	16.053	14.232	12.992
0.5	12.313	11.825	11.593	11.825	14.232	11.458	14.232	15.486	14.232	12.992
LOW	7.570	8.343	7.570	10.754	14.016	10.754	14.232	15.486	14.232	12.992

Table D-7. Test of Sampling Intervals for Long-Term Mean, NYC Station #27

	SAMPLING INTERVAL (NO. OF 3HR. INCREMENTS)									
	1	2	3	4	6	8	12	16	24	32
OF COMPARISONS	2908	1455	971	726	487	363	244	183	122	92
	219.172	222.330	211.113	223.472	217.879	222.523	218.633	227.267	200.226	230.048
DARD DEVIATION	291.636	293.329	268.625	302.703	299.000	303.053	288.587	249.350	252.688	290.694
IBUTION PERCENTILES										
HIGH	4299.195	3066.919	2701.377	3066.919	2701.377	3066.919	2169.680	1252.273	2100.954	1881.481
99.5	1941.269	1966.193	1943.708	1943.708	2169.680	1881.481	2100.954	1198.266	961.624	1881.481
99.0	1371.320	1480.056	1252.273	1529.304	1881.481	1397.415	1881.481	1098.758	961.624	1063.134
95.0	707.808	742.280	644.657	736.137	705.749	673.698	736.137	739.577	590.375	790.474
90.0	484.260	475.932	465.660	465.632	421.053	465.632	508.893	553.902	402.921	635.949
80.0	303.159	307.748	303.056	308.271	307.457	299.632	307.748	325.250	303.117	299.352
70.0	224.557	223.898	226.580	221.448	236.473	209.868	239.061	242.539	238.244	241.272
60.0	170.030	176.953	163.168	167.957	166.363	172.390	153.098	184.510	152.299	176.197
50.0	131.601	132.469	126.392	130.372	125.970	132.962	125.097	132.633	125.091	128.493
40.0	100.972	99.717	96.439	99.454	94.947	100.534	92.553	100.288	90.952	104.087
30.0	73.043	74.053	71.745	72.428	68.664	72.995	64.121	77.567	63.216	73.612
20.0	52.856	53.300	50.436	51.938	50.156	52.636	45.906	56.210	39.207	40.982
10.0	31.865	30.966	29.927	30.536	30.091	29.648	27.136	32.031	26.790	26.251
5.0	22.773	23.245	21.613	21.045	22.831	23.683	21.968	25.149	20.520	19.588
1.0	13.736	14.125	13.378	13.415	14.834	13.415	14.125	16.236	12.018	9.460
0.5	12.238	12.900	12.019	12.018	12.018	10.524	12.018	13.736	12.018	9.460
LOW	7.697	8.308	10.648	8.308	10.648	8.308	12.018	13.736	12.018	9.460

Table D-8. Test of Sampling Intervals for Long-Term Mean, NYC Station #28

	SAMPLING INTERVAL (NO. OF 3HR. INCREMENTS)									
	1	2	3	4	6	8	12	16	24	32
. OF COMPARISONS	2909	1455	971	726	487	363	244	183	122	92
[illegible]	104.510	107.267	100.923	112.841	109.312	116.109	111.587	107.540	97.930	125.269
NDARD DEVIATION	201.778	203.934	191.474	226.677	226.328	239.962	243.387	157.363	210.280	275.519
TRIBUTION PERCENTILES										
HIGH	3628.716	2228.474	2228.474	2228.474	2228.474	2228.474	2228.474	1061.241	2171.677	2228.474
99.5	1465.095	1494.640	1465.095	1721.561	2037.450	1858.517	2171.677	866.417	456.883	2228.474
99.0	966.978	984.789	853.033	1275.094	1056.618	1061.241	1580.818	657.943	456.883	966.978
95.0	367.304	373.934	344.640	384.905	371.613	401.222	345.021	400.790	289.098	326.292
90.0	239.150	245.479	239.150	245.479	232.743	248.132	243.916	290.294	206.113	293.741
80.0	132.786	138.596	132.786	138.332	136.105	140.268	137.123	142.343	113.751	161.915
70.0	95.620	95.750	95.419	96.465	98.484	97.611	100.217	107.351	85.718	101.718
60.0	65.358	65.508	64.332	65.911	67.188	70.360	76.517	72.056	60.713	58.778
50.0	45.360	46.260	45.685	45.557	47.018	45.557	48.722	55.984	39.382	37.819
40.0	30.743	31.409	31.598	32.322	31.920	32.920	32.249	30.702	27.046	23.208
30.0	20.518	20.574	20.646	21.763	21.331	20.574	22.045	21.693	18.384	18.892
20.0	11.627	11.845	11.979	12.360	12.124	10.139	13.479	9.817	11.945	13.554
10.0	4.797	5.153	5.009	5.141	4.835	4.218	4.955	3.674	3.822	2.882
5.0	2.282	2.367	2.335	2.335	2.335	2.442	2.841	1.972	2.819	1.198
1.0	1.037	1.137	1.040	1.089	1.056	1.089	0.724	0.758	1.507	0.769
0.5	0.766	0.770	0.724	1.027	0.724	1.027	0.574	0.624	1.507	0.769
LOW	0.540	0.680	0.574	0.680	0.574	0.701	0.574	0.624	1.507	0.769

Table D-9. Test of Sampling Intervals for Long-Term Mean, NYC Station #31

	SAMPLING INTERVAL (NO. OF 3HR. INCREMENTS)									
	1	2	3	4	6	8	12	16	24	32
L. OF COMPARISONS	2908	1455	971	726	407	363	244	183	122	92
AN	229.735	241.046	226.607	231.531	215.407	227.346	220.429	225.715	222.160	180.183
ANDARD DEVIATION	323.365	343.807	321.031	329.912	265.853	305.453	296.560	275.632	350.617	173.042
ISTRIBUTION PERCENTILES										
HIGH	5960.945	5960.945	4451.039	4368.219	2255.448	2719.606	2255.448	2719.606	2255.448	768.912
99.5	1867.116	1937.761	1954.683	1937.761	1589.476	1728.543	1954.683	1381.560	1954.683	768.912
99.0	1589.476	1634.799	1641.931	1546.815	1256.083	1536.477	1589.476	867.547	1954.683	757.669
95.0	741.992	788.572	752.727	781.190	757.669	768.146	788.572	614.959	867.547	496.619
90.0	512.542	533.587	509.927	507.649	500.094	483.653	546.887	476.242	558.009	461.178
80.0	324.438	335.556	317.480	326.283	310.661	310.187	301.345	336.625	288.864	328.462
70.0	226.034	234.525	218.797	227.748	218.896	216.320	204.366	244.577	167.440	179.270
60.0	170.534	170.081	163.335	168.523	162.547	166.687	157.055	205.559	129.295	147.882
50.0	132.716	135.058	131.769	132.323	127.600	138.733	127.873	154.975	91.471	132.458
40.0	103.678	103.794	97.399	98.973	94.699	97.310	90.201	108.502	82.514	100.765
30.0	78.339	77.952	75.776	76.767	74.145	75.147	68.567	77.522	64.927	61.539
20.0	54.704	54.704	51.846	53.813	50.215	53.054	48.450	51.097	46.893	33.677
10.0	27.159	28.690	26.905	28.190	27.159	26.484	25.388	24.417	25.388	15.496
5.0	13.717	14.285	13.192	13.111	12.921	14.418	11.716	13.439	11.113	10.544
1.0	6.899	7.659	7.715	6.519	8.308	4.199	8.413	8.225	8.413	5.537
0.5	5.928	6.197	6.199	6.199	7.805	4.034	7.805	6.475	8.413	5.537
LOW	3.411	3.411	4.792	3.411	6.199	3.411	7.805	6.475	8.413	5.537

Table D-10. Test of Sampling Intervals for Long-Term Mean, NYC Station #36

	SAMPLING INTERVAL (NO. OF 3HR. INCREMENTS)									
	1	2	3	4	6	8	12	16	24	32
O. OF COMPARISONS	2908	1455	971	726	487	363	244	183	122	92
EAN	181.226	166.738	180.199	186.565	174.734	182.503	173.487	191.367	147.569	152.878
TANDARD DEVIATION	291.102	327.662	277.667	307.146	222.837	275.903	237.539	265.489	174.524	186.137
ISTRIBUTION PERCENTILES										
HIGH	5667.062	5667.062	4731.906	4504.641	1494.365	2592.053	1484.365	2592.053	898.161	977.365
99.5	1430.839	1913.059	1365.122	1513.628	1195.562	1484.345	1365.445	932.382	878.647	977.365
99.0	1235.465	1129.198	1120.555	1275.472	1064.759	1275.472	1195.562	888.536	878.647	919.146
95.0	658.050	662.346	662.546	727.600	670.129	742.322	691.732	662.465	548.661	490.811
90.0	442.817	444.690	438.133	462.565	429.354	400.523	365.978	474.598	318.605	318.938
80.0	257.551	258.354	253.644	258.067	260.158	251.673	232.882	305.734	221.584	224.346
70.0	186.616	189.668	186.195	184.658	192.463	182.105	184.659	209.096	171.151	171.900
60.0	136.010	137.192	142.161	133.530	137.192	131.732	133.527	155.580	132.362	147.788
50.0	95.498	98.916	98.072	91.826	105.553	86.925	104.919	106.180	105.553	109.210
40.0	65.916	67.266	66.416	65.358	67.605	62.542	64.537	68.591	71.015	57.448
30.0	43.257	43.257	42.939	41.831	40.495	36.235	37.585	53.595	36.882	29.912
20.0	20.491	20.961	19.167	19.204	16.660	16.380	14.800	18.204	11.119	14.344
10.0	6.940	6.915	6.510	6.892	6.288	6.799	5.266	6.892	4.554	5.029
5.0	4.661	3.991	3.653	3.827	3.810	3.848	3.644	4.670	3.212	2.877
1.0	2.226	2.256	2.245	1.942	2.562	1.976	2.520	1.966	2.124	1.695
0.5	1.960	1.930	1.902	1.527	2.124	1.475	2.124	1.942	2.124	1.695
LOW	0.977	0.977	1.527	0.977	1.976	0.977	2.124	1.942	2.124	1.695